

Skyrme Model Description of Heavy Baryons with Strangeness

by

Jacobus Petrus Blanckenberg

*Dissertation presented for the degree of PhD in Theoretical
Physics in the Faculty of Natural Sciences at Stellenbosch
University*



Department of Physics,
University of Stellenbosch,
Private Bag X1, Matieland 7602, South Africa.

Promoters:

Prof. Herbert Weigel
Prof. Frederik G. Scholtz

March 2015

Declaration

By submitting this dissertation electronically, I declare that the entirety of the work contained therein is my own, original work, that I am the sole author thereof (save to the extent explicitly otherwise stated), that reproduction and publication thereof by Stellenbosch University will not infringe any third party rights and that I have not previously in its entirety or in part submitted it for obtaining any qualification.

Date:

Copyright © 2015 Stellenbosch University
All rights reserved.

Abstract

Skyrme Model Description of Heavy Baryons with Strangeness

J.P. Blanckenberg

*Department of Physics,
University of Stellenbosch,
Private Bag X1, Matieland 7602, South Africa.*

Dissertation: PhD Theoretical Physics

March 2015

We are interested in the soliton description of baryons with a single heavy quark (charm or bottom). In this approach such baryons emerge as bound composites of a soliton of meson fields built from light quarks (up, down and strange) and a meson field that contains a heavy quark. The soliton must then be quantised as a diquark because the fermionic character arises from binding the heavy meson field.

We are particularly interested in heavy baryons that have non-zero strangeness. In the quark model that corresponds to, say, up-strange-bottom (usb) baryons. Thus the flavour symmetry breaking among the light quarks must be fully incorporated when constructing diquark states. In the soliton model that symmetry breaking is parameterised by differences between the masses and decay constants of kaons and pions.

Here we will compute the mass differences between the different heavy baryons and compare these results to experimental data.

Uittreksel

Skyrme Model Beskrywing van Swaar Barione met 'Strangeness'

("Skyrme Model Description of Heavy Baryons with Strangeness")

J.P. Blanckenberg

Departement Fisika,

Universiteit van Stellenbosch,

Privaatsak X1, Matieland 7602, Suid Afrika.

Proefskrif: PhD Teoretiese Fisika

Maart 2015

Ons stel belang in 'soliton' beskrywing van barione met n' enkele swaar kwark ('charm' of 'bottom'). In hierdie benadering kom sulke barione voor as samestellings van mesoon velde gebou uit ligte kwarke ('up', 'down' en 'strange'), en n' mesoon veld wat n' swaar kwark bevat. Die 'soliton' moet dan as n' dikwark gekwantiseer word, want die fermioniese gedrag kom voor as gevolg van die binding van die swaar mesoon.

Ons stel spesifiek belang in swaar barione met nie-nul 'strangeness'. In die kwark model stem dit ooreen met iets soos 'up'-'strange'-'bottom' (usb) barione. Dus moet die breek van geur simmetrie tussen die ligte kwarke ten volle inkorporeer word wanneer dikwark toestande konstrueer word. In die 'soliton' model word daardie breek van simmetrie deur die verskil tussen die massas en verval konstantes van die pion en kaon geparametriseer.

Hier sal ons die verskille tussen die massas van verskillende swaar barione bereken en die resultate met eksperimentele data vergelyk.

Acknowledgements

I would like to express my sincere gratitude to the following people and organizations:

- My promoter, Prof. H. Weigel, for his continuing support and guidance during my research.
- My co-promoter, Prof. F.G. Scholtz along with the NRF and NIThep for financially supporting my research.
- My Lord Jesus Christ who has given me the opportunities to discover more about the nature He created, and who has given me the strength and the capacity for that discovery.

Contents

Declaration	i
Abstract	ii
Uittreksel	iii
Acknowledgements	iv
Contents	v
List of Figures	viii
List of Tables	x
1 Introduction and Motivation	1
2 Strong Interactions	3
2.1 QCD	3
2.2 Quark Model	5
2.3 Baryons	6
2.3.1 Isospin	6
2.3.2 Strangeness	7
2.3.3 Heavy Flavours	8
2.4 Mesons	9
2.5 Chiral Symmetry	12
2.5.1 Sigma Model	15
2.5.2 Spontaneous Symmetry Breaking	17
3 SU(3) and the quark model	19
3.1 Mesons	22
3.2 Baryons	23
3.3 Beyond strangeness	26
3.4 SU(3) and chiral solitons	27
4 Skyrme Soliton Model	29
4.1 From large N_c to soliton models.	29

4.1.1	Equivalence to effective meson theory	30
4.1.2	Hadron Mass in large N_c	31
4.1.3	Hadron Interaction in large N_c	33
4.2	Pions	34
4.3	Skyrme term for stable solitons	35
5	Skyrmion Quantisation	39
5.1	SU(2)	39
5.2	Wess-Zumino term	44
5.2.1	Baryon number current	46
5.3	SU(3)	47
5.4	Flavour Symmetry Breaking	50
5.4.1	Numeric Calculations	53
5.4.2	Perturbation Theory	57
6	Heavy Flavour Symmetry	61
6.1	Parity Degeneracy	61
6.2	Heavy Meson Lagrangian	62
6.3	Covariant Heavy Meson Lagrangian	63
7	Heavy Meson Solitons	65
7.1	The Bound State Approach	65
7.2	S & P wave bound states	67
7.3	Normalisation of bound state wave functions	71
8	Heavy Solitons in Flavour SU(3)	73
8.1	Modified constraint on R_8	73
8.2	Heavy symmetry breaking	75
9	Hyperfine Splitting	77
9.1	Flavour Rotations and Spin	77
10	Numerical Results	81
11	Conclusion	89
	Appendices	90
A	Notation & Conventions	91
B	Conventional Matrices	93
B.1	Gell-Mann Matrices	93
B.2	Dirac Matrices	94
C	Radial Functions	95

CONTENTS

vii

List of References

97

List of Figures

3.1	SU(3) triplet (3) representation.	20
3.2	SU(3) anti-triplet ($\bar{\mathbf{3}}$) representation.	21
3.3	Mesons constructed from $\mathbf{3} \otimes \bar{\mathbf{3}} = \mathbf{8} \oplus \mathbf{1}$	23
3.4	$J = 0$ mesons.	23
3.5	$J = 1$ mesons.	24
3.6	Combinations of three quarks in $\mathbf{3} \otimes \mathbf{3} \otimes \mathbf{3}$	24
3.7	$J_z = \frac{3}{2}$ baryons in the decuplet (10).	25
3.8	$J_z = \frac{1}{2}$ baryons in the octet (8).	25
3.9	Left representation or flavour representation of SU(3) sextet and anti-triplet with labels corresponding to baryons made up of a charm quark bound in the background field of a diquark in the corresponding representation.	26
3.10	Left representation or flavour representation of SU(3) sextet (6).	28
3.11	Left representation or flavour representation of SU(3) anti-triplet ($\bar{\mathbf{3}}$).	28
3.12	Right representation or spin representation of SU(3) sextet (6).	28
4.1	Gluon Feynmann and double line diagram.	29
4.2	Gluon self interaction Feynmann and double line diagram.	30
4.3	Planar and non-planar gluon self-interaction diagram.	30
4.4	Quark bilinear coupling to loops in QCD. Coupling points are indicated by “ \times ”.	31
4.5	Gluon exchange between linked quark pairs inside a baryon.	32
4.6	Gluon exchange between non-linked quark pairs inside a baryon.	32
4.7	Baryon baryon interaction through the exchange of a single quark and gluon.	33
4.8	Baryon meson interaction through the exchange of a single quark and gluon.	34
4.9	Chiral angle as a function of radius with $e_{sk} = 4.25$, $m_\pi = 138\text{MeV}$ and $f_\pi = 93\text{MeV}$	38
5.1	Intrinsic eigenfunctions of a spin-1 diquark, with $Y = -\frac{1}{3}$ and $I = \frac{1}{2}$, for different values of symmetry breaking strength ($\gamma\beta^2$).	55

5.2	Comparison between numerical and 2^{nd} order perturbation theory calculations (by Momen <i>et al.</i> (1994)) of eigen-energies of solitons in heavy baryons as a function of flavour symmetry breaking strength.	58
5.3	Comparison between numerical and 2^{nd} order perturbation theory calculations (by Park <i>et al.</i> (1989)) of eigen-energies as a function of flavour symmetry breaking strength for light baryons.	59
5.4	Comparison between numerical and 3^{rd} order perturbation theory calculations (by Park <i>et al.</i> (1989)) of eigen-energies as a function of flavour symmetry breaking strength for light baryons.	60
7.1	Wave functions of the pseudoscalar and vector fields for the P-wave of the heavy meson containing a bottom quark with $\epsilon_H = 595$ MeV and $e_{sk} = 6.62$	71
7.2	Wave functions of the pseudoscalar and vector fields for the S-wave of the heavy meson containing a bottom quark with $\epsilon_H = 338$ MeV and $e_{sk} = 6.62$	72
10.1	Wave functions of the pseudoscalar and vector fields for the P-wave of the heavy meson containing a charm quark with $\epsilon_B = 314$ MeV. Here the vertical axis is in arbitrary units.	82
10.2	Wave functions of the pseudoscalar and vector fields for the S-wave of the heavy meson containing a charm quark with $\epsilon_B = 28$ MeV. Here the vertical axis is in arbitrary units.	83

List of Tables

2.1	Information on the different flavours of quarks. The second last column represents the ‘bottom’ charge, not to be confused with the baryon number which is $\frac{1}{3}$ for all quarks. The masses were taken from Olive <i>et al.</i> (2014) which also shows the different ways in which the masses were calculated since confinement prevents observing a single quark. The u , d and s masses are estimates of the so-called “current quark masses”. The c and b masses are “running” masses in the $\overline{\text{MS}}$ scheme.	6
2.2	Lightest baryons and their quark content according to Olive <i>et al.</i> (2014).	8
2.3	List of baryons containing strange and lighter quarks ($S = -1$) according to Olive <i>et al.</i> (2014).	9
2.4	Baryons containing a single charm quark ($C = +1$) and light quarks according to Olive <i>et al.</i> (2014).	10
2.5	Baryons containing a single bottom quark ($B = -1$) and light quarks according to Olive <i>et al.</i> (2014). The mass and mean lifetime of the Σ_b^0 is not known empirically, but it should be close to that of the Σ_b^+	11
3.1	Triplet (3) eigenstates and corresponding weights.	20
5.1	Quantum numbers of diquark members of $SU(3)$ irreps. Commutators ‘[,]’ and anti-commutators ‘{,}’ refer to anti-symmetric and symmetric light flavour combinations, respectively. The last column denotes the heavy baryons for which the diquarks are relevant.	56
5.2	Coefficients of 2 nd order perturbation theory obtained by Momen <i>et al.</i> (1994).	58
6.1	Masses of pseudoscalar and vector mesons where ‘q’ indicates an up or down quark and 0^- and 1^- represent the pseudoscalar and vector components respectively. All masses were taken from Olive <i>et al.</i> (2014)	62
8.1	Heavy pseudoscalar and vector meson masses according to Olive <i>et al.</i> (2014).	76

10.1	Bound state energies of bottom and charm mesons where ϵ_H is defined in eq.(7.2.14).	81
10.2	Comparison of mass differences between S and P-wave to experimentally observed mass differences between heavy mesons of opposite parity. Here $e_{sk} = 6.62$. The experimentally determined masses were taken from Olive <i>et al.</i> (2014).	82
10.3	Relevant quantum numbers for the baryons under investigation. . .	84
10.4	Numerical and experimental results for masses of $J = 1/2$ heavy baryons relative to the mass of the Λ_c with $e_{sk} = 6.62$	85
10.5	Numerical and experimental results for masses of $J = 3/2$ heavy baryons relative to the mass of the Λ_c with $e_{sk} = 6.62$	85
10.6	Numerical and experimental results for masses of $J = 1/2$ heavy baryons relative to the mass of the Λ_c with $e_{sk} = 4.25$	86
10.7	Numerical and experimental results for masses of $J = 3/2$ heavy baryons relative to the mass of the Λ_c with $e_{sk} = 4.25$	86
10.8	Numerical and experimental results for masses of $J = 1/2$ heavy baryons relative to the mass of the Λ_c with $e_{sk} = 4.84$ and $f_\pi = 54$ as used by Adkins and Nappi (1984).	87
10.9	Numerical and experimental results for masses of $J = 3/2$ heavy baryons relative to the mass of the Λ_c with $e_{sk} = 4.84$ and $f_\pi = 54$ as used by Adkins and Nappi (1984).	87
10.10	Numerical and experimental results for S-wave masses of $J = 1/2$ heavy baryons relative to the ground state mass of the Λ_c with different values of e_{sk} and f_π	88
10.11	Numerical and experimental results for S-wave masses of $J = 3/2$ heavy baryons relative to the ground state mass of the Λ_c with different values of e_{sk} and f_π	88

Chapter 1

Introduction and Motivation

In recent years high energy particle colliders, such as the Large Hadron Collider (LHC), have enabled physicists to observe particles with larger masses than ever before. Along with the theoretical models that help interpret the experimental data, these observations help us gain more insight into the laws of nature which govern the formation and interaction of these particles. The group of such particles that we will be focusing on in this study are the hadrons and more specifically, the baryons. Many experiments during the twentieth century have given us a great deal of knowledge about the low mass baryons such as protons and neutrons and others containing up, down and/or strange quarks. Along with all this experimental data, models were developed that explained and predicted observations.

The Skyrme model has been used very successfully in the calculation of mass differences between light baryons, (baryons containing up, down and strange quarks) as well as many of their static properties (see Zahed and Brown (1986)), Schwesinger *et al.* (1989), Meissner (1988), Weigel (2008)). The Skyrme model has also been used to describe baryons (in the valence quark picture) containing a single heavy quark (charm or bottom) as a heavy meson in the background field of a light soliton containing up and down quarks (see Schechter *et al.* (1995)). This study is based on combining these two approaches to describe baryons containing up, down or strange quarks as well as a single heavy quark.

We will start in chapter 2 with an introduction to strong interactions and the quark model, including the associated symmetries with a large focus on chiral symmetry. This will be followed, in chapter 3, by a discussion on group theory focused on aspects relevant to the $SU(3)$ treatment of the three-flavour quark model. In chapter 4, we will then present arguments, based on large N_c (number of colour degrees of freedom), for baryons arising as solitons in an effective meson theory, followed by a description of the Skyrme model for such solitons.

In chapter 5 we will introduce collective coordinates to quantise the soliton. At this point, flavour symmetry breaking will need to be introduced in order to account for the strange quark in our solitons. Numerical results of this symmetry breaking, will be compared to results obtained through second and third order perturbation theories, used by Momen *et al.* (1994) and Park *et al.* (1989) respectively. In this discussion we will already consider diquark solitons with some foreshadowing to the fact that, when considering heavy baryons, the soliton is forced to be quantised as a diquark.

Then we will move on to the discussion of the heavy meson, containing the heavy quark, that will be bound in the background of the soliton. We will see, in chapter 6, that there is some parity degeneracy which needs to be taken into account when setting up a Lagrangian for heavy mesons. Some results will be shown for the wave functions of heavy meson solitons in chapter 7 and these will be compared to similar results obtained by Schechter *et al.* (1995). In chapter 8 we will discuss the effect which this heavy meson has on the Lagrangian of the soliton, including forcing the soliton to be quantised as a diquark. Finally, in chapter 9, we will discuss the hyperfine splitting between baryons with different spin, which has, until the time of publication, not yet been considered in a Skyrme model description of heavy baryons with strangeness. Mass differences (relative to other heavy baryons) of all baryons containing two light (up, down or strange) quarks and a single heavy (charm or bottom) quark will be presented in chapter 10. These mass differences will be presented for both parity states and, where possible, will be compared to experimental data, primarily obtained from Olive *et al.* (2014). Some intermediate results have already been published in Blanckenberg and Weigel (2014).

We will conclude this study in chapter 11. Some clarifying remarks on notation, used in this text, are made in appendix A and a few technical details are summarised in further appendices.

Chapter 2

Strong Interactions

2.1 QCD

The strong interaction is one of the four fundamental forces or interactions of nature, along with the electromagnetic, weak and gravitational forces¹. Gauge theory has been very effective in describing the electromagnetic interaction between particles as an exchange of photons, which are referred to as gauge bosons. In this case, the gauge theory is called quantum electrodynamics (QED). Similarly a gauge theory is used to describe the strong interaction between quarks, via the exchange of gauge bosons called gluons. This is referred to as quantum chromodynamics (QCD), a name which stems from the fact that quarks have $N_c = 3$ colour charges. QED is a $U(1)$ gauge theory, so its gauge boson has no charge and the electric charge of interacting particles is conserved. QCD is an $SU(N_c)$ gauge theory which is why its gauge bosons have two colour charges, one for each of the interacting particles. In QCD, colour is the conserved charge.

For completeness sake we include the QCD Lagrangian² (see Alkofer and Reinhardt (1995)) here,

$$\mathcal{L}_{\text{QCD}} = \bar{q}(i\gamma^\mu\partial_\mu - m^0)q - \frac{1}{4}(F_{\mu\nu}^a)^2 + g\bar{q}\gamma^\mu A_\mu q, \quad (2.1.1)$$

although we will not be deriving anything directly from it. Here q is the quark field, in the form of a six flavour (up, down, strange, charm, bottom, top) spinor, and the first term in brackets gives the kinetic and mass terms of a free quark with m^0 being the diagonal matrix containing the six current quark

¹There has been some progress in unifying the electromagnetic and weak interaction and the search continues for a unification of all four interactions.

²In literature, it is common practice to discuss the Lagrangian, but write the Lagrange density, since the Lagrangian is just the spatial integral, of the lagrange density. In order to make the distinction clear, in this text, the Lagrangian and Lagrange density are indicated by L and \mathcal{L} , respectively.

masses. The next term is the Yang-Mills Lagrangian with field strength,

$$F_{\mu\nu}^a = \partial_\mu A_\nu^a - \partial_\nu A_\mu^a + gf^{abc}A_\mu^b A_\nu^c. \quad (2.1.2)$$

A_μ^a is the gauge field and $A_\mu = A_\mu^a \frac{\lambda^a}{2}$ is the gluon field.³ These λ^a 's are the generators of the colour gauge group. Formally they are equal to the SU(3) flavour Gell-Mann matrices (see Appendix B.1), but act in a different manifold. Furthermore, g is the gauge coupling constant and f^{abc} are the group structure constants. The last term in eq.(2.1.1) represents the coupling of gluons to the colour of the quarks.

Because the strong interaction is the interaction between quarks, it is responsible for keeping them together, to form hadrons like protons and neutrons. We will discuss the particles constructed from quarks more in the next section. The strong interaction is not just confined to keeping hadrons in one piece though. It is also responsible for keeping hadrons together, like keeping protons and neutrons together in a nucleus. This gives us a way of comparing the strengths and ranges of the strong interaction to the electromagnetic or Coulomb interaction. In a helium nucleus, for instance, the Coulomb interaction pushes the two protons apart, but the strong interaction between the two protons and two neutrons is enough to keep the whole unit together. Larger nuclei demonstrate the range differences though, since larger nuclei need a higher ratio of neutrons to protons in order to be stable. The strong interaction is a short range interaction compared to the Coulomb interaction, but at short ranges it is also much stronger than the Coulomb interaction. As an indication of their comparative strengths, we can look at their respective coupling constants. The coupling constants are dependent on the energy scale, but at the energy scale where QED is relevant, $\alpha_{\text{QED}} = 1/137$. At the scale of the mass the Z-boson, the QCD coupling constant, $\alpha_{\text{QCD}} \approx 0.115$. We can see that the strong coupling constant, α_{QCD} , is about two orders of magnitude stronger than the electromagnetic coupling constant, α_{QED} . Hence the strong interaction is much stronger than the electromagnetic interaction. We should also note that, at low energies, α_{QCD} becomes large. In a perturbative expansion, which needs to include higher powers of α_{QCD} , this becomes a problem, since it means that higher order terms start to dominate the expansion, unlike in QED, where higher order terms become negligible. Because of this, the perturbative expansion of QCD fails at low energies.

There is another parameter that can give us an idea of the strength of the strong interaction and that is the QCD scale, Λ_{QCD} . It is related to the

³In this study in general we use the Einstein summation over repeated indices and, unless stated otherwise, lower-case greek indices run from 0 to 3 and lower-case latin indices run from 1 to 3.

running coupling constant via.

$$\alpha_{\text{QCD}}(Q^2) = \frac{1}{-b_0 \ln \frac{Q^2}{\Lambda_{\text{QCD}}^2}}, \quad (2.1.3)$$

where Q is the energy scale we are interested in, and b_0 is the 1-loop β -function coefficient related to the renormalisation of the field theory. For the energy scale of the mass of the Z-boson, $\Lambda_{\text{QCD}} \approx 250$ MeV .

It should be noted that the strong interaction between quarks is unique in that it seems to get stronger as the distance between the quarks increases. One can think of it heuristically as stretching a rubber band. When it is stretched too far, this 'rubber band' will suddenly break in two and the ends will collapse. In terms of the quarks, this means that as you pull the quarks apart, the energy required to pull them apart against the force of the strong interaction becomes so great that it is energetically more viable for a quark - anti-quark pair to form in the middle, one of them going to each of the two quarks you are trying to separate. Hence quarks cannot be detected on their own. This is known as confinement. There are some experiments being done in probing so called quark gluon plasmas (QGP) formed in large density and high temperature heavy ion collisions, but these fall outside the spectrum of this study.

2.2 Quark Model

Quarks come in 6 flavours, namely up, down, strange, charm, bottom (sometimes called beauty) and top (listed in order of increasing mass). They are shown along with more information in table 2.1. The fact that they have fractional electric charges, along with the fact that all observed particles have integer electric charges, places a limitation on the possible combinations in which quarks can form hadrons. There are mainly two possible combinations that will yield integer charge. An anti-symmetric⁴ combination of a quark and anti-quark that yields integer charge is called a meson, whereas a combination of three quarks that yields integer charge is called a baryon.⁵ These baryons are the particles we are interested in. More specifically, we are interested in baryons that contain a heavy quark, like the charm or bottom quark. Baryons are fermions, and therefore their wave functions must be anti-symmetric. The

⁴Since only colour singlet particles can exist, the colours of the quarks must match, for instance red and anti-red.

⁵There are, at least theoretically, other, more exotic combinations such as pentaquarks, but these have not been experimentally observed. There are also tetraquarks, consisting of two quarks and two anti-quarks, which have been observed Collaboration (2014), but these particles fall outside the Quark model.

Quark data				Quantum Numbers				
Name	Symbol	Mass (MeV)	charge (Q)	I_z	S	C	B	T
Up	u	$2.3^{+0.7}_{-0.5}$	$\frac{2}{3}$	$+\frac{1}{2}$	0	0	0	0
Down	d	$4.8^{+0.7}_{-0.3}$	$-\frac{1}{3}$	$-\frac{1}{2}$	0	0	0	0
Strange	s	95 ± 5	$-\frac{1}{3}$	0	-1	0	0	0
Charm	c	1275 ± 25	$\frac{2}{3}$	0	0	+1	0	0
Bottom	b	4180 ± 30	$-\frac{1}{3}$	0	0	0	-1	0
Top	t	$(173.5 \pm 1.4) \times 10^3$	$\frac{2}{3}$	0	0	0	0	+1

Table 2.1: Information on the different flavours of quarks. The second last column represents the ‘bottom’ charge, not to be confused with the baryon number which is $\frac{1}{3}$ for all quarks. The masses were taken from Olive *et al.* (2014) which also shows the different ways in which the masses were calculated since confinement prevents observing a single quark. The u , d and s masses are estimates of the so-called “current quark masses”. The c and b masses are “running” masses in the $\overline{\text{MS}}$ scheme.

quark model works with symmetric wave functions though, so in order to have an anti-symmetric wave function we need to introduce a quantum number with the same number of possibilities as the number of quarks in a baryon, i.e. three. This new quantum number is the colour of QCD and its possible values are red, green and blue. All observable hadrons must be colour singlets so they must contain either three different colours in the case of baryons or a single colour and its anti-colour in the case of mesons.

2.3 Baryons

2.3.1 Isospin

Light baryons are baryons that contain up, down and/or strange quarks. The most common baryons are, of course, the proton (consisting of 2 up quarks and 1 down quark, uud) and the neutron (consisting of 1 up quark and 2 down quarks, udd). According to Olive *et al.* (2014), the mass of the proton is 938.27 MeV and the mass of the neutron is 939.57 MeV⁶. These masses have been determined to a very high accuracy. Due to the similarity of the mass of the proton and neutron, they are often considered to be two sides of the same particle, the nucleon, with the only difference being that one is electri-

⁶Looking at these masses and the masses of the up and down quarks in table 2.1, it is clear that the mass of the baryon is not simply the mass of the quarks. As with atoms, the bulk of the mass of the baryon is made up of the binding energy holding its constituents together.

cally positive and the other is neutral. This is called isospin symmetry and the nucleon is referred to as an isospin doublet. Isospin (denoted by I) is one defining property of a particle. In order to differentiate between the different states⁷ of an isospin doublet, we assign them an isospin projection, I_z . Isospin and isospin projection are counted in a similar way to spin, so in order to have a doublet, the isospin of the nucleon must be $I = \frac{1}{2}$ with the isospin projection of the proton being $I_z = \frac{1}{2}$ and the neutron $I_z = -\frac{1}{2}$. Such defining properties are called quantum numbers.

This kind of symmetry goes hand in hand with a charge and, in this case, it is the electric charge, Q . The electric charge of a hadron is given by

$$Q = I_z + \frac{1}{2}(B + S), \quad (2.3.1)$$

where B is the baryon number and S is the strangeness (discussed in section 2.3.2). In particle physics then, the symbols for protons and neutrons are N^+ and N^0 respectively, indicating that they are the same particle but with different charges. If isospin symmetry means that the proton and neutron are the same, then of course their constituent quarks must be the same, so under isospin symmetry, the up and down quarks are considered to be the same as well, but again with different electric charges, $\frac{2}{3}$ and $-\frac{1}{3}$ respectively. Assigning baryon number $B = \frac{1}{3}$ to all quarks makes eqn.(2.3.1) consistent with the entries in table 2.1. This two way symmetry is also a property of the SU(2) group, which is why these light baryons are treated in SU(2).

There are other baryons consisting of only up and down quarks, but as with the heavier baryons, they are unstable and only occur as short lived resonances. These are the Δ baryons and they have isospin $I = \frac{3}{2}$ and spin $J = \frac{3}{2}$. They are listed along with their quark content in table 2.2. The mean lifetimes⁸ of the baryons are also listed, and we can draw some conclusions from them. The proton has a mean lifetime that is much longer than the age of the universe, so it is considered absolutely stable. The Δ s have a very short lifetime, associated with decay via the strong interaction, while neutrons have a (relatively) much longer lifetime, and decay through the weak interaction.

2.3.2 Strangeness

The next heavier quark in the list, is the strange quark. Whereas the masses of the up and down quarks are quite close (see table 2.1), the mass of the

⁷Since we have established that they are considered to be the same particle, the difference between protons and neutrons are just attributed to different states of the nucleon.

⁸The error margins for the masses and mean lifetimes have been omitted here but can be found in Olive *et al.* (2014) where the data is originally from.

Baryon	Quarks	I	I_z	J	Mass $m(\text{MeV})$	Mean life $\tau(\text{s})$
N^+	uud	$\frac{1}{2}$	$\frac{1}{2}$	$\frac{1}{2}$	938.272046	$> 6.6 \times 10^{36}$
N^0	udd	$\frac{1}{2}$	$-\frac{1}{2}$	$\frac{1}{2}$	939.565379	8.80×10^2
Δ^{++}	uuu	$\frac{3}{2}$	$\frac{3}{2}$	$\frac{3}{2}$	1232	5.63×10^{-24}
Δ^+	uud	$\frac{3}{2}$	$\frac{1}{2}$	$\frac{3}{2}$	1232	5.63×10^{-24}
Δ^0	udd	$\frac{3}{2}$	$-\frac{1}{2}$	$\frac{3}{2}$	1232	5.63×10^{-24}
Δ^-	ddd	$\frac{3}{2}$	$-\frac{3}{2}$	$\frac{3}{2}$	1232	5.63×10^{-24}

Table 2.2: Lightest baryons and their quark content according to Olive *et al.* (2014).

strange quark differs considerably from them. Even so, it is still considered a light quark since its mass is smaller than the QCD scale, Λ_{QCD} , introduced in eq.(2.1.3). The charge that goes with flavour symmetry is the strangeness, S . Therefore a particle that contains a strange quark has $S \neq 0$. In order to include a strange quark, flavour symmetry must be broken. The breaking of flavour symmetry will form an important part of this study since we are interested in baryons containing both a strange quark and a heavy quark.

In table 2.3 (and table 2.1) we can see that each strange quark contributes a strangeness charge of -1 to the total strangeness of the baryon. One can also see a degeneracy between the Λ^0 and Σ^0 in this table. This degeneracy is also present in the flavour $SU(3)$ octet which is discussed in more detail in section 3.2. Furthermore, table 2.3 contains members from the decuplet (also discussed in section 3.2), the Σ^*s and Ξ^*s . They have the same isospin and strangeness as the corresponding octet baryons (ones without the ‘*’ superscript) but they have different spin, J .

2.3.3 Heavy Flavours

The next set of baryons, which we will consider in this study, are those containing a single charm quark. The names of these baryons are similar to the light baryons, but with a subscript ‘c’, to indicate that one of the strange quarks is replaced by a charm quark. These are listed in table 2.4. Similarly, baryons containing a single bottom quark have a subscript ‘b’ and are listed in table 2.5.

The baryons listed in the tables 2.4 and 2.5 are the ones we are most interested in. Models, such as the Skyrme model, are already quite good at determining the mass differences⁹ of the light baryons. Baryons with two heavy

⁹In general these models seem to overestimate the actual masses of the baryons, but they do give good results for the known mass differences between them. This is sufficient, since a

Baryon	Quarks	S	I	I_z	J	Mass $m(\text{MeV})$	Mean life $\tau(\text{s})$
Λ^0	uds	-1	0	0	$\frac{1}{2}$	1115.683	2.632×10^{-10}
Σ^+	uus	-1	1	1	$\frac{1}{2}$	1189.37	0.8018×10^{-10}
Σ^0	uds	-1	1	0	$\frac{1}{2}$	1192.642	7.4×10^{-20}
Σ^-	dds	-1	1	-1	$\frac{1}{2}$	1197.449	1.479×10^{-10}
Σ^{+*}	uus	-1	1	1	$\frac{3}{2}$	1382.80	1.83×10^{-23}
Σ^{0*}	uds	-1	1	0	$\frac{3}{2}$	1383.7	1.8×10^{-23}
Σ^{-*}	dds	-1	1	-1	$\frac{3}{2}$	1387.2	1.67×10^{-23}
Ξ^0	uss	-2	$\frac{1}{2}$	$\frac{1}{2}$	$\frac{1}{2}$	1314.86	2.90×10^{-10}
Ξ^-	dss	-2	$\frac{1}{2}$	$-\frac{1}{2}$	$\frac{1}{2}$	1321.71	1.639×10^{-10}
Ξ^{0*}	uss	-2	$\frac{1}{2}$	$\frac{1}{2}$	$\frac{3}{2}$	1531.80	7.2×10^{-23}
Ξ^{-*}	dss	-2	$\frac{1}{2}$	$-\frac{1}{2}$	$\frac{3}{2}$	1535.0	6.6×10^{-23}
Ω^-	sss	-3	0	0	$\frac{3}{2}$	1672.45	0.821×10^{-10}

Table 2.3: List of baryons containing strange and lighter quarks ($S = -1$) according to Olive *et al.* (2014).

quarks, like the Λ_{cc} containing two charm quarks, have also been observed, but they fall outside the scope of this study since they would require doubling the heavy meson bound states.

2.4 Mesons

The other important hadrons, alluded to earlier, are the mesons. These too will become important to our study later on, specifically the heavy mesons, or mesons containing a single heavy quark. As stated earlier, mesons consist of a quark and an anti-quark, combined in a way to give integer charge. The anti-quarks have opposite quantum numbers to their quark partners. Therefore a strange anti-quark will have a charge of $\frac{1}{3}$ and strangeness $+1$. We will not list all known mesons here, since there are a lot of them. In fact, the sheer number of different mesons that have been discovered were one of the main reasons for the development of the quark model. A complete list of mesons, that have been experimentally observed, can be found in Olive *et al.* (2014). We will however look more closely at some of the mesons that will be important to our study.

model that can give the mass differences can still be used to predict masses of baryons that have yet to be seen by experiment, based on the masses of baryons that have already been seen.

Baryon	Quarks	C	S	I	I_z	J	Mass $m(\text{MeV})$	Mean life $\tau(\text{s})$
Λ_c^+	udc	1	0	0	0	$\frac{1}{2}$	2286.46	200×10^{-15}
Σ_c^{++}	uuc	1	0	1	1	$\frac{1}{2}$	2453.98	2.91×10^{-22}
Σ_c^+	udc	1	0	0	0	$\frac{1}{2}$	2452.9	$> 1.43200 \times 10^{-22}$
Σ_c^0	ddc	1	0	1	-1	$\frac{1}{2}$	2453.74	3.04×10^{-22}
Σ_c^{++*}	uuc	1	0	1	1	$\frac{3}{2}$	2517.9	4.41×10^{-23}
Σ_c^{+*}	udc	1	0	0	0	$\frac{3}{2}$	2517.5	$> 3.9 \times 10^{-23}$
Σ_c^{0*}	ddc	1	0	1	-1	$\frac{3}{2}$	2518.8	4.53×10^{-23}
Ξ_c^+	usc	1	-1	$\frac{1}{2}$	$\frac{1}{2}$	$\frac{1}{2}$	2467.8	442×10^{-15}
Ξ_c^0	dsc	1	-1	$\frac{1}{2}$	$-\frac{1}{2}$	$\frac{1}{2}$	2470.88	112×10^{-15}
Ξ_c^{+*}	usc	1	-1	$\frac{1}{2}$	$\frac{1}{2}$	$\frac{3}{2}$	2645.9	$> 2.1 \times 10^{-22}$
Ξ_c^{0*}	dsc	1	-1	$\frac{1}{2}$	$-\frac{1}{2}$	$\frac{3}{2}$	2645.9	$> 1.2 \times 10^{-22}$
Ω_c^0	ssc	1	-2	0	0	$\frac{3}{2}$	2695.2	69×10^{-15}

Table 2.4: Baryons containing a single charm quark ($C = +1$) and light quarks according to Olive *et al.* (2014).

The first important meson will be the pion (π^\pm, π^0) with a mass of 139.6 MeV and quark content of $u\bar{d}$, $d\bar{u}$ or $(u\bar{u} - d\bar{d})/\sqrt{2}$. The $(u\bar{u} + d\bar{d})/\sqrt{2}$ combination refers to a scalar particle, σ , but due to chiral symmetry breaking, which is discussed in section 2.5, it is not fundamental to model building. These scalar particles are unstable with respect to the strong interaction with a short half life time. Including them, when building a model, would complicate matters without resulting in much added insight. There are other mesons that have zero charges in the other flavours such as the $s\bar{s}$ combination, which contains two strange quarks, but have a total strangeness of 0. The next important mesons to us, will be the kaons or K mesons which have $S = \pm 1$. These mesons contain either a strange quark or anti-quark, along with an up or down anti-quark or quark. The mass of the K^\pm is 493.7 MeV which is nearly four times as much as the π . These are still considered light mesons.

As a rule of thumb we consider mesons as light when their spin excitation is significantly heavier than their ground state. For the pion, this is the ρ -meson (770 MeV) and for the kaon, the K^* (880 MeV). On a more fundamental level, the criteria is that quark components have current masses less than Λ_{QCD} .

The heavy mesons which will be important to us later on are the D mesons ($C = \pm 1$) and the B mesons ($B = \pm 1$). The mass of the D^\pm is 1869.6 MeV and that of the B^\pm is 5279.25 MeV. There are of course more D and B mesons

Baryon	Quarks	B	S	I	I_z	J	Mass $m(\text{MeV})$	Mean life $\tau(\text{s})$
Λ_b^0	udb	-1	0	0	0	$\frac{1}{2}$	5619.4	1.429×10^{-12}
Σ_b^+	uub	-1	0	1	1	$\frac{1}{2}$	5811.3	0.68×10^{-22}
Σ_b^0	udb	-1	0	0	0	$\frac{1}{2}$		
Σ_b^-	ddb	-1	0	1	-1	$\frac{1}{2}$	5815.5	1.3×10^{-22}
Σ_b^{*+}	uub	-1	0	1	1	$\frac{3}{2}$	5832.1	0.572×10^{-22}
Σ_b^{*0}	udb	-1	0	0	0	$\frac{3}{2}$		
Σ_b^{*-}	ddb	-1	0	1	-1	$\frac{3}{2}$	5835.1	0.88×10^{-22}
Ξ_b^0	usb	-1	-1	$\frac{1}{2}$	$\frac{1}{2}$	$\frac{1}{2}$	5788	1.49×10^{-12}
Ξ_b^-	dsb	-1	-1	$\frac{1}{2}$	$-\frac{1}{2}$	$-\frac{1}{2}$	5791.1	1.56×10^{-12}
Ξ_b^{*0}	usb	-1	-1	$\frac{1}{2}$	$\frac{1}{2}$	$\frac{3}{2}$	5945.5	3.1×10^{-22}
Ω_b^-	ssb	-1	-2	0	0	$\frac{1}{2}$	6071	1.1×10^{-12}

Table 2.5: Baryons containing a single bottom quark ($B = -1$) and light quarks according to Olive *et al.* (2014). The mass and mean lifetime of the Σ_b^0 is not known empirically, but it should be close to that of the Σ_b^+ .

than these, but we list them just to give an idea of the masses of these mesons. D and B mesons with non-zero strangeness are identified by a subscript ‘s’ as in D_s and B_s .

This concludes our first look at the well established quark model. We did not mention any hadrons containing the top quark because the lifetime of the top quark is too short to bind to others in a hadron.

2.5 Chiral Symmetry

Considering the masses of nucleons and the mass of their constituent quarks, we can see that the mass of the quarks are negligible, compared to the mass of the baryon they form. The contribution of mass to the baryon from a single light quark, or the current quark mass, comes from the highly relativistic motion of the nearly massless quark. In order to study this motion, consider the Dirac equation,

$$H\psi = E\psi \quad (2.5.1)$$

$$H = \vec{\alpha} \cdot \vec{p} + \beta m, \quad (2.5.2)$$

where $\vec{\alpha}$ ¹⁰ and β are the Dirac operators and the relations,

$$\{\alpha_i, \beta\} = 0 \quad (2.5.3)$$

$$\alpha_i^2 = \beta^2 = 1, \quad (2.5.4)$$

are demanded by the mass energy relation. They are also 4×4 matrices. Now the Dirac equation for a free particle (see Bhaduri (1988)) is given by,

$$(\vec{\alpha} \cdot \vec{p} + \beta m)\psi(t, \vec{x}) = i \frac{\partial}{\partial t} \psi(t, \vec{x}) \quad (2.5.5)$$

We would like to consider the particles in a vector potential though. Including this, in the form $V_0(\vec{x})$, the Dirac equation for a particle in a vector potential is given by

$$[\vec{\alpha} \cdot \vec{p} + \beta m + V_0(\vec{x})]\psi(t, \vec{x}) = i \frac{\partial}{\partial t} \psi(t, \vec{x}) \quad (2.5.6)$$

The Dirac operators can be explicitly written in terms of the Dirac-Pauli representation,

$$\vec{\alpha} = \begin{pmatrix} 0 & \vec{\sigma} \\ \vec{\sigma} & 0 \end{pmatrix} \quad (2.5.7)$$

$$\beta = \begin{pmatrix} I & 0 \\ 0 & -I \end{pmatrix}, \quad (2.5.8)$$

where $\vec{\sigma}$ are the Pauli spin matrices. Choosing the stationary solution as

$$\psi(t, \vec{x}) = \psi(\vec{x})e^{-iEt}, \quad (2.5.9)$$

causes eq.(2.5.6) to take the form

$$[-i\vec{\alpha} \cdot \vec{\nabla} + \beta m + V_0]\psi(\vec{x}) = E\psi(\vec{x}). \quad (2.5.10)$$

¹⁰Throughout this study we will use the arrow as in $\vec{\alpha}$ to indicate either a three component vector such as \vec{p} or a three component operator such as the three Pauli spin matrices $\vec{\sigma}$

Here $\psi(\vec{x})$ is a four component spinor and we can rewrite it in terms of the two two component spinors, ϕ and χ ,

$$\psi(\vec{x}) = \begin{pmatrix} \phi \\ \chi \end{pmatrix}. \quad (2.5.11)$$

In order to solve the Dirac equation then, we need to solve the two coupled equations,

$$\begin{aligned} (\vec{\sigma} \cdot \vec{p})\chi + (m + V_0)\phi &= E\phi \\ (\vec{\sigma} \cdot \vec{p})\phi - (m - V_0)\chi &= E\chi, \end{aligned} \quad (2.5.12)$$

where $\vec{p} = -i\vec{\nabla}$. If we consider a free particle again, eq.(2.5.12) simplifies to,

$$\begin{aligned} (\vec{\sigma} \cdot \vec{p})\chi + m\phi &= E\phi \\ (\vec{\sigma} \cdot \vec{p})\phi - m\chi &= E\chi. \end{aligned} \quad (2.5.13)$$

Now we define two new two component spinors,

$$\begin{aligned} \phi_R &= \frac{1}{2}(\phi + \chi) \\ \phi_L &= \frac{1}{2}(\phi - \chi). \end{aligned} \quad (2.5.14)$$

Substituting these new spinors into eq.(2.5.13) yields,

$$\begin{aligned} (\vec{\sigma} \cdot \vec{p})\phi_R + m\phi_L &= E\phi_R \\ (\vec{\sigma} \cdot \vec{p})\phi_L - m\phi_R &= -E\phi_L. \end{aligned} \quad (2.5.15)$$

What we are really interested in, however, are light quarks, which, we have already argued, may as well be taken as massless particles. In the massless case, eqs.(2.5.15) decouple. We divide both sides of the equations by $|\vec{p}|$ which results in,

$$\begin{aligned} (\vec{\sigma} \cdot \hat{p})\phi_R &= \frac{E}{|\vec{p}|}\phi_R \\ (\vec{\sigma} \cdot \hat{p})\phi_L &= -\frac{E}{|\vec{p}|}\phi_L. \end{aligned} \quad (2.5.16)$$

We can now see that, for a positive energy solution, the spin, σ , must be aligned along the same direction as the momentum, \vec{p} , in ϕ_R . In ϕ_L they must be aligned in opposite directions. Here $(\vec{\sigma} \cdot \hat{p})$ is called the helicity operator and ϕ_R and ϕ_L are both eigenstates of this operator with eigenvalues 1 and -1 respectively. We call ϕ_R and ϕ_L the right- and left-handed spinors, respectively.

Eqn.(2.5.5) can also be written as

$$(i\gamma^\mu\partial_\mu - m)\psi = 0, \quad (2.5.17)$$

where γ_μ are the Dirac matrices given in Appendix B.2. Multiplying by γ^5 should not change the equation,

$$\gamma_5(i\gamma^\mu\partial_\mu - m)\psi = 0. \quad (2.5.18)$$

Using the commutation relation $\{\gamma^\mu, \gamma_5\} = 0$,

$$(i\gamma^\mu\partial_\mu + m)(\gamma_5\psi) = 0. \quad (2.5.19)$$

This means that, in the case where $m = 0$, both ψ and its chiral partner, $\gamma_5\psi$, are eigenstates of the Dirac Hamiltonian. Taking linear combinations of these two eigenstates then, we can define two new four-component spinors,

$$\psi_R = \frac{1}{2}(1 + \gamma_5)\psi \quad (2.5.20)$$

$$\psi_L = \frac{1}{2}(1 - \gamma_5)\psi. \quad (2.5.21)$$

It turns out that,

$$\psi_R = \begin{pmatrix} \phi_R \\ \phi_R \end{pmatrix}, \quad (2.5.22)$$

$$\psi_L = \begin{pmatrix} \phi_L \\ -\phi_L \end{pmatrix}. \quad (2.5.23)$$

If we look at the Dirac equation in terms of QCD, we need to add the quark interaction term (from the last term in eq.(2.1.1) to the Dirac equation for the free particle in eq.(2.5.5), which then becomes

$$(\vec{\alpha} \cdot \vec{p} + \beta m + g_{\text{QCD}}(A_0 - \vec{\alpha} \cdot \vec{A})\psi(t, \vec{x}) = i\frac{\partial}{\partial t}\psi(t, \vec{x}). \quad (2.5.24)$$

The energy scale (and thus the strength), of the interaction term, is of the order of $\Lambda_{\text{QCD}} \approx 250$ MeV, whereas the βm term is less than 10 MeV, and is therefore negligible. Therefore, in QCD, we truly can consider the $m = 0$ case as a good starting point. Furthermore, because of the commutation relation,

$$[\gamma_5, \vec{\alpha}] = 0, \quad (2.5.25)$$

the new term does not change the conclusions from eqs.(2.5.18) and (2.5.19). Therefore QCD exhibits chiral symmetry to a good approximation. If this were a true symmetry in nature though, we would expect to have a degeneracy between the π triplet and σ singlet, but in nature, the σ does not exist (at least at the mass scale of the pion), indicating that the chiral symmetry in QCD is spontaneously broken. In order to investigate all these aspects of QCD, we will look at the sigma-model.

2.5.1 Sigma Model

As a starting point when looking at chiral symmetry in QCD, we will consider the sigma-model in $SU(2)_L \times SU(2)_R$. We will look at the same Lagrangian as eq.(4.5.1) in Bhaduri (1988),

$$\begin{aligned} \mathcal{L}_\sigma = & i\bar{\psi}\gamma^\mu\partial_\mu\psi + g\bar{\psi}(\sigma + i\vec{\tau}\cdot\vec{\pi}\gamma_5)\psi + \frac{1}{2}(\partial_\mu\sigma)^2 \\ & + \frac{1}{2}(\partial_\mu\vec{\pi})^2 - C^2(\sigma^2 + \vec{\pi}^2 - A)^2. \end{aligned} \quad (2.5.26)$$

Here, σ is an isoscalar field and $\vec{\pi} = (\pi_1, \pi_2, \pi_3)$ is an isotriplet field. Now we want to find the vector and axial vector currents, $j^{\mu i}$ and $j_5^{\mu i}$, respectively, using the Gell-Mann Levy technique. First, let's look at a chiral transformation,

$$\psi(x) \rightarrow \left(1 - i\epsilon_i\gamma_5\frac{\tau^i}{2}\right)\psi(x) \quad (2.5.27)$$

$$\pi_i \rightarrow \pi_i + \epsilon_i\sigma \quad (2.5.28)$$

$$\sigma \rightarrow \sigma - \epsilon_i\pi^i, \quad (2.5.29)$$

where ϵ_i is a small x -dependent iso-triplet and \mathcal{L}_σ transforms as

$$\mathcal{L}_\sigma \rightarrow \mathcal{L}_\sigma + \delta\mathcal{L}_\sigma. \quad (2.5.30)$$

While

$$\frac{\partial}{\partial\epsilon^i}\delta\mathcal{L}_\sigma = 0, \quad (2.5.31)$$

from global symmetry we get a current from

$$j^{\mu i} = \frac{\partial}{\partial(\partial_\mu\epsilon_i)}\delta\mathcal{L}_\sigma, \quad (2.5.32)$$

which results in the axial vector current,

$$\vec{j}_5^\mu(x) = \bar{\psi}\gamma^\mu\gamma_5\frac{\vec{\tau}}{2}\psi + \sigma(\partial^\mu\vec{\pi}) - (\partial^\mu\sigma)\vec{\pi}. \quad (2.5.33)$$

The axial vector charge is given by

$$Q_5^i = \int d^3x j_5^{0i}(\vec{x}, t). \quad (2.5.34)$$

Next we will look at a rotation in isospin space to get the vector current and charge,

$$\psi \rightarrow \left(1 - i\epsilon_i\frac{\tau^i}{2}\right)\psi \quad (2.5.35)$$

$$\pi_i \rightarrow \pi_i + \epsilon^{ijk}\epsilon_j\pi_k. \quad (2.5.36)$$

Because σ is an isoscalar, it is unaffected by a rotation in isospin space. The vector current and vector charge are now given by

$$\vec{j}^\mu = \bar{\psi}\gamma^\mu\frac{\vec{\tau}}{2}\psi + (\vec{\pi} \times \partial^\mu\vec{\pi}) \quad (2.5.37)$$

and

$$Q^i = \int d^3x j^{0i}(\vec{x}, t) \quad (2.5.38)$$

respectively.

We can now define generators of the chiral transformations like eq.(4.5.9) in Bhaduri (1988)

$$Q_R^i = \frac{1}{2}(Q^i + Q_5^i) \propto (1 + \gamma_5)\tau^i \quad (2.5.39)$$

$$Q_L^i = \frac{1}{2}(Q^i - Q_5^i) \propto (1 - \gamma_5)\tau^i. \quad (2.5.40)$$

These Left and Right generators obey the same commutation relations as SU(2),

$$\begin{aligned} [Q_R^i, Q_R^j] &= i\epsilon^{ijk}Q_R^k \\ [Q_L^i, Q_L^j] &= i\epsilon^{ijk}Q_L^k \\ [Q_R^i, Q_L^j] &= 0, \end{aligned} \quad (2.5.41)$$

and therefore their combination forms a closed algebra. Of course this is not an exact symmetry in nature, and the fact that Q_L and Q_R have different spectra leads to a spontaneous breaking of chiral symmetry, but we will still need to break the symmetry explicitly, in order to account for the pion mass.

In order to demonstrate a chiral transformation, recall

$$\begin{aligned} \psi_L &= \frac{1}{2}(1 - \gamma_5)\psi \\ \psi_R &= \frac{1}{2}(1 + \gamma_5)\psi. \end{aligned}$$

Then the coupling to a matrix representation (U) for mesons is given by

$$\psi^\dagger U \psi = \psi_L^\dagger U \psi_R + \psi_R^\dagger U^\dagger \psi_L. \quad (2.5.42)$$

Now if we vary these independently,

$$\begin{aligned} \psi'_L &= g_L \psi_L \\ \psi'_R &= g_R \psi_R \end{aligned} \quad (2.5.43)$$

$$U = g_L U g_R^{-1}, \quad (2.5.44)$$

it can be shown that

$$\mathcal{L}_{\text{nl}\sigma} = \frac{f_\pi^2}{4} \text{tr}[\partial_\mu U \partial^\mu U^\dagger] \quad (2.5.45)$$

will be invariant. Therefore the first term in our Lagrangian (where f_π is the pion decay constant), eq.(2.5.45) Weigel (2008), displays chiral symmetry¹¹.

2.5.2 Spontaneous Symmetry Breaking

Let us take another look at the mesonic part of eq.(2.5.26)¹². If we want the ground state of the Lagrangian, we need to minimise the potential term,

$$U = C^2(\sigma^2 + \vec{\pi}^2 - A)^2. \quad (2.5.46)$$

Now if $A > 0$, the minimum of U is obtained when,

$$\sigma^2 + \vec{\pi}^2 = A \quad (2.5.47)$$

Since $\vec{\pi}$ is pseudoscalar, we want to keep $\langle \vec{\pi} \rangle = 0$ and therefore

$$\langle \sigma \rangle = -\sqrt{A} \quad (2.5.48)$$

We really want fields that vanish at the ground state though, so we need to define a new field instead of σ in the form,

$$\tilde{\sigma} = \sigma + \sqrt{A}. \quad (2.5.49)$$

Now we need to rewrite eq.(2.5.26) in terms of $\tilde{\sigma}$

$$\begin{aligned} \mathcal{L}_\sigma &= i\bar{\psi}\gamma^\mu\partial_\mu\psi - g\sqrt{A}\bar{\psi}\psi + g\bar{\psi}(\tilde{\sigma} + i\vec{\tau}\cdot\vec{\pi}\gamma_5)\psi \\ &+ \frac{1}{2}(\partial_\mu\tilde{\sigma})^2 + \frac{1}{2}(\partial_\mu\vec{\pi})^2 - 4C^2A\tilde{\sigma}^2 \\ &+ 4\sqrt{A}C^2\tilde{\sigma}(\tilde{\sigma}^2 + \vec{\pi}^2) - C^2(\tilde{\sigma}^2 + \vec{\pi}^2)^2. \end{aligned} \quad (2.5.50)$$

Since we chose $\langle \vec{\pi} \rangle = 0$ in deriving this Lagrangian, the pion field is massless, and it is therefore called a Goldstone boson. We can now specify matrix representations from eq.(2.5.42) with,

$$U = \langle \sigma \rangle e^{i\vec{\tau}\cdot\vec{\pi}/f_\pi}. \quad (2.5.51)$$

The fact that the fields $\tilde{\sigma}$ and $\vec{\pi}$ have different masses means that the symmetry is spontaneously broken. Nonetheless, in order to give a realistic description

¹¹This term does actually have spontaneous breaking of the chiral symmetry at $r = 0$, but we will still have to add explicit symmetry breaking for a realistic model.

¹²The mesonic part contains only the terms with no ψ component.

of hadrons, we need to break the chiral symmetry explicitly with a term containing the pion mass and the pion decay constant.

$$\mathcal{L}_m = \frac{m_\pi^2 f_\pi^2}{4} \text{tr}[U + U^\dagger - 2] \quad (2.5.52)$$

We now have the first two terms of our Lagrangian that take into account chiral symmetry,

$$\mathcal{L} = \frac{f_\pi^2}{4} \text{tr}[\partial_\mu U \partial^\mu U^\dagger] + \frac{m_\pi^2 f_\pi^2}{4} \text{tr}[U + U^\dagger - 2]. \quad (2.5.53)$$

This, so called, non-linear σ -model sets up an effective model that we will discuss in more detail later.

Chapter 3

SU(3) and the quark model

In this study we will be dealing with the quark model and SU(3) a lot, so we will provide a brief overview of the relevant properties and diagrams that illustrate the link between SU(3) group theory and particles observed in experiments. This is by no means a full description of SU(3), and should be seen merely as a reference for discussions in this study.

SU(3) is the group of unitary 3×3 matrices with determinant 1 in the defining representation. It has $3^2 - 1 = 8$ generators that can be obtained from the Gell-Mann matrices, λ_a , in B.1.1 according to

$$T_a = \frac{1}{2}\lambda_a \quad (3.0.1)$$

Of these generators, a maximum of two may commute with each other, and these are the Cartan generators:

$$H_1 = \frac{1}{2}\lambda_3 \quad (3.0.2)$$

$$H_2 = \frac{1}{2\sqrt{3}}\lambda_8. \quad (3.0.3)$$

Now if $|\phi\rangle$ is an eigenstate of both H_1 and H_2 with eigenvalues p and q respectively, we can identify this eigenstate by a point in a two dimensional plane with coordinates (p, q) which is referred to as the weight¹. We will now look at some of the irreducible representations (irreps) in SU(3). The simplest one is the singlet (**1**), which contains only one state with a weight of $(0, 0)$. When it comes to identifying baryons with states in SU(3), the totally antisymmetric singlet will account for the colour factor in the baryon wave function. We are more interested in states with higher weights though, such as the triplet (**3**). The eigenstates of the triplet and their respective weights are given in table 3.1.

¹Strictly speaking, p and q refer to the highest weights in a given representation and not to the weights of individual states

Eigenstate	Weight	Flavour
$\begin{pmatrix} 1 \\ 0 \\ 0 \end{pmatrix}$	$\left(\frac{1}{2}, \frac{1}{2\sqrt{3}}\right)$	u
$\begin{pmatrix} 0 \\ 1 \\ 0 \end{pmatrix}$	$\left(-\frac{1}{2}, \frac{1}{2\sqrt{3}}\right)$	d
$\begin{pmatrix} 0 \\ 0 \\ 1 \end{pmatrix}$	$\left(0, -\frac{1}{\sqrt{3}}\right)$	s

Table 3.1: Triplet ($\mathbf{3}$) eigenstates and corresponding weights.

In table 3.1 we have already added the flavor names to the states, alluding to the quark model, but that will become clearer later. If we plot the points of these three weights on a normal two dimensional plane, we get fig. 3.1. This representation is called the triplet ($\mathbf{3}$) because it has three states. The solid lines represent the three axes of symmetry, while the dashed lines represent the directions of raising and lowering operators. In higher dimensional representations, more states will be allowed, and they will fall on these intersections. The intersection between the three solid lines fall on the origin in this figure. Counting upwards by an amount p , and to the right by an amount q , from the origin brings you to the eigenstate corresponding to that weight.

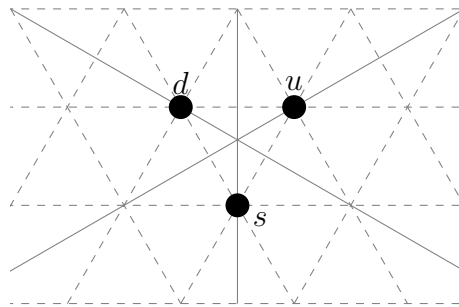


Figure 3.1: $SU(3)$ triplet ($\mathbf{3}$) representation.

The complex conjugate of the triplet is also a three dimensional, irreducible representation in $SU(3)$ and is called the anti-triplet ($\bar{\mathbf{3}}$). The weights of the states in the anti-triplet, are simply the negative of the weights of the triplet

and they are shown in fig. 3.2.

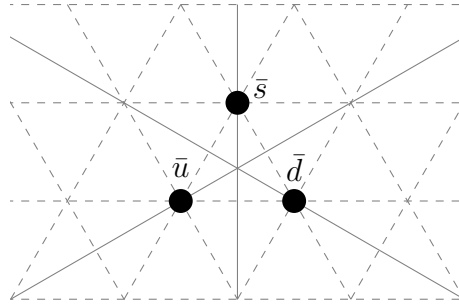
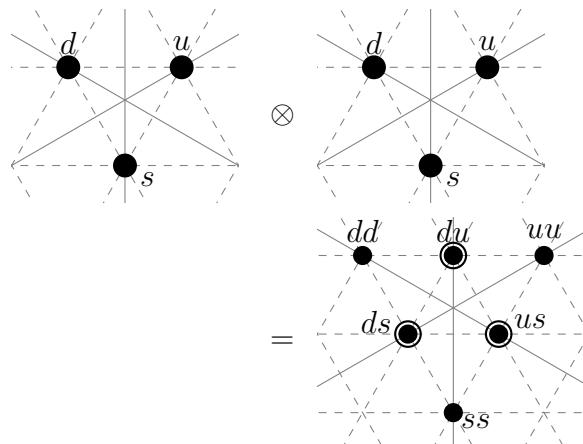


Figure 3.2: $SU(3)$ anti-triplet ($\bar{\mathbf{3}}$) representation.

We can now use these weight diagrams to simplify the tensor product (denoted by \otimes) between two irreps. To find the states in the tensor product between two irreps, we need to take the tensor product of each state in the one irrep, with each state in the other. The simplest way to demonstrate this is by example, so we will look at the states in $\mathbf{3} \otimes \mathbf{3}$. The states of $\mathbf{3} \otimes \mathbf{3}$ will be given by $u \otimes u$, $u \otimes d$, $u \otimes s$ and the same for the other two states in the left factor. Hence, in this case there will be nine states. To find the weight of the tensor product of two states, we simply need to add the weights of the two states in question. As an example the weight of $u \otimes d$ is

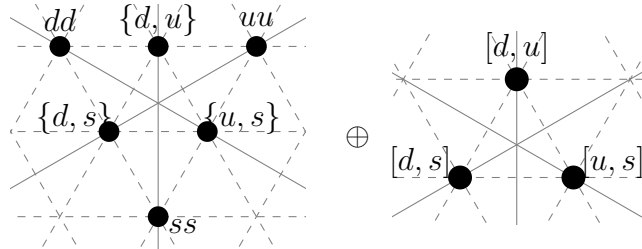
$$\left(\frac{1}{2}, \frac{1}{2\sqrt{3}}\right) + \left(-\frac{1}{2}, \frac{1}{2\sqrt{3}}\right) = \left(0, \frac{1}{\sqrt{3}}\right). \quad (3.0.4)$$

We will clearly get the same result for $d \otimes u$ so there can be some degeneracies. This method becomes even simpler when looking at the weight diagrams.



$$(3.0.5)$$

The resultant weight diagram is similar to that of the $SU(3)$ sextet (**6**), with the difference being the three weights that have two corresponding states marked on the diagram by a circle around the dot. Those three degenerate weights correspond to the weights of the anti-triplet, which means this diagram can now be decomposed into $\mathbf{6} \oplus \bar{\mathbf{3}}$,



$$(3.0.6)$$

where we have introduced the brackets ‘{ }’ and ‘[]’ to show the symmetric and anti-symmetric combinations of the quarks respectively, defined as,

$$\{d, u\} = \frac{1}{\sqrt{2}}(du + ud) \quad (3.0.7)$$

$$[d, u] = \frac{1}{\sqrt{2}}(du - ud) \quad (3.0.8)$$

We now have the tools needed to look at the quark model in terms of $SU(3)$ representations. We have already identified the three states of the triplet with the three quark flavours, so now we can build up more particles by combining quarks through the tensor product.

3.1 Mesons

We will start with the most simple hadrons, the mesons. Since they consist of a quark anti-quark pair, we build them from $\mathbf{3} \otimes \bar{\mathbf{3}}$ which yields fig. 3.3. This can be decomposed into the octet (**8**) and the singlet.

In order to match these eigenstates with actual particles, we need to find an analogy between the numbers in the weights, and the quantum numbers of real particles. The first weight, p , is equated to the isospin projection, I_3 , and for the second weight, q , we introduce the hypercharge,

$$Y = \frac{2}{\sqrt{3}}q, \quad (3.1.1)$$

which is related to baryon number (B) and the strangeness (S) via.

$$Y = B + S. \quad (3.1.2)$$

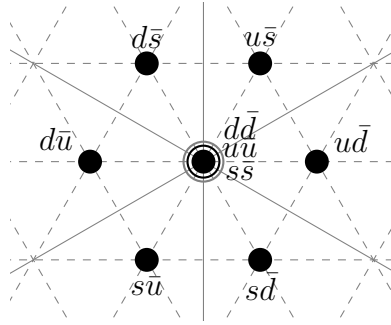


Figure 3.3: Mesons constructed from $\mathbf{3} \otimes \bar{\mathbf{3}} = \mathbf{8} \oplus \mathbf{1}$.

Each quark has $B = \frac{1}{3}$ so that a baryon, consisting of three quarks, has $B = 1$ and a meson, consisting of a quark and an anti-quark has $B = 0$. Each strange quark has $S = -1$. There is still the total spin, J , which can be either 0 or 1 for mesons, so this leads to two different, but related sets of mesons. The octet representations are shown in fig. 3.4 and 3.5. Of course there is a singlet associated with each of the two octets, for a total of nine states each. On each of the figures, we have only provided a label for one of the degenerate $I_3 = 0$ states. This is because linear combinations of the other $I_3 = 0$ state in the octet and the associated singlet states form the physical states. These physical states are (linear combinations of) the η and η' for $J = 0$ and the ω and ϕ for $J = 1$.

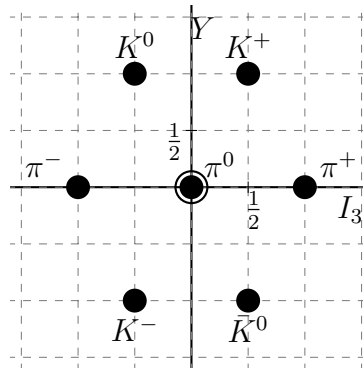


Figure 3.4: $J = 0$ mesons.

3.2 Baryons

The baryons are constructed of three quarks, so we need to look at the tensor product $\mathbf{3} \otimes \mathbf{3} \otimes \mathbf{3}$. We have already seen what $\mathbf{3} \otimes \mathbf{3}$ looks like in figure 3.0.5 so we will simply take the product of that with the triplet. The full result of

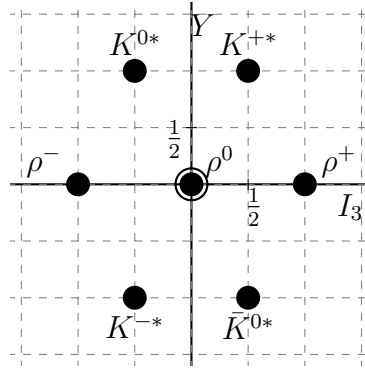


Figure 3.5: $J = 1$ mesons.

that product is shown in figure 3.6. This can be decomposed as follows:

$$\mathbf{3} \otimes \mathbf{3} \otimes \mathbf{3} = \mathbf{10} \oplus \mathbf{8} \oplus \mathbf{8}' \oplus \mathbf{1}. \quad (3.2.1)$$

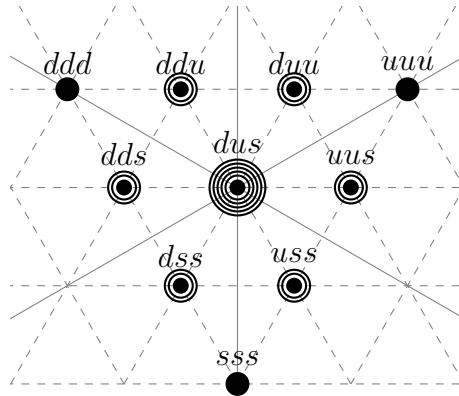


Figure 3.6: Combinations of three quarks in $\mathbf{3} \otimes \mathbf{3} \otimes \mathbf{3}$.

Because the constituents of the baryons are fermions, their wave functions must be completely anti-symmetric. The three factors contributing to the symmetry of the wave functions are the colour, flavour and spin. The decuplet ($\mathbf{10}$) contains flavour combinations such as ‘ ddd ’, which are symmetric in flavour. They are always antisymmetric in colour though, so in order to have an antisymmetric wave function, the spin must be a symmetric combination $(\frac{1}{2}, \frac{1}{2}, \frac{1}{2})$, i.e. $J_z = \frac{3}{2}$. The baryon decuplet is shown in figure 3.7.

The two octets in eq.(3.2.1) have mixed symmetry, but we can choose a combination of the two octets such that, along with having $J_z = \frac{1}{2}$, the wave functions will be symmetric. Finally, along with the colour, they are again completely anti-symmetric. The baryon octet is shown in figure 3.8.

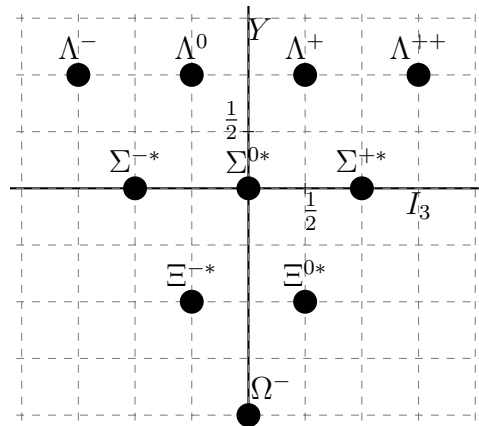


Figure 3.7: $J_z = \frac{3}{2}$ baryons in the decuplet (10).

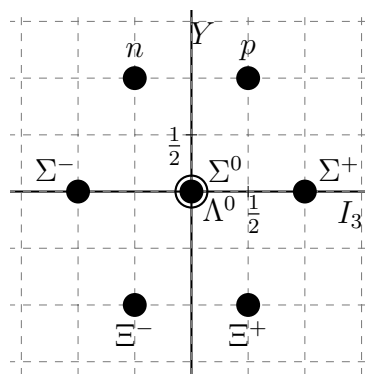


Figure 3.8: $J_z = \frac{1}{2}$ baryons in the octet (8).

If we attempt the same for the singlet, we find that the singlet must be antisymmetric in flavour, and of course in colour, so it will have to be antisymmetric in spin, but this is impossible for $J = \frac{1}{2}$ and therefore there is no singlet baryon in the non-relativistic quark model.

3.3 Beyond strangeness

Thus far in this chapter we have only considered three flavours of quarks, though we know that there are six. The problem is that $SU(3)$ or strangeness symmetry is not nearly as good a symmetry as the $SU(2)$ or isospin symmetry. This can be remedied by incorporating symmetry breaking. Upon breaking this $SU(3)$ symmetry, the resultant states are no longer pure eigenstates of specific irreps in $SU(3)$, but are instead admixtures of states from higher irreps such as the 15-plet or 27-plet.

When looking at the heavier flavours (charm, bottom and top), the deviation from $SU(N)$ symmetry is so big that there is not a lot to be gained from looking at something like $SU(6)$, and it is more fruitful to seek out alternative methods of dealing with the heavy flavours. Phenomenologically we can consider the heavy baryon as a part consisting of only light quarks, and therefore in $SU(3)$, and a heavy part consisting of a charm or bottom spectator quark. The light part is described as a soliton in the $SU(3)$ sextet and anti-triplet so it is a diquark. In section 8.1 we will see that we are actually forced to quantise this light soliton as a diquark. Fig. 3.9 shows labels of heavy baryons, on nodes corresponding to the diquark soliton contained in that baryon, in our model. Only the charm baryons are shown here, but it would look the same for bottom baryons except that the subscript ‘ c ’ is replaced with ‘ b ’.

If one takes into account isospin symmetry, like we do in this model, the nine distinct baryons in fig. 3.9 are reduced to just five baryons for each heavy flavour. A quick look at the masses in tables 2.4 and 2.5 however, shows that the mass differences between the heavy baryons with different isospins, are no more than a few MeV, so isospin symmetry is still a good symmetry for these baryons.

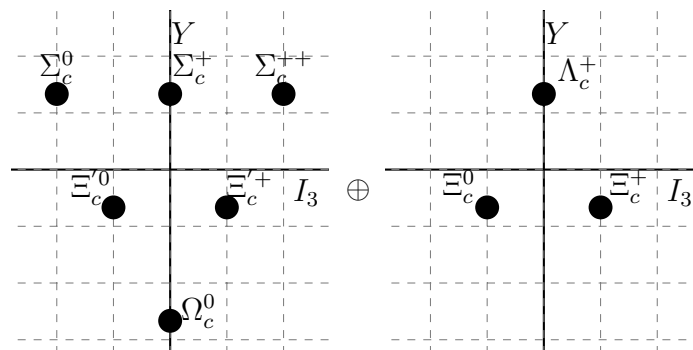


Figure 3.9: Left representation or flavour representation of $SU(3)$ sextet and anti-triplet with labels corresponding to baryons made up of a charm quark bound in the background field of a diquark in the corresponding representation.

3.4 $SU(3)$ and chiral solitons

Since we have just introduced $SU(3)$, it is worth commenting on its role in the soliton description of baryons, even though details will be provided later. In this study we will consider baryons containing heavy flavours as a heavy quark in the background of a soliton, quantised as a system of two quarks. The two quarks in the soliton can be up, down or strange, so they will still be eigenstates in the $SU(3)$ representations, under the approximation of light flavour symmetry. Figs. 3.10 and 3.11 show the $SU(3)$ sextet and anti-triplet representations for diquarks. We refer to these representations as the left (or flavour) representations, and their associated generators are the left (or flavour) generators, L_a . We have already identified the weights of the left generators with the physical quantum numbers Y and I_3 . By performing a rotation on these left generators (as will be shown in eq.(5.3.16)), we obtain the right generators, R_a . Due to the particular structure of the soliton, these are the generators of rotations in space, and therefore we can identify one of the weights of the right generators with the spin projection quantum number, $R_i = -J_i$ for $i = 1, 2, 3$. The other weight is identified with the right hypercharge, Y_R , defined as

$$Y_R = \frac{2}{\sqrt{3}}R_8. \quad (3.4.1)$$

Because these generators are related by a rotation,

$$\sum_{a=1}^8 R_a^2 = \sum_{a=1}^8 L_a^2. \quad (3.4.2)$$

Hence the multiplets will have the same weights and therefore the same representations. Fig. 3.12 shows the $SU(3)$ sextet spin representation. In section 8.1 we will see that, for heavy baryons, Y_R is constrained to be $\frac{2}{3}$ which, according to Fig. 3.12 means that the spin projection, J_3 , of the soliton must be integer valued, and therefore the soliton must be a diquark. When coupling to a heavy quark, this will lead to half-integer spin for the baryon.

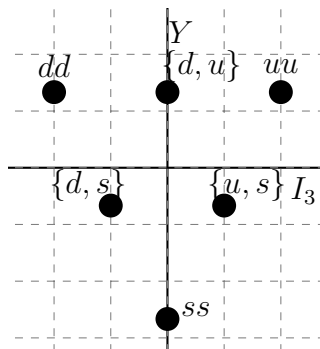


Figure 3.10: Left representation or flavour representation of $SU(3)$ sextet (**6**).

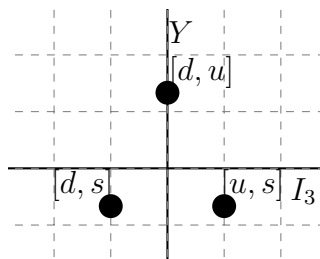


Figure 3.11: Left representation or flavour representation of $SU(3)$ anti-triplet ($\bar{\mathbf{3}}$).

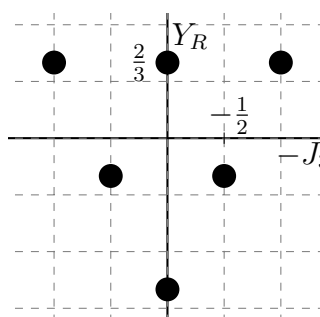


Figure 3.12: Right representation or spin representation of $SU(3)$ sextet (**6**).

Chapter 4

Skyrme Soliton Model

In this chapter we will motivate and explain the use of a soliton model in describing baryons. We will start by looking at large N_c QCD to motivate the use of solitons (in a similar way to Bhaduri (1988) and Weigel (2008)) before giving an actual Lagrangian for describing pions. Finally we will discuss the Skyrme term for producing stable solitons.

4.1 From large N_c to soliton models.

In this section, we are going to look at QCD in the large N_c limit, where N_c represents the colour degrees of freedom of the theory. We will use combinatorics to determine the leading contributions to Green's functions, which will then be used to determine some hadron properties. As we have already seen, QCD is the study of colour interactions between quarks. Each quark has a single colour charge. The gauge boson responsible for this interaction carries two colour charges. One couples to the quark, and the other to the anti-quark. Therefore, when calculating the combinatorics of Feynmann diagrams, we can consider the gluons as quark anti-quark pairs, and draw gluon lines as double lines for the quark anti-quark pair as in figure 4.1.

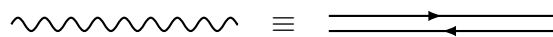


Figure 4.1: Gluon Feynmann and double line diagram.

As a first step we look at the diagram of the gluon self interaction in figure 4.2. This diagram must be of the order unity to establish a converging $1/N_c$ expansion. As usual each three-gluon vertex contributes g_{QCD} (QCD coupling constant), and each four-gluon vertex contributes g_{QCD}^2 to the diagram. While the colours of the outer quark line in the loop are determined by the gluon, the inner loop has an undetermined colour which must be summed over. Hence

this loop contributes a factor N_c . In order for the diagram to be of the order unity then,

$$g_{\text{QCD}} = \mathcal{O}\left(\frac{1}{\sqrt{N_c}}\right). \quad (4.1.1)$$

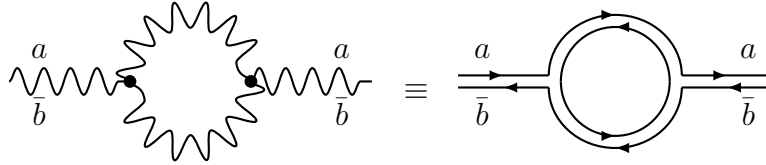


Figure 4.2: Gluon self interaction Feynmann and double line diagram.

We can now compute the combinatorial factors of other Feynmann diagrams. Two similar sets of diagrams are shown in figure 4.3, but the upper one is planar, and the lower one is not, because the upper diagram has an extra four gluon vertex in the middle. In the double line notation, it is clear that the planar case has four undetermined colour loops, as opposed to only one in the non-planar case. In the planar case, the vertices result in a factor g_{QCD}^8 which, together with the four colour loops, means the diagram is $\mathcal{O}(N_c^0)$. In the non-planar diagram, the vertices result in a factor g_{QCD}^6 , but since there is only one colour loop the diagram is $\mathcal{O}(1/N_c^2)$. This result can be generalised so that, for large N_c , all non-planar diagrams are suppressed.

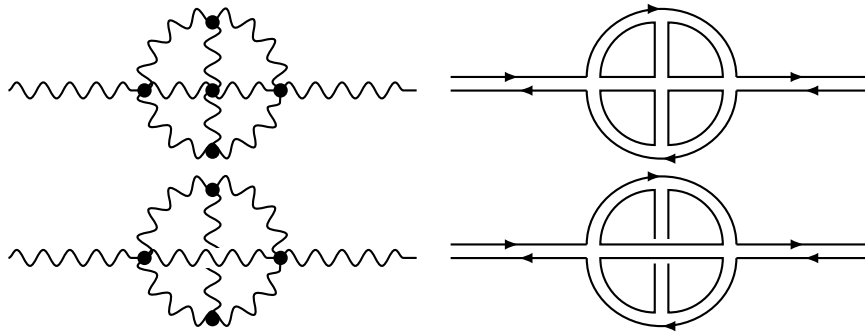


Figure 4.3: Planar and non-planar gluon self-interaction diagram.

4.1.1 Equivalence to effective meson theory

In order to discuss properties of hadrons, we will need matrix elements of colour singlet quark bilinears, like $\bar{q}\gamma_\mu q$ and $\bar{q}(i\partial_\mu - g_{\text{QCD}}A_\mu)q$. Hence we need to consider Feynmann diagrams that these quark bilinears can couple to. Fig.

4.4 shows the general form of the necessary Feynmann diagrams, to leading order, as well as the double line notation version of it.

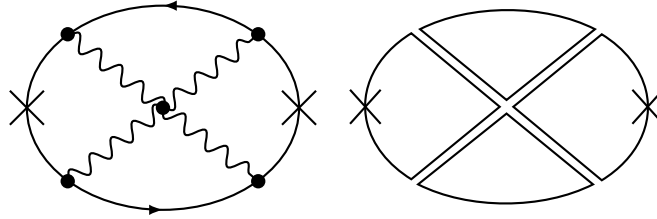


Figure 4.4: Quark bilinear coupling to loops in QCD. Coupling points are indicated by “ \times ”.

The following properties are required for all these leading order diagrams (see Witten (1979)):

1. All internal lines consist of gluons.
2. All diagrams are planar.
3. Only quark lines run along the edges.

All diagrams that satisfy these conditions, scale as N_c . In order to consider intermediate states between the quark bilinears, we can cut through the diagram at any point. Due to the fact that there are no internal quark lines and all the gluon lines are in the same plane, the colour indices along any cut are combined in a single trace. Therefore, in the large- N_c limit, all intermediate states are quark bilinear colour singlets i.e. mesons.

We can consider a diagram with two meson operators a or a^\dagger inserted. Since the diagram is of $\mathcal{O}(N_c)$, the matrix element of a (or a^\dagger) is $\mathcal{O}(\sqrt{N_c})$. Any interaction of n mesons is described by n such operators times the vertex function. This product must again be $\mathcal{O}(N_c)$. Hence the vertex is $\mathcal{O}(N_c^{1-n/2})$. In particular, the coupling constant for meson-meson scattering ($n = 4$) is suppressed as $1/N_c$. Along with the fact that the meson mass is unaffected at large N_c , this means that mesons will be stable and non-interacting at large N_c . Therefore, at large N_c , QCD may be seen as a theory of weakly coupled mesons (see Hooft (1974) and Witten (1979)).

4.1.2 Hadron Mass in large N_c

Let us now look at hadrons in the large N_c limit. Since a meson consists of a quark anti-quark pair, the number of colours doesn't affect the meson masses. For the baryon to be a colour singlet though, it must contain N_c quarks. If we

assume the mass of every quark to be m_q , the contribution to the total mass of the baryon from only the masses of the individual quarks, is $m_q N_c$.

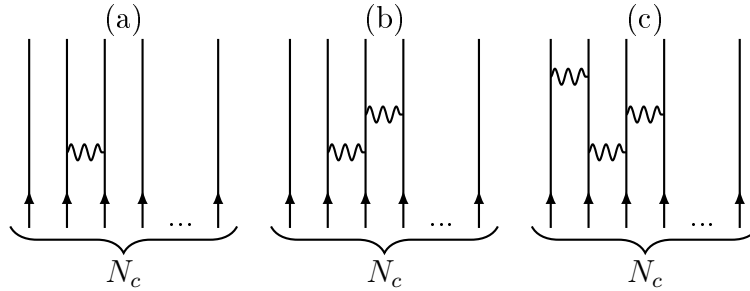


Figure 4.5: Gluon exchange between linked quark pairs inside a baryon.

Next we consider a single quark pair interaction by gluon exchange as shown in (a) of figure 4.5. There are two vertices so together they contribute a factor $1/N_c$. The choice of which pair interacts, gives a factor $\frac{1}{2}N_c(N_c - 1)$, so the total contribution from the single pair interaction is proportional to N_c . In (c) in figure 4.5 there are six vertices and four quarks to choose, so the contribution is $\frac{1}{N_c^3} \times N_c^4$ which is proportional to N_c once again. The same holds for more quark pair interactions. Notice that in all three diagrams in figure 4.5, the interactions are all linked to form a cluster of interacting quarks. If we want to look at interactions that are not linked, like in figure 4.6, summing over these to all orders means that they end up not contributing to the energy, so the only contribution comes from the linked quark clusters. Therefore the mass of the baryon, M_B is proportional to N_c . This also means that

$$M_B \propto g_{\text{QCD}}^{-2}. \quad (4.1.2)$$

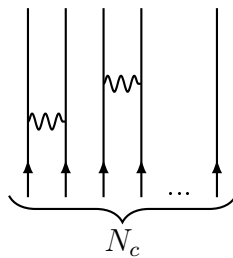


Figure 4.6: Gluon exchange between non-linked quark pairs inside a baryon.

Furthermore, soliton-like states with masses that go inversely as the coupling strength may emerge from such a theory. Witten (1979) further conjectured that baryons may be considered as such soliton states. We will use this picture to build baryons as solitons in an effective meson theory.

4.1.3 Hadron Interaction in large N_c

We will see how hadron interactions depend on N_c by first looking at baryon baryon interactions. Since baryons are colour singlets, there cannot be a gluon exchange between two of them, without an accompanying quark exchange. Figure 4.7 shows this. The two vertices together contribute $1/N_c$. Then one also needs to choose the quark from each baryon, so that contributes N_c for each baryon. In total then, the baryon baryon interaction is proportional to N_c to leading order.

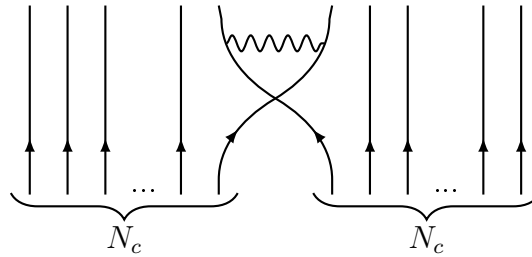


Figure 4.7: Baryon baryon interaction through the exchange of a single quark and gluon.

Baryon meson interactions are similar and figure 4.8 shows this. Again the two vertices contribute $1/N_c$ and the meson can interact with any one of the N_c quarks in the baryon. Since the meson is also a colour singlet, its wave function contains

$$|1\rangle_c = \frac{1}{\sqrt{N_c}} \sum_i^{N_c} (q\bar{q}). \quad (4.1.3)$$

which gives a factor $\sqrt{N_c}$. Putting things together then, the baryon meson interaction goes like,

$$\frac{1}{N_c} \times N_c \times \sqrt{N_c} = \sqrt{N_c}. \quad (4.1.4)$$

In the large N_c limit baryon-meson interactions are then only moderately strong, compared to baryon-baryon interactions.

In fact, in nuclear physics interactions between nucleons is not considered to be an exchange of gluons, but rather an exchange of mesons. According to what we have just seen about meson-baryon interactions, there will be a $\sqrt{N_c}$ contribution from each nucleon interacting with the meson, which gives a total contribution of N_c so large N_c QCD agrees with this picture of nucleon nucleon interactions. Again, the scaling behaviour in the large- N_c limit, corresponds

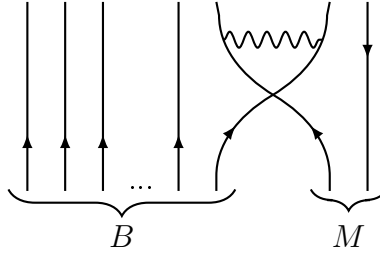


Figure 4.8: Baryon meson interaction through the exchange of a single quark and gluon.

to that of a soliton model with coupling constant proportional to $1/N_c$ and masses being scattering fluctuations about the soliton.

Staying with hadrons in large N_c , Ioffe and Shifman (1982) found that the nucleon mass goes like

$$M_N^3 \sim N_c^2 \langle \bar{q}q \rangle_0. \quad (4.1.5)$$

We have already shown that the mass of baryons goes as N_c so clearly $\bar{q}q_0$, the QCD vacuum quark condensate, must also go as N_c . Assuming the relation (see Cheng and Li (1984)),

$$m_\pi^2 = -\frac{1}{f_\pi^2} \langle \bar{q}q \rangle_0 (m_u + m_d), \quad (4.1.6)$$

between the pion mass and pion decay constant, it follows that

$$f_\pi \propto \sqrt{N_c} \quad (4.1.7)$$

$$\Rightarrow f_\pi \propto \frac{1}{g_{\text{QCD}}} \quad (4.1.8)$$

This relationship enables us to encapsulate all the N_c dependence for our model in f_π , while the rest of the model is completely N_c independent. Furthermore, f_π can be determined experimentally.

4.2 Pions

Above we argued that baryons can be formed as solitons in a low energy meson theory. To construct these baryons then, we need a Lagrangian that contains all the meson degrees of freedom. As a starting point, we will consider only the two flavour situation, and then move on to three flavours to include strangeness. Hence we start with only pion degrees of freedom, but in section 5.4 we will extend the Lagrangian to include kaon degrees of freedom. We will start, therefore, with the non-linear σ -model Lagrangian,

$$\mathcal{L}_{\text{nl}\sigma} = \frac{f_\pi^2}{4} \text{tr}[\partial_\mu U \partial^\mu U^\dagger], \quad (4.2.1)$$

with

$$U = e^{i\vec{r}\cdot\vec{\pi}/f_\pi} \quad (4.2.2)$$

As we have seen earlier, this Lagrangian is chirally symmetric, but for a realistic description of hadrons, that symmetry needs to be broken. To that end we introduce a symmetry breaking term proportional to the pion mass (m_π) and pion decay constant (f_π),

$$\mathcal{L}_m = \frac{m_\pi^2 f_\pi^2}{4} \text{tr}[U + U^\dagger - 2]. \quad (4.2.3)$$

Now finding the equation of motion of $\mathcal{L} = \mathcal{L}_{\text{nl}\sigma} + \mathcal{L}_m$ will lead to the Klein Gordon equation for pions.

Upon expansion, one finds the four pion coupling to be proportional to $1/f_\pi^2$ and therefore proportional to $1/N_c$. This is in agreement with the large- N_c conclusions. Also by expansion the axial current is,

$$\vec{A}_\mu \propto f_\pi \partial_\mu \vec{\pi} + \dots \quad (4.2.4)$$

which shows that f_π is indeed the decay constant measured in the weak decay, $\pi \rightarrow \mu \bar{\nu}_\mu$, to be $f_\pi = 93$ MeV.

4.3 Skyrme term for stable solitons

According to Derrick's theorem, we need to include higher order derivative terms to ensure that the theory has stable solutions. We will show the application of the theorem here. We have not yet given any form to our field, $U(\vec{r})$, but let us assume that it is stable. If that is the case, the energy, E must be at least a local minimum or maximum.

$$E = - \int d^3r \mathcal{L}(U) \quad (4.3.1)$$

$$E[U] = - \int d^3r (\mathcal{L}_{\text{nl}\sigma}(U) + \mathcal{L}_m(U)). \quad (4.3.2)$$

Now we introduce a new field with a scalar factor,

$$U_s = U(\lambda \vec{r}) \quad (4.3.3)$$

Since $E[U]$ is an extremum, $E[U_s]$ must be an extremum at $\lambda = 1$,

$$\left. \frac{\partial E[U_s]}{\partial \lambda} \right|_{\lambda=1} = 0 \quad (4.3.4)$$

Let us now see if this holds true when we look at eq.(4.3.2) for the new field, U_s .

$$E[U_s] = - \int d^3r (\mathcal{L}_{\text{nl}\sigma}(U_s) + \mathcal{L}_m(U_s)) \quad (4.3.5)$$

$$= - \int d^3r (\mathcal{L}_{\text{nl}\sigma}(U(\lambda\vec{r})) + \mathcal{L}_m(U(\lambda\vec{r}))) \quad (4.3.6)$$

$$= - \int d^3r \left(\frac{f_\pi^2}{4} \text{tr}[\partial_r U \partial_r U^\dagger] + \frac{m_\pi^2 f_\pi^2}{4} \text{tr}[U + U^\dagger - 2] \right). \quad (4.3.7)$$

Next we perform a change of variable,

$$\vec{s} = \lambda\vec{r}. \quad (4.3.8)$$

This changes eq.(4.3.7) into,

$$E[U_s] = - \frac{1}{\lambda^3} \int d^3s \left(\frac{f_\pi^2}{4} \lambda^2 \text{tr}[\partial_s U \partial_s U^\dagger] + \frac{m_\pi^2 f_\pi^2}{4} \text{tr}[U + U^\dagger - 2] \right) \quad (4.3.9)$$

$$= \frac{1}{\lambda} E_{\text{nl}\sigma}[U] + \frac{1}{\lambda^3} E_m[U], \quad (4.3.10)$$

where $E_{\text{nl}\sigma}$ and E_m are non-negative. We can now look at the derivative in eq.(4.3.4),

$$\frac{\partial E[U_s]}{\partial \lambda} = - \frac{1}{\lambda^2} E_{\text{nl}\sigma} - \frac{3}{\lambda^4} E_m \quad (4.3.11)$$

$$\left. \frac{\partial E[U_s]}{\partial \lambda} \right|_{\lambda=1} = -(E_{\text{nl}\sigma} + 3E_m), \quad (4.3.12)$$

but

$$0 \neq -(E_{\text{nl}\sigma} + 3E_m) \quad (4.3.13)$$

$$\neq \left. \frac{\partial E[U_s]}{\partial \lambda} \right|_{\lambda=1} \quad (4.3.14)$$

This contradicts eq.(4.3.4) which means that our assumption that a stable solution exists, must have been incorrect. One can see by inspection, that including a term with a fourth or higher order in the derivative will result in eq.(4.3.12) changing to something like

$$\left. \frac{\partial E[U_s]}{\partial \lambda} \right|_{\lambda=1} = -(E_{\text{nl}\sigma} + 3E_m - E_{\text{Sk}}), \quad (4.3.15)$$

which can be zero, even though all individual E 's are non-negative. To that end, the four derivative term,

$$\mathcal{L}_{\text{Sk}} = \frac{1}{32e_{\text{sk}}^2} \text{tr}([\alpha_\mu, \alpha_\nu][\alpha^\mu, \alpha^\nu]), \quad (4.3.16)$$

$$\alpha_\mu = U^\dagger \partial_\mu U, \quad (4.3.17)$$

was suggested by Skyrme (1961). In eq.(4.3.16), e_{sk} is a free parameter that can, in principle, be determined from $\pi\pi$ scattering data, although this has not yet been done satisfactorially. Eq.(4.3.16) contains a $\pi\pi$ scattering vertex, which is proportional to $1/(e_{\text{sk}}f_\pi^4)$. From this we can deduce that $e_{\text{sk}} \propto \frac{1}{\sqrt{N_c}}$.

We now have the Lagrangian for our Skyrme model soliton, often called a Skyrmion.

$$\mathcal{L} = \mathcal{L}_{\text{nl}\sigma} + \mathcal{L}_m + \mathcal{L}_{\text{Sk}}. \quad (4.3.18)$$

Thus far we have not placed any restrictions on the field, U , so we can choose a field with high symmetry. The field we will be using is of hedgehog type (see Pauli (1946)),

$$U(r) = U_0(r) = e^{i\tau \cdot \hat{r}F(r)}. \quad (4.3.19)$$

Here $F(r)$ is the chiral angle. Now we can write down the classical energy functional,

$$E_{\text{cl}}(F(r)) = - \int d^3r (\mathcal{L}_{\text{nl}\sigma} + \mathcal{L}_m + \mathcal{L}_{\text{Sk}}) \quad (4.3.20)$$

$$= f_\pi^2 \int_0^\infty dr 4\pi r^2 \left\{ \left(\frac{F'^2}{2} + \frac{\sin^2 F}{r^2} \right) + m_\pi^2 (1 - \cos F) + \frac{1}{e_{\text{sk}}^2 f_\pi^2} \frac{\sin^2 F}{r^2} \left(F'^2 + \frac{\sin^2 F}{2r^2} \right) \right\}. \quad (4.3.21)$$

In order to simplify matters, we can introduce dimensionless quantities,

$$x = r e_{\text{sk}} f_\pi \quad (4.3.22)$$

$$\mu_\pi = \frac{m_\pi}{e_{\text{sk}} f_\pi}. \quad (4.3.23)$$

Now the classical energy functional is given by:

$$E_{\text{cl}}[F(x)] = \frac{2\pi f_\pi}{e_{\text{sk}}} \int_0^\infty dx \left\{ x^2 F'^2 + 2 \sin^2 F + 2\mu_\pi^2 x^2 (1 - \cos F) + \sin^2 F \left(2F'^2 + \frac{\sin^2 F}{x^2} \right) \right\} \quad (4.3.24)$$

In view of the above explained scaling laws, it is obvious that E_{cl} is of the order N_c , in agreement with the results of large- N_c QCD. It should be noted that F' denotes the derivative of $F(x)$ with respect to x . We now use the variational principle to obtain a second order differential equation for the stationary solution of F .

$$F'' = \frac{\left(\mu_\pi^2 x^2 \sin F - \sin 2F (F'^2 - 1 - \frac{\sin^2 F}{x^2}) - 2xF' \right)}{(x^2 + 2 \sin^2 F)} \quad (4.3.25)$$

Eq.(4.3.25) can be solved numerically with the appropriate boundary conditions ($F(0) = \pi$ and $F(\infty) = 0^1$) to obtain the chiral angle as in figure (4.9). Notice that for the figure we have changed back to the dimensionful quantities.

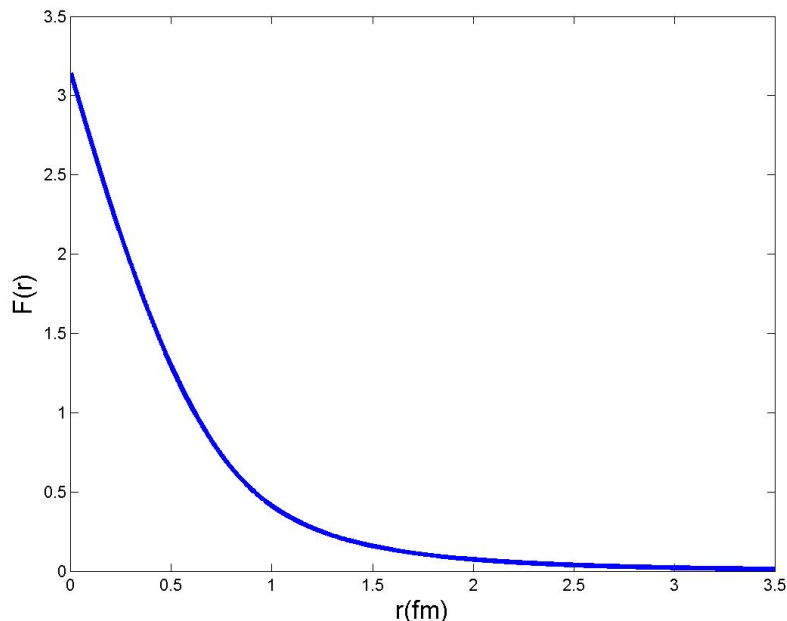


Figure 4.9: Chiral angle as a function of radius with $e_{sk} = 4.25$, $m_{\pi} = 138\text{MeV}$ and $f_{\pi} = 93\text{MeV}$.

Now the integral for the classical energy functional can be solved numerically and the result is $E_{cl} = 1.65$ GeV. According to the theory then, 1.65 GeV is the lower limit to the mass of the nucleon. The actual mass of the nucleon is 0.939 GeV, though. This raises an issue that is shared among theories of this kind, which hope to predict the masses of baryons. Most of these theories will overestimate the masses of the particles they are trying to describe. The problem is, that there are quantum corrections to the classical masses we are trying to predict. Unfortunately though, the Skyrme model is non-renormalisable, and therefore the quantum corrections cannot be calculated unambiguously. Fortunately though, these corrections should be the same for all baryons and therefore we can eliminate this problem by focusing on calculating the differences between their masses, rather than their absolute masses.

¹The origin and consequence of these boundary conditions will be discussed in section 5.2.1

Chapter 5

Skyrmion Quantisation

Thus far we have not assigned any quantum numbers to our soliton. Furthermore, the soliton spontaneously breaks rotation and flavour symmetry in reality. These need to be taken into account in our theory. Since we are dealing with a field theory though, there are an infinite number of degrees of freedom, so we introduce collective coordinates in the form of Euler angles to quantise the most important modes. We will first quantise the soliton in flavour SU(2) before moving on to flavour SU(3) in order to accommodate a third flavour, i.e. strangeness. Finally we will introduce symmetry breaking, since the mass of the strange quark is much greater than that of the up and down quarks¹.

5.1 SU(2)

Adkins *et al.* (1983) quantised the two-flavour soliton as a rigid rotator. In order to do this, they introduced time-dependent SU(2) matrices to construct a time-dependent configuration of the hedgehog field. We parametrise these matrices by three time dependent Euler angles,

$$A(t) = e^{i\Phi(t)\frac{\tau_3}{2}} e^{i\Theta(t)\frac{\tau_2}{2}} e^{i\Psi(t)\frac{\tau_3}{2}} \quad (5.1.1)$$

$$U(x, t) = A(t)U_0(x)A^\dagger(t), \quad (5.1.2)$$

where τ_i represent the Pauli matrices,

$$\tau_1 = \begin{pmatrix} 0 & 1 \\ 1 & 0 \end{pmatrix}, \quad \tau_2 = \begin{pmatrix} 0 & -i \\ i & 0 \end{pmatrix}, \quad \tau_3 = \begin{pmatrix} 1 & 0 \\ 0 & -1 \end{pmatrix}, \quad (5.1.3)$$

and Φ , Θ and Ψ are the Euler angles we use as our collective coordinates. Substituting eq.(5.1.2) into our Lagrangian results in the Lagrange function of the rigid rotator,

$$L = \frac{1}{2}\alpha^2[F]\vec{\Omega} \cdot \vec{\Omega} - E_{\text{cl}}[F], \quad (5.1.4)$$

¹We will however, still maintain isospin symmetry.

where α^2 is a moment of inertia and $\vec{\Omega}$ is an angular velocity.

$$\alpha^2 = \frac{8\pi}{3} \int_0^\infty dr r^2 \sin^2 F \left\{ f_\pi^2 + \frac{1}{e_{\text{sk}}^2} \left(F'^2 + \frac{\sin^2 F}{r^2} \right) \right\} \quad (5.1.5)$$

$$\vec{\Omega} = -i \operatorname{tr}[A^\dagger(t)\dot{A}(t)\vec{\tau}]. \quad (5.1.6)$$

If A was not time dependent, we would simply have $L = -E_{\text{cl}}$, but since A is time dependent, it leads to terms containing two time derivatives, hence the Ω^2 term. With $e_{\text{sk}} = 4.25$ and $m_\pi = 138$ MeV, one finds numerically that $\alpha^2 = 5.11/\text{GeV}$. Substituting eq.(5.1.6) into eq.(5.1.4) and writing it out in terms of the Euler angles yields

$$L = \frac{1}{2}\alpha^2[F](\dot{\Phi}^2 + \dot{\Theta}^2 + \dot{\Psi}^2 + 2\cos\Theta\dot{\Phi}\dot{\Psi}) - E_{\text{cl}}[F]. \quad (5.1.7)$$

Now we quantise eq.(5.1.7) by substituting it into the Hamiltonian according to Lee (1982):

$$\frac{1}{2}\dot{\xi}_i g_{ij}(\xi)\dot{\xi}_j \rightarrow -\frac{1}{2\sqrt{g}}\frac{\partial}{\partial\xi_i}(g^{-1})_{ij}\sqrt{g}\frac{\partial}{\partial\xi_j} \quad (5.1.8)$$

$$g = \det(g_{ij}). \quad (5.1.9)$$

In our case

$$\xi_i = (\Phi, \Theta, \Psi), \quad (5.1.10)$$

$$(g_{ij}) = \alpha^2 \begin{pmatrix} 1 & 0 & \cos\Theta \\ 0 & 1 & 0 \\ \cos\Theta & 0 & 1 \end{pmatrix} \quad (5.1.11)$$

$$\Rightarrow H = -\frac{1}{2\alpha^2} \left\{ \frac{1}{\sin\Theta} \frac{\partial}{\partial\Theta} \sin\Theta \frac{\partial}{\partial\Theta} + \frac{1}{\sin^2\Theta} \left(\frac{\partial^2}{\partial\Phi^2} + \frac{\partial^2}{\partial\Psi^2} - 2\cos\Theta \frac{\partial^2}{\partial\Phi\partial\Psi} \right) \right\} + E_{\text{cl}}. \quad (5.1.12)$$

Now we see that the differential operator in H is just the spin operator for the Wigner D-function,

$$H D_{mm'}^j(\Phi, \Theta, \Psi) = \left(E_{\text{cl}} + \frac{j(j+1)}{2\alpha^2} \right) D_{mm'}^j(\Phi, \Theta, \Psi). \quad (5.1.13)$$

Eq.(5.1.13) gives us the spectrum of our Skyrmion (skyrme model soliton), but the structure of any other two flavour hedgehog soliton will be identical. The calculation and values of E_{cl} and α^2 may differ for other models though.

We have just introduced three quantum numbers j , m and m' , but we have yet to give them a physical meaning. To that end we consider

$$\vec{J} = \frac{\partial L}{\partial \vec{\Omega}} \quad (5.1.14)$$

$$= \alpha^2 \vec{\Omega} \quad (5.1.15)$$

$$= \alpha^2 \begin{bmatrix} \cos \Psi \sin \Theta \\ \sin \Psi \sin \Theta \\ \cos \Theta \end{bmatrix} \dot{\Phi} + \begin{bmatrix} -\sin \Psi \\ \cos \Psi \\ 0 \end{bmatrix} \dot{\Theta} + \begin{bmatrix} 0 \\ 0 \\ 1 \end{bmatrix} \dot{\Psi}. \quad (5.1.16)$$

We define the conjugate momenta, $P_{\xi_i} = \frac{\partial L}{\partial \xi_i}$ and rewrite \vec{J} in terms thereof,

$$P_{\Phi} = \alpha^2 (\dot{\Phi} + \dot{\Psi} \cos \Theta) \quad (5.1.17)$$

$$P_{\Theta} = \alpha^2 \dot{\Theta} \quad (5.1.18)$$

$$P_{\Psi} = \alpha^2 (\dot{\Psi} + \dot{\Phi} \cos \Theta) \quad (5.1.19)$$

$$\begin{aligned} \vec{J} &= \frac{1}{\sin \Theta} \begin{bmatrix} \cos \Psi \\ \sin \Psi \\ 0 \end{bmatrix} P_{\Phi} + \begin{bmatrix} -\sin \Psi \\ \cos \Psi \\ 0 \end{bmatrix} P_{\Theta} \\ &+ \begin{bmatrix} -\cos \Psi \cot \Theta \\ -\sin \Psi \cot \Theta \\ 1 \end{bmatrix} P_{\Psi}. \end{aligned} \quad (5.1.20)$$

We postulate canonical commutation relations between the Euler angles and their conjugate momenta, e.g.

$$[\Psi, P_{\Psi}] = i, \quad (5.1.21)$$

which leads to:

$$[J_i, J_j] = i\epsilon_{ijk} J_k. \quad (5.1.22)$$

These are exactly the commutation relations of $SU(2)$ operators. We now define a rotation operator,

$$D_{ij}(A) \equiv \frac{1}{2} \text{tr}[\tau_i A \tau_j A^\dagger], \quad (5.1.23)$$

and apply the rotation on the operators, J_i ,

$$I_i = -D_{ij} J_j. \quad (5.1.24)$$

These new operators satisfy the commutation relations:

$$[I_i, I_j] = i\epsilon_{ijk} I_k \quad (5.1.25)$$

$$[I_i, J_j] = 0. \quad (5.1.26)$$

Again they are $SU(2)$ operators.

Still, we haven't given any physical interpretation to the generators \vec{I} and \vec{J} (although the symbols used do hint at their physical interpretation). In order to do this we will construct Noether currents and charges. First let us look at the infinitesimal transformation for isospin,

$$U \rightarrow LUR^\dagger, \quad (5.1.27)$$

with $L = R$. This transformation can be written as,

$$U \rightarrow U - i\vec{\epsilon} \cdot \left[U, \frac{\vec{\tau}}{2} \right] + \dots \quad (5.1.28)$$

We now construct the conserved Noether charge as

$$\vec{I} = - \int d^3x \text{tr} \left(\frac{\partial \mathcal{L}}{\partial \vec{U}} \left[U, \frac{i}{2} \vec{\tau} \right] + \text{h.c.} \right), \quad (5.1.29)$$

which is the isospin. Here h.c. is the Hermitian conjugate. \mathcal{L} is the Lagrangian density in question. From the definitions in eqs.(5.1.2) and (5.1.6) we find

$$\dot{U} = \dot{A}U_0A^\dagger + AU_0\dot{A}^\dagger \quad (5.1.30)$$

$$= A \left[\frac{i}{2} \vec{\tau} \cdot \vec{\Omega}, U_0 \right] A^\dagger \quad (5.1.31)$$

$$= \left[\frac{i}{2} \vec{\tau} \cdot \vec{\Omega}', U \right], \quad (5.1.32)$$

where

$$\vec{\tau} \cdot \vec{\Omega}' = A\vec{\tau} \cdot \vec{\Omega}A^\dagger \quad (5.1.33)$$

and

$$\Omega_i = \Omega'_j D_{ij}. \quad (5.1.34)$$

Taking the derivative of eq.(5.1.32),

$$\frac{\partial \dot{U}}{\partial \vec{\Omega}'} = \left[\frac{i}{2} \vec{\tau}, U \right], \quad (5.1.35)$$

we get exactly the term after the derivative in eq.(5.1.29). Substituting eq.(5.1.35) in eq.(5.1.29), using the chain rule and doing the spatial integral over the Lagrange density, we get

$$\vec{I} = - \int d^3x \text{tr} \left(\frac{\partial \mathcal{L}}{\partial \vec{U}} \frac{\partial \dot{U}}{\partial \vec{\Omega}'} + \text{h.c.} \right) \quad (5.1.36)$$

$$= - \frac{\partial L}{\partial \vec{\Omega}'}. \quad (5.1.37)$$

$$(5.1.38)$$

Using eqs.(5.1.34) and (5.1.4) this reduces to,

$$\vec{I} = -D \cdot \frac{\partial L}{\partial \vec{\Omega}} \quad (5.1.39)$$

$$= -\alpha^2 D \cdot \vec{\Omega}. \quad (5.1.40)$$

Therefore \vec{I} is the generator for isospin. Now let us look at an infinitesimal coordinate rotation,

$$U \rightarrow U - \vec{\epsilon}' \cdot [i\vec{x} \times \partial, U] + \dots \quad (5.1.41)$$

Since we are using the hedgehog field, eq.(4.3.19),

$$[i\vec{x} \times \partial, U] = - \left[U, A \frac{\vec{\tau}}{2} A^\dagger \right] \quad (5.1.42)$$

$$= -D^\dagger \cdot \left[U, \frac{\vec{\tau}}{2} \right] \quad (5.1.43)$$

$$\Rightarrow \vec{J} = \frac{\partial L}{\partial \vec{\Omega}} \quad (5.1.44)$$

$$= \alpha^2 \vec{\Omega} \quad (5.1.45)$$

$$= -D^\dagger \cdot \vec{I}. \quad (5.1.46)$$

The relationship between \vec{I} and \vec{J} in eq.(5.1.46) is exactly that in eq.(5.1.24) which, together with eq.(5.1.15) shows that the \vec{J} in eq.(5.1.15) is in fact a quantity conserved because of rotational invariance, i.e. the spin. Furthermore, \vec{I} is the soliton isospin. We now have the physical quantities to go into the Wigner D-functions (eq.(5.1.13)). The wave functions of the soliton in collective coordinates are given by

$$\langle A | J = I, I_3, J_3 \rangle = \langle \Phi, \Theta, \Psi | J = I, I_3, J_3 \rangle \quad (5.1.47)$$

$$= \left[\frac{2J+1}{8\pi^2} \right]^{\frac{1}{2}} D_{I_3, -J_3}^{J=I}(\Phi, \Theta, \Psi). \quad (5.1.48)$$

The states described by the wave function in eq.(5.1.48) must have identical spin and isospin. Exactly this property is a feature of nucleons and the Δ 's, the most prominent baryons in the up-down sector. Here the identification arose from the hedgehog structure of the soliton, which allows us to phrase isospin rotations as ordinary rotations.

Now that we have established that using collective coordinates is a sensible step that leads to physical states in SU(2), we can move on to the more relevant SU(3) case in order to obtain a more realistic description of baryons as solitons.

5.2 Wess-Zumino term

Before we can actually move on to the $SU(3)$ case, we need to look at an important non-local contribution to the action: The Wess-Zumino term. In $SU(2)$, it only contributes when gauged by (external) vector fields. This gauge principle is a convenient construction procedure to find the coupling of vector fields, like the photon, to the chiral field, U . The linear coupling to such vector fields determines the currents. We particularly require the singlet vector field, from whose coupling we determine the baryon number, B , carried by the considered field configuration, $U(\vec{x}, t)$. In $SU(3)$ the Wess-Zumino term is crucial for the quantization procedure. Most importantly, it enforces configurations with unit baryon number to be quantized as fermions. Since our soliton description is an effective meson theory, based on pions and kaons, we will use Witten's argument (see Witten (1983)), for including the Wess-Zumino term, which relies on their pseudoscalar nature.

The parts in our Lagrangian thus far are invariant under parity transformations,

$$t \rightarrow t \quad (5.2.1)$$

$$\vec{x} \rightarrow -\vec{x}. \quad (5.2.2)$$

The symmetry here is too much, though. Because this is a pseudoscalar field theory, the basic fields should transform as

$$\begin{aligned} \vec{\pi}(\vec{x}, t) &\rightarrow -\vec{\pi}(-\vec{x}, t) \\ &\Leftrightarrow \\ U(\vec{x}, t) &\rightarrow U^\dagger(-\vec{x}, t). \end{aligned} \quad (5.2.3)$$

The theory, as a whole, should only be invariant under both the transformations in eqs.(5.2.2) and (5.2.3) together. There is no local Lagrangian that can accomplish this in 3+1 dimensions, because any such candidate would contain the Levi-Cevita tensor, but

$$\epsilon_{\mu\nu\rho\sigma} \text{tr}[\alpha^\mu \alpha^\nu \alpha^\rho \alpha^\sigma] = 0. \quad (5.2.4)$$

Witten (1983) suggested adding a 5 dimensional integral to the meson action,

$$\Gamma_{\text{WZ}} = i\lambda \epsilon_{\mu\nu\rho\sigma\tau} \int_{M_5} d^5x \text{tr}[\alpha^\mu \alpha^\nu \alpha^\rho \alpha^\sigma \alpha^\tau]. \quad (5.2.5)$$

Here the boundary of the manifold, M_5 , is just the 4 dimensional Minkowski space. Now we want to use the variational principle to obtain the equations of motion for the pseudoscalar fields. One possible way to vary the field is by,

$$U(x) \rightarrow U(x)e^{i\epsilon(x)}. \quad (5.2.6)$$

To linear order this corresponds to,

$$\alpha_\mu \rightarrow \alpha_\mu + i\partial_\mu \epsilon + \dots \quad (5.2.7)$$

Due to the global axial symmetry, the terms without derivatives of ϵ will cancel, hence they are omitted. Since we are only interested in the parity properties, we will only consider the combination of the non-linear sigma model with the Wess-Zumino term for now,

$$\Gamma = \int d^4x \mathcal{L}_{\text{nl}\sigma} + \Gamma_{\text{WZ}}. \quad (5.2.8)$$

We use the variational principle on eq.(5.2.8) and then apply the fact that

$$\epsilon_{\mu\nu\rho\sigma} \alpha^\mu \alpha^\nu \alpha^\rho \alpha^\sigma = \epsilon_{\mu\nu\rho\sigma} \partial^\mu (\alpha^\nu \alpha^\rho \alpha^\sigma), \quad (5.2.9)$$

as well as Stoke's theorem to find,

$$\begin{aligned} \delta\Gamma &= \frac{f_\pi^2}{2} \int_{M_4} d^4x \text{tr}[i\alpha_\mu \partial^\mu \epsilon] + 5i\lambda \epsilon_{\mu\nu\rho\sigma\tau} \int_{M_5} d^5x \text{tr}[(i\partial^\mu \epsilon) \alpha^\nu \alpha^\rho \alpha^\sigma \alpha^\tau] \\ &= \frac{f_\pi^2}{2} \int_{M_4} d^4x \text{tr}[i\alpha_\mu \partial^\mu \epsilon] + 5i\lambda \epsilon_{\mu\rho\sigma\tau} \int_{M_4} d^4x \text{tr}[(i\partial^\mu \epsilon) \alpha^\rho \alpha^\sigma \alpha^\tau] \end{aligned} \quad (5.2.10)$$

$$= \int_{M_4} d^4x \left\{ \frac{f_\pi^2}{2} \text{tr}[i\alpha_\mu \partial^\mu \epsilon] + 5i\lambda \epsilon_{\mu\rho\sigma\tau} \text{tr}[(i\partial^\mu \epsilon) \alpha^\rho \alpha^\sigma \alpha^\tau] \right\}. \quad (5.2.11)$$

This yields the following equations of motion:

$$\frac{f_\pi^2}{2} \partial_\mu \alpha^\mu + 5i\lambda \epsilon_{\mu\nu\rho\sigma} \alpha^\mu \alpha^\nu \alpha^\rho \alpha^\sigma = 0. \quad (5.2.12)$$

Now we see that the first term² in the equations of motion is odd in α^μ , but the second term is even. In this case the parity transformation eq.(5.2.3) turns into

$$\alpha_\mu \rightarrow -U \alpha_\mu U^\dagger \quad (5.2.13)$$

$$\Leftrightarrow$$

$$\partial_\mu \alpha^\mu \rightarrow -U \partial_\mu \alpha^\mu U^\dagger. \quad (5.2.14)$$

Performing this transformation on eq.(5.2.12) results in a relative sign, but so does the transformation in eqs.(5.2.1) and (5.2.2). Because there is an odd number of spatial derivatives in the second term of eq.(5.2.12), they cancel each other. Therefore the Wess-Zumino term successfully enforces the pseudoscalar nature of the Goldstone bosons in our effective meson theory.

²Even though we only included the non-linear sigma model in this argument, the same holds for the other terms in eq.(4.3.18).

5.2.1 Baryon number current

In order to specify λ in eq.(5.2.12), we need to look at the topological structure of the Wess-Zumino action. There is a manifold \bar{M}_5 , complimentary to M_5 which has the same boundary, M_4 . Since the physics must not be changed whether we choose M_5 or \bar{M}_5 to calculate the Wess-Zumino term, we demand that,

$$i\lambda\epsilon_{\mu\nu\rho\sigma\tau}\int_{M_5\cup\bar{M}_5}d^5x\text{tr}[\alpha^\mu\alpha^\nu\alpha^\rho\alpha^\sigma\alpha^\tau]=2\pi m, \quad (5.2.15)$$

where m is a non-zero³ integer as it leaves $e^{i\Gamma_{\text{wz}}}$ in the path integral invariant. Now $M_5\cup\bar{M}_5$ is compact and isomorphic to the symmetric group of degree five, \mathbb{S}_5 , because we evaluate the generating functional with initial and final time steps identified. If we define.

$$j_\mu(x)=\frac{i}{2\pi}\frac{1}{240\pi^2}\epsilon_{\mu\nu\rho\sigma\tau}\text{tr}[\alpha^\mu\alpha^\nu\alpha^\rho\alpha^\sigma\alpha^\tau], \quad (5.2.16)$$

then eq.(5.2.15) is proportional to,

$$Q=\int_{\mathbb{S}_5}d^5x\ j_0. \quad (5.2.17)$$

By construction, $j_\mu(x)$ is the winding number current for a mapping of \mathbb{S} onto $SU(3)$. Since j_μ will have zero divergence, Q is conserved. In fact, Q is actually an integer and therefore eq.(5.2.15) constrains λ to,

$$\lambda=\frac{m}{240\pi^2} \quad (5.2.18)$$

According to C.4 in Appendix C of Weigel (2008), the integer, m , must be identified with the number of colour degrees of freedom, N_C , because the Wess-Zumino term is used to compute the decay width of the π^0 , which depends on N_C . Furthermore, as described in the same appendix, the baryon number current is given by,

$$B_\mu=\frac{1}{24\pi^2}\epsilon_{\mu\nu\rho\sigma}\text{tr}[\alpha^\nu\alpha^\rho\alpha^\sigma], \quad (5.2.19)$$

and it is the topological current for the mapping $\mathbb{S}_3\rightarrow SU(2)$ in the form of a winding number. Substituting the hedgehog field in eq.(4.3.19) into eq.(5.2.19) results in:

$$B_\mu=-g_{\mu 0}F'\frac{\sin^2 F}{2\pi^2}. \quad (5.2.20)$$

Imposing boundary conditions on F such that $F(\infty)=0$ and $F(0)=n\pi$ will yield integer baryon number, $B=n$. In our work with baryons then, we need $B=1$ and therefore $F(0)=\pi$.

³The trivial solution $m=0$ would completely remove the Wess-Zumino term which we need.

5.3 SU(3)

In this section we will quantise the soliton in the flavour symmetric SU(3) case. Of course this flavour symmetry is not realistic, so it will be explicitly broken later on. One important difference between the SU(3) and SU(2) case is that, in the SU(3) case, the Wess-Zumino term will arise and that will force us to quantise the soliton as a spin $\frac{1}{2}$ object. It will also be very important eventually when we start looking at quantising the heavy baryon. The field we consider will still be based on the hedgehog field (eq.(4.3.19)), but it needs to be embedded in an SU(2) submanifold of SU(3). In order to yield the lowest classical energy, it must be embedded as follows⁴:

$$U(\vec{x}) = U_0(\vec{x}) = \begin{pmatrix} e^{i\vec{\tau} \cdot \hat{x} F(r)} & 0 \\ & 0 \\ 0 & 0 & 1 \end{pmatrix}. \quad (5.3.1)$$

Similar to the SU(2) case, we will define SU(3) Euler angles as follows:

$$A(t) = e^{-i\alpha \frac{\lambda_3}{2}} e^{-i\beta \frac{\lambda_2}{2}} e^{-i\gamma \frac{\lambda_3}{2}} e^{-i\nu \lambda_4} \\ \cdot e^{-i\alpha' \frac{\lambda_3}{2}} e^{-i\beta' \frac{\lambda_2}{2}} e^{-i\gamma' \frac{\lambda_3}{2}} e^{-i\rho \frac{\lambda_8}{\sqrt{3}}}, \quad (5.3.2)$$

where λ_i are the Gell-Mann matrices shown in Appendix B.1.1. We will now briefly describe the calculation of the generators of SU(3). The generators can be written as linear combinations of differential operators,

$$R_a = i d_{ba}(\alpha) \frac{\partial}{\partial \alpha_b}, \quad (5.3.3)$$

where α is a vector containing the eight Euler angles in eq.(5.3.2). All we have to do now is find the coefficients d_{ba} . To do that, we look at the defining equations of the SU(3) algebra,

$$AR_a A^\dagger = \frac{1}{2} A \lambda_a A^\dagger \quad (5.3.4)$$

$$= \frac{1}{2} \lambda_b D_{ba}(\alpha). \quad (5.3.5)$$

Here D_{ab} is defined similarly to eq.(5.1.23),

$$D_{ab}(A) \equiv \frac{1}{2} \text{tr}[\lambda_a A \lambda_b A^\dagger]. \quad (5.3.6)$$

⁴Strictly speaking, this embedding is only really forced on us when we include SU(3) symmetry breaking in section 5.4.

From eq.(5.3.3) and eq.(5.3.5) we get an expression for d_{ab} ,

$$d_{ab}(\vec{\alpha}) = (M^{-1}(\vec{\alpha}))_{ac} D_{cb}(\vec{\alpha}). \quad (5.3.7)$$

We have defined M as a matrix that contains the derivatives explicitly calculated,

$$M_{bc}(\vec{\alpha}) = \frac{1}{2} \text{tr} \left[\lambda_b A i \frac{\partial}{\partial \alpha_c} A^\dagger \right]. \quad (5.3.8)$$

Once we have these coefficients, we simply put them back into eq.(5.3.3) and calculate the generators of $SU(3)$, R_a . These are explicitly listed in Appendix D of Weigel (2008). Getting back to the soliton and physical interpretation, if we look closely at the matrix elements in eq.(5.3.2), we can see that it consists of a matrix in ν , pinched between two matrices of the same form as eq.(5.1.1) (plus a term in λ_8 at the end). This ν is the strangeness changing angle.

Now the equivalent of eq.(5.1.2) becomes

$$U(\vec{x}, t) = A(t) U_0(\vec{x}) A^\dagger(t). \quad (5.3.9)$$

Substituting this into our Lagrangian results in

$$L(A, \Omega_\alpha) = -E_{\text{cl}} + \frac{1}{2} \alpha^2 \sum_{i=1}^3 \Omega_i^2 + \frac{1}{2} \beta^2 \sum_{\alpha=4}^7 \Omega_\alpha^2 - \frac{N_c}{2\sqrt{3}} \Omega_8, \quad (5.3.10)$$

where the Ω_α are the angular velocities and α^2 and β^2 are the moments of inertia defined as follows.

$$\frac{i}{2} \sum_{\alpha=1}^8 \Omega_\alpha \lambda_\alpha = A^\dagger(t) \frac{dA(t)}{dt} \quad (5.3.11)$$

$$\alpha^2[F] = \frac{8\pi}{3} \int_0^\infty dr r^2 \sin^2 F \left[f_\pi^2 + \frac{1}{e_{\text{sk}}^2} \left(F'^2 + \frac{\sin^2 F}{r^2} \right) \right] \quad (5.3.12)$$

$$\beta^2[F] = \pi \int dr r^2 \sin^2 \frac{F}{2} \left[4f_\pi^2 + \frac{1}{e_{\text{sk}}^2} \left(F'^2 + \frac{2 \sin^2 F}{r^2} \right) \right] \quad (5.3.13)$$

The first two terms in eq.(5.3.10) are exactly the same as in the $SU(2)$ case, and again the α^2 term comes from the fact that the Skyrmion breaks rotational invariance, ie. the $SU(2)$ symmetry. Likewise, the β^2 term arises because the Skyrmion breaks the $SU(3)$ symmetry. It is important to realise that the soliton configuration in eq.(5.3.1) commutes with λ_8 , which means that the local Lagrangian will not contribute any Ω_8 terms. The only source of an Ω_8 term is the non-local Wess-Zumino term. It is also the only contribution from the Wess-Zumino term.

The right generators are defined in the usual way and result in

$$R_i = -\frac{\partial L}{\partial \Omega_i} \quad (5.3.14)$$

$$= \begin{cases} -\alpha^2 \Omega_i = J_i, & i = 1, 2, 3 \\ -\beta^2 \Omega_i, & i = 4, 5, 6, 7 \\ \frac{N_c}{2\sqrt{3}}, & i = 8 \end{cases} \quad (5.3.15)$$

These generators are the conjugates to the angular coordinates. The Wess-Zumino term is the only factor that contributes to R_8 , and that constraint in eq.(5.3.15) means that, according to eq.(3.4.1), $Y_R = 1$. Looking at the relationship between I_3 and Y described in section (3.2) and its analogy to the relationship between J_3 and Y_R described in section (3.3), $Y_R = 1$ forces the soliton to have half-integer spin when $N_c = 3$ (more generally, when N_c is odd).

Now the left generators can be found from the right generators by rotation,

$$L_i = D_{ij} R_j. \quad (5.3.16)$$

These left⁵ generators are the flavour generators for $SU(3)$. Similarly to eq.(5.3.15),

$$L_i = I_i, \quad i = 1, 2, 3, \quad (5.3.17)$$

and L_8 relates to the hypercharge, Y . Defining the Casimir operator in the usual way we can write the collective coordinate hamiltonian of our soliton as

$$H_{SU(3)} = E_{cl} + \frac{1}{2} \left(\frac{1}{\alpha^2} - \frac{1}{\beta^2} \right) \mathbf{J}^2 + \frac{1}{2\beta^2} C_2 - \frac{N_c^2 B^2}{24\beta^2} \quad (5.3.18)$$

$$C_2 = \sum_{a=1}^8 R_a^2 = \sum_{a=1}^8 L_a^2. \quad (5.3.19)$$

The last term in eq.(5.3.18) comes from the Wess-Zumino term where N_c is again the number of colours and B is the baryon number, discussed in section 5.2.1. This is still a fully symmetric $SU(3)$ hamiltonian and the energy eigenvalues of the equation

$$C_2 \Psi = \mu \Psi \quad (5.3.20)$$

are just the known $SU(3)$ eigenvalues that can be calculated as follows:

$$\mu_{SU(3)} = p^2 + q^2 + pq + 3p + 3q \quad (5.3.21)$$

⁵The notation reflects that R_a acts like a right multiplication with $\frac{\lambda^a}{2}$ on A , while L acts as a left multiplication.

where p and q are the highest weights, of the $SU(3)$ irreps, described in chapter 3. The wave function Ψ is a function of the strangeness changing angle, ν , pinched between two $SU(2)$ Wigner D-functions (see Yabu and Ando (1988)),

$$\begin{aligned} \Psi(I, I_3, Y; J, J_3, Y_R) &= \sum_{M_L, M_R} D_{I_3, M_L}^{(I)*}(\alpha, \beta, \gamma) f_{M_L, M_R}^{(I, Y; J, Y_R)}(\nu) \\ &\times e^{iY_R \rho} D_{M_R, -J_3}^{(J)*}(\alpha', \beta', \gamma'), \end{aligned} \quad (5.3.22)$$

where the sums over M_L and M_R run from $-I$ to I and $-J$ to J respectively and are further constrained by,

$$M_L - M_R = \frac{(Y - Y_R)}{2}. \quad (5.3.23)$$

In eq.(5.3.22), $f(\nu)$ is referred to as the intrinsic function. We list some of these functions here for the pure $SU(3)$ case with $\mu = 3$ and $Y_R = 1$ (see Weigel (2008)):

$$\begin{aligned} N : f_{\frac{1}{2}, \frac{1}{2}}^{\frac{1}{2}, 1; \frac{1}{2}, 1}(\nu) &= \cos^2 \nu \\ N : f_{-\frac{1}{2}, -\frac{1}{2}}^{\frac{1}{2}, 1; \frac{1}{2}, 1}(\nu) &= \cos \nu \\ \Sigma : f_{0, \frac{1}{2}}^{1, 0; \frac{1}{2}, 1}(\nu) &= \frac{1}{\sqrt{2}} \cos \nu \sin \nu \\ \Sigma : f_{-1, -\frac{1}{2}}^{1, 0; \frac{1}{2}, 1}(\nu) &= \sin \nu \\ \Lambda : f_{0, \frac{1}{2}}^{0, 0; \frac{1}{2}, 1}(\nu) &= \sqrt{\frac{3}{2}} \cos \nu \sin \nu \\ \Xi : f_{-\frac{1}{2}, \frac{1}{2}}^{1, -1; \frac{1}{2}, 1}(\nu) &= \sin^2 \nu. \end{aligned} \quad (5.3.24)$$

Due to the collective coordinates, in principle, the hamiltonian gives rise to eight second order partial differential equations (DEQ).

5.4 Flavour Symmetry Breaking

We started with $SU(3)$ in order to have a three flavour model, those flavours being up, down and strange. Of course $SU(3)$ in itself is completely flavour symmetric. In $SU(2)$ with only up and down flavours, this symmetry is not a problem because isospin symmetry is a very good symmetry in nature. Strangeness cannot be symmetric with the other two however. This is obvious when looking at the masses of the pion and kaon of 139.6 MeV and 493.7 MeV respectively. In order to break this symmetry, we need to add a symmetry breaking term, \mathcal{L}_{sb} to our Lagrange density. We will obtain this term from the bosonisation of the quark flavour interactions, but we need to ensure that it has the same

chiral properties as the rest of the terms in the Lagrange density in eq.(4.3.18). This bosonisation is characterised by,

$$\bar{q}\hat{m}_0q = \bar{q}_L\hat{m}_0^\dagger q_R + \bar{q}_R\hat{m}_0 q_L \quad (5.4.1)$$

$$\rightarrow \hat{m}_0(M + M^\dagger), \quad (5.4.2)$$

where q represents the quark flavour spinor, \hat{m}_0 is the diagonal current quark mass matrix and M is the meson field. We can see that a chiral transformation,

$$\hat{m}_0 \rightarrow R\hat{m}_0L^\dagger \quad (5.4.3)$$

$$q_L \rightarrow Lq_L \quad (5.4.4)$$

$$q_R \rightarrow q_R R, \quad (5.4.5)$$

will leave eq.(5.4.1) invariant and so should a chiral transformation on M ,

$$M \rightarrow RML^\dagger. \quad (5.4.6)$$

In our three flavour case, with the masses of the up and down quarks being equal ($m_{0,u} = m_{0,d}$), but the strange quark mass being much greater,

$$\hat{m}_0 = \begin{pmatrix} m_{0,u} & 0 & 0 \\ 0 & m_{0,u} & 0 \\ 0 & 0 & m_{0,s} \end{pmatrix} \quad (5.4.7)$$

$$= \frac{2}{3}m_{0,u} \left(I + \frac{\sqrt{3}}{2}\lambda_8 \right) + \frac{1}{3}m_{0,s} \left(I - \sqrt{3}\lambda_8 \right) \quad (5.4.8)$$

$$= \frac{2m_{0,u} + m_{0,s}}{3}I + \frac{\sqrt{3}(m_{0,u} - m_{0,s})}{3}\lambda_8. \quad (5.4.9)$$

We are only interested in a symmetry breaking term up to linear order in \hat{m}_0 so the general form of this Lagrange density can be written as,

$$\begin{aligned} \mathcal{L}_{\text{sb}} &= \sum_i c_i \text{tr}[F_i(M, \partial_\mu M) + \text{h.c.}] \\ &\quad + \sum_i \tilde{c}_i \text{tr}[\lambda_8 \tilde{F}_i(M, \partial_\mu M) + \text{h.c.}]. \end{aligned} \quad (5.4.10)$$

Importantly, under the transformation in eq.(5.4.6), the functionals, F_i and \tilde{F}_i , must transform as

$$F_i(LMR^\dagger, \partial_\mu(LMR^\dagger)) = LF_i(M, \partial_\mu M)R^\dagger. \quad (5.4.11)$$

These functionals and their associated constant, c_i and \tilde{c}_i , can be determined from experiment, but we want a minimal set of symmetry breaking terms. Therefore we will only consider terms which describe the differences between

the pion and kaon masses, as well as between their decay constants, in such a way that expanding the Lagrange density to quadratic order will result in Klein Gordon equations for those fields. It is straightforward to verify that adding

$$\begin{aligned} \mathcal{L}_{\text{sb}} = & \frac{f_\pi^2 m_\pi^2 + 2f_K^2 m_K^2}{12} \text{tr}[U + U^\dagger - 2] \\ & + \sqrt{3} \frac{f_\pi^2 m_\pi^2 - f_K^2 m_K^2}{6} \text{tr}[\lambda_8(U + U^\dagger)] \\ & + \frac{f_K^2 - f_\pi^2}{12} \text{tr}[(1 - \sqrt{3}\lambda_8)(U\partial_\mu U^\dagger\partial^\mu U + U^\dagger\partial_\mu U\partial^\mu U^\dagger)] \end{aligned} \quad (5.4.12)$$

to the Skyrme model Lagrangian satisfies all requirements.

We now have all the building blocks of a starting point for a theory describing three-flavour baryons in $SU(3)$, in terms of an effective meson action,

$$\Gamma = \int d^4x \{ \mathcal{L}_{\text{nl}\sigma} + \mathcal{L}_m + \mathcal{L}_{\text{Sk}} + \mathcal{L}_{\text{sb}} \} + \Gamma_{\text{WZ}} \quad (5.4.13)$$

We substitute the rotating hedgehog field, eq.(5.3.9), into eq.(5.4.12) and introduce γ to simplify matters a bit.

$$L_{\text{sb}} = -\frac{1}{2}\gamma[F](1 - D_{88}(A)) \quad (5.4.14)$$

$$\begin{aligned} \gamma[F] = & \frac{4}{3} \int d^3r \left\{ (m_K^2 f_K^2 - m_\pi^2 f_\pi^2)(1 - \cos F) \right. \\ & \left. + \frac{1}{2}(f_K^2 - f_\pi^2) \cos F \left(F'^2 + \frac{2 \sin^2 F}{r^2} \right) \right\}. \end{aligned} \quad (5.4.15)$$

D_{88} is just according to the definition in eq.(5.3.6) and actually

$$D_{88} = 1 + \frac{3}{2} \sin^2 \nu, \quad (5.4.16)$$

so it depends only on ν , the strangeness changing angle. Including this new term in our eigenvalue equation induces the eigenvalue problem

$$[C_2 + \gamma\beta^2(1 - D_{88})]\Psi = \epsilon_{\text{sb}}\Psi, \quad (5.4.17)$$

which is no longer simple to solve and the eigenfunctions are no longer pure elements of $SU(3)$ irreps. However, it turns out that all angles except ν factor out, and we are left with some coupled ordinary DEQs in ν only. These can be approximated using perturbation theory, but a much simpler option is to solve them exactly in a numerical approach.

5.4.1 Numeric Calculations

In order to solve the eigenvalue equation (5.4.17), we need to look at the action of the Casimir operator on the wave function, eq.(5.3.22), which is given by

$$\begin{aligned}
C_2\Psi(I, I_3, Y; J, J_3, Y_R) &= \sum_{M_L, M_R} D_{I_3, M_L}^{(I)*}(\alpha, \beta, \gamma) e^{iY_R\rho} D_{J_3, M_R}^{(J)*}(\alpha', \beta', \gamma') \\
&\left\{ -\frac{1}{4} \left[\frac{d^2}{d\nu^2} + (3 \cot \nu - \tan \nu) \frac{d}{d\nu} \right] + \frac{I^2 + J^2}{\sin^2 \nu} + \frac{M_L^2}{\cos^2 \nu} \right. \\
&\quad + \frac{M_R^2}{4} \left(3 + \frac{1}{\cos^2 \nu} \right) - \frac{1 + \cos^2 \nu}{\sin^2 \nu \cos^2 \nu} M_L M_R + \frac{3Y_R M_L}{2 \cos^2 \nu} \\
&\quad \left. - 3 \frac{1 + \cos^2 \nu}{4 \cos^2 \nu} Y_R M_R + \left(\frac{3}{4} + \frac{9}{16} \tan^2 \nu \right) Y_R^2 \right\} f_{M_L, M_R}^{(I, Y; J, Y_R)}(\nu) \\
&- \frac{\cos \nu}{\sin^2 \nu} \sqrt{(I + M_L + 1)(I - M_L)(J + M_R + 1)(J - M_R)} f_{M_L+1, M_R+1}^{(I, Y; J, Y_R)}(\nu) \\
&- \frac{\cos \nu}{\sin^2 \nu} \sqrt{(I - M_L + 1)(I + M_L)(J - M_R + 1)(J + M_R)} f_{M_L-1, M_R-1}^{(I, Y; J, Y_R)}(\nu).
\end{aligned} \tag{5.4.18}$$

When solving the eigenvalue problem in eq.(5.3.20) using eq.(5.4.18) we find that the dependence on all the angles except ν are factorised. This fact is not altered by symmetry breaking, since we can see in eq.(5.4.16) and eq.(5.4.17) that the symmetry breaking also only depends on ν . Therefore we are left with an ordinary differential equation in ν ,

$$\begin{aligned}
0 &= \sum_{M_L, M_R} \left\{ -\frac{1}{4} \left[\frac{d^2}{d\nu^2} + (3 \cot \nu - \tan \nu) \frac{d}{d\nu} \right] - \epsilon_{sb} + \frac{I^2 + J^2}{\sin^2 \nu} + \frac{M_L^2}{\cos^2 \nu} \right. \\
&\quad + \frac{M_R^2}{4} \left(3 + \frac{1}{\cos^2 \nu} \right) - \frac{1 + \cos^2 \nu}{\sin^2 \nu \cos^2 \nu} M_L M_R + \frac{3Y_R M_L}{2 \cos^2 \nu} \\
&\quad \left. - 3 \frac{1 + \cos^2 \nu}{4 \cos^2 \nu} Y_R M_R + \left(\frac{3}{4} + \frac{9}{16} \tan^2 \nu \right) Y_R^2 \right\} f_{M_L, M_R}^{(I, Y; J, Y_R)}(\nu) \\
&- \frac{\cos \nu}{\sin^2 \nu} \sqrt{(I + M_L + 1)(I - M_L)(J + M_R + 1)(J - M_R)} f_{M_L+1, M_R+1}^{(I, Y; J, Y_R)}(\nu) \\
&- \frac{\cos \nu}{\sin^2 \nu} \sqrt{(I - M_L + 1)(I + M_L)(J - M_R + 1)(J + M_R)} f_{M_L-1, M_R-1}^{(I, Y; J, Y_R)}(\nu).
\end{aligned} \tag{5.4.19}$$

In eq.(5.4.19), the intrinsic functions $f_{M_L-1, M_R-1}^{(I, Y; J, Y_R)}(\nu)$ are still undetermined, but we can see that for different intrinsic spin and isospin quantum numbers, M_L and M_R , they depend on each other. Eq.(5.4.19) contains up to three different intrinsic functions. The total number of intrinsic functions depends on the range of M_L and M_R , which of course depends on the I and J of the specific baryon we are considering. Moreover, the number of intrinsic functions in eq.(5.4.19) for a specific set of M_L and M_R may be further limited.

For instance, if $M_L = -I$ then $-I - 1$ is not an allowable quantum number for $f(\nu)$, hence $f_{-I-1, M_R-1}^{(I, Y; J, Y_R)}(\nu)$ is non-existent. In those cases where the intrinsic function would be non-existent, the coefficient under the square root sign will be zero.

Eq.(5.4.19) also contains a first and second order derivative of one of the intrinsic functions, which means it can be re-written as an ordinary second order DEQ, or two coupled first order DEQs. Together with the limitations on the number of intrinsic functions, this gives up to six coupled first order DEQs for the quantum numbers we will be considering.⁶

In order to solve these DEQs we employ the 'shooting method' over a suitable range of ν , $[0, \frac{\pi}{2}]$, and completely independent boundary conditions for the intrinsic functions at the start and end of the range. In general, the intrinsic functions will start at either 0 or 1 (or close to them since exact zero is something one wants to avoid in numerics). Even if the 'wrong' choice is made though, the numerics will fix the intrinsic function such that, if it is made to start close to π , but the correct form requires it to start close to zero, the numerics will eventually force it into that form. At the end of the range, the boundary conditions are typically a form of power law decay. Again the exact values are not important, since the numerics will fix them. The intrinsic functions are started at these boundary conditions and then 'shot', using a Runga-Kuta method, to some matching point in the middle, where both the value of $f_{M_L-1, M_R-1}^{(I, Y; J, Y_R)}(\nu)$ and its first derivative need to match up. They will only be able to match for proper eigenvalues, so another important starting condition, is the eigenvalue, ϵ_{sb} . Using a Newton-Raphson method we can then close in on the exact eigenvalues. In the symmetric case, we can get the exact SU(3) eigenvalues, and the intrinsic functions are exactly the functions listed in eq.(5.3.24).

In order to include symmetry breaking, we need to solve eq.(5.4.17). Clearly if $\gamma\beta^2 = 0$, we are back to the symmetric case. From now on we will refer to $\gamma\beta^2$ as the symmetry breaking strength, and it is just a number. Of course we have seen definitions for both γ and β^2 earlier on, and these will be used later to determine the actual symmetry breaking strength, but for now we will consider it as just a number, in order to investigate the effect of symmetry breaking on the eigenvalue and the intrinsic functions.

Fig. 5.1 shows the effect of symmetry breaking on the intrinsic functions. Here we are looking at a spin 1 diquark that contains two intrinsic functions⁷. Table 5.1 shows the quantum numbers and SU(3) irreps of the diquarks that

⁶Looking at higher order irreps of SU(3) with higher allowable values of I and J will require solving more DEQs.

⁷The reason for looking at a diquark rather than a baryon will become clear in section

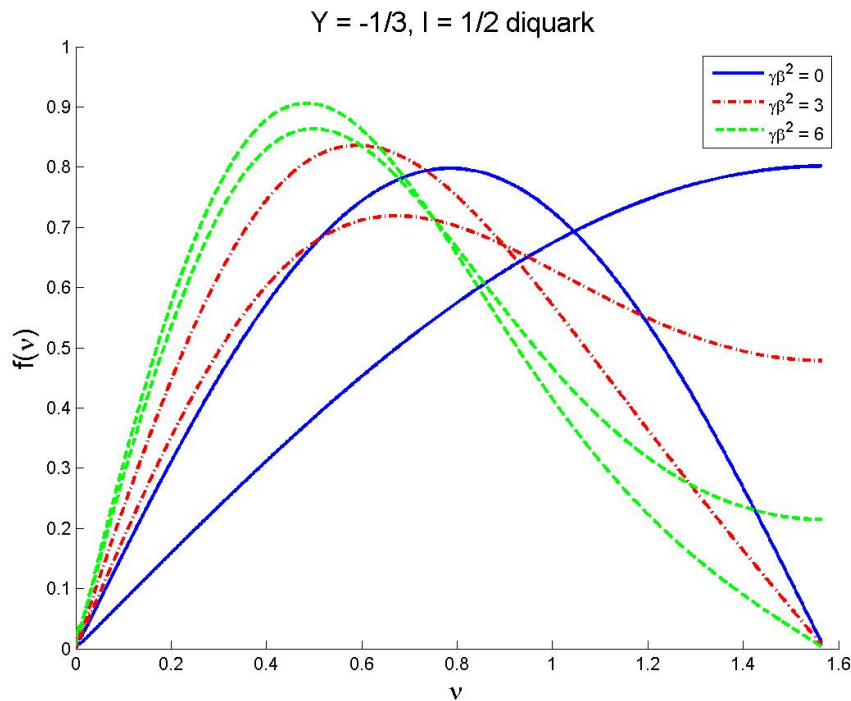


Figure 5.1: Intrinsic eigenfunctions of a spin-1 diquark, with $Y = -\frac{1}{3}$ and $I = \frac{1}{2}$, for different values of symmetry breaking strength ($\gamma\beta^2$).

are important to our study. In fig. 5.1 the two solid lines represent the two different intrinsic functions for the diquark, with no symmetry breaking. When there is no symmetry breaking ($\gamma\beta^2 = 0$), the two intrinsic functions are simple trigonometric functions. The ‘-.’ and ‘--’ lines represent the same two intrinsic functions, but for different symmetry breaking strengths. As the symmetry breaking is turned on, the intrinsic functions get pushed toward $\nu = 0$. This is exactly the effect we want, because we want the wave functions to be more pronounced at small values of the strangeness changing angle, which means that strangeness modes are less likely to be excited.

8.1 when we look at the effect of the heavy meson on the soliton, but at this stage the choice of which particle to look at is irrelevant since it is just to demonstrate the effect of symmetry breaking.

Diquark	SU(3) Irrep	I	J	Baryon
$[u,d]$	$\bar{\mathbf{3}}$	0	0	Λ_Q
$[u,s]$ & $[d,s]$	$\bar{\mathbf{3}}$	$\frac{1}{2}$	0	Ξ_Q
$\{s,s\}$	$\mathbf{6}$	0	1	Ω_Q
$\{u,s\}$ & $\{d,s\}$	$\mathbf{6}$	$\frac{1}{2}$	1	Ξ'_Q
$\{u,u\}$, $\{u,d\}$, $\{d,d\}$	$\mathbf{6}$	1	1	Σ_Q

Table 5.1: Quantum numbers of diquark members of SU(3) irreps. Commutators ‘ $[,]$ ’ and anti-commutators ‘ $\{, \}$ ’ refer to anti-symmetric and symmetric light flavour combinations, respectively. The last column denotes the heavy baryons for which the diquarks are relevant.

5.4.2 Perturbation Theory

Momen *et al.* (1994) approached the problem of symmetry breaking in heavy baryons in a soliton model using perturbation theory. Though we will not use perturbation theory, it is interesting to compare our numerical results to results of perturbation theory. The perturbation operator is

$$H' = \gamma(1 - D_{88}) \quad (5.4.20)$$

$$\gamma = \gamma_{\text{light}} + \gamma_{\text{heavy}}, \quad (5.4.21)$$

where

$$\gamma_{\text{heavy}} = \frac{1}{3}(M - M_s), \quad (5.4.22)$$

in the heavy limit. Later, in eqs.(8.2.6) and (8.2.6), we will give definitions for γ_{heavy} for ground states of heavy baryons. In eq.(5.4.21), γ_{light} is given in definition (5.4.15).

The matrix elements of H' between eigenstates of the unperturbed Hamiltonian (i.e. SU(3) eigenstates) are denoted by H'_{ab} and mass differences are calculated according to

$$\Delta m_a = H'_{aa} - \sum_{n \neq a} \frac{|H'_{na}|^2}{m_n - m_a} + \dots \quad (5.4.23)$$

where the contributing states are determined from SU(3) decompositions,

$$\bar{\mathbf{3}} \otimes \mathbf{8} = \bar{\mathbf{3}} \oplus \mathbf{6} \oplus \bar{\mathbf{15}} \quad (5.4.24)$$

$$\mathbf{6} \otimes \mathbf{8} = \bar{\mathbf{3}} \oplus \mathbf{6} \oplus \bar{\mathbf{15}} \oplus \mathbf{24}. \quad (5.4.25)$$

The octet on the left hand side arises from the D_{88} term in H' which means that it transforms as an octet.

Finally Momen *et al.* (1994) obtain expressions for the mass differences in the form, $\Delta M = a\tau + b\tau^2\beta^2 + c$, with the coefficients listed in table 5.2.

Using these coefficients, the eigenvalue of eq.(5.4.17) in second order perturbation theory is given by

$$\epsilon_p = (1 - a)\gamma\beta^2 + \frac{1}{2}b(\gamma\beta^2)^2. \quad (5.4.26)$$

Fig. 5.2 shows this dependence of the eigenvalue, ϵ_p , on $\gamma\beta^2$ for Momen *et al.* (1994) as well as our numerical results. Up to $\gamma\beta^2 \approx 5$ the numeric results and perturbation theory agree quite well, but beyond that the perturbation

Matrix Element	a	b	c
Λ_Q	$\frac{1}{4}$	$-\frac{9}{160}$	0
$\Xi_Q(\mathbf{3})$	$-\frac{1}{8}$	$-\frac{27}{640}$	0
Σ_Q	$\frac{1}{10}$	$-\frac{29}{250}$	$\frac{1}{\alpha^2}$
$\Xi_Q(\mathbf{6})$	$-\frac{1}{20}$	$-\frac{123}{2000}$	$\frac{1}{\alpha^2}$
Ω_Q	$-\frac{1}{5}$	$-\frac{3}{125}$	$\frac{1}{\alpha^2}$

Table 5.2: Coefficients of 2nd order perturbation theory obtained by Momen *et al.* (1994).

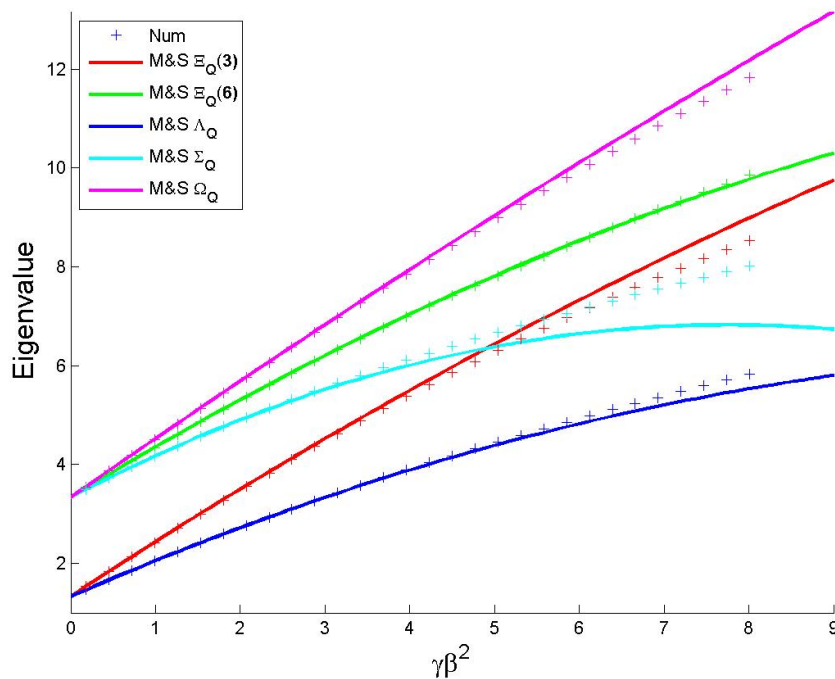


Figure 5.2: Comparison between numerical and 2nd order perturbation theory calculations (by Momen *et al.* (1994)) of eigen-energies of solitons in heavy baryons as a function of flavour symmetry breaking strength.

theory starts to deviate, especially for Σ_Q states. In order to improve on the perturbation theory, one would have to go to third order or even higher.

Park *et al.* (1989) did a similar calculation for light baryons, which isn't strictly speaking relevant to our study, aside from the fact that it allows us to compare our numeric results against third order perturbation theory. We will

repeat the results obtained in eq.(10) of Park *et al.* (1989)

$$\begin{aligned}
 2\beta^2\delta E(p) &= -0.3\gamma\beta^2 - 0.0287(\gamma\beta^2)^2 + 0.0006(\gamma\beta^2)^3 + \dots \\
 2\beta^2\delta E(\Lambda) &= -0.1\gamma\beta^2 - 0.0180(\gamma\beta^2)^2 + 0.0003(\gamma\beta^2)^3 + \dots \\
 2\beta^2\delta E(\Sigma) &= 0.1\gamma\beta^2 - 0.0247(\gamma\beta^2)^2 + 0.0002(\gamma\beta^2)^3 + \dots \\
 2\beta^2\delta E(\Xi) &= 0.2\gamma\beta^2 - 0.0120(\gamma\beta^2)^2 + 0.0006(\gamma\beta^2)^3 + \dots
 \end{aligned} \tag{5.4.27}$$

where

$$2\beta^2\delta E = \epsilon - 3 - \gamma\beta^2. \tag{5.4.28}$$

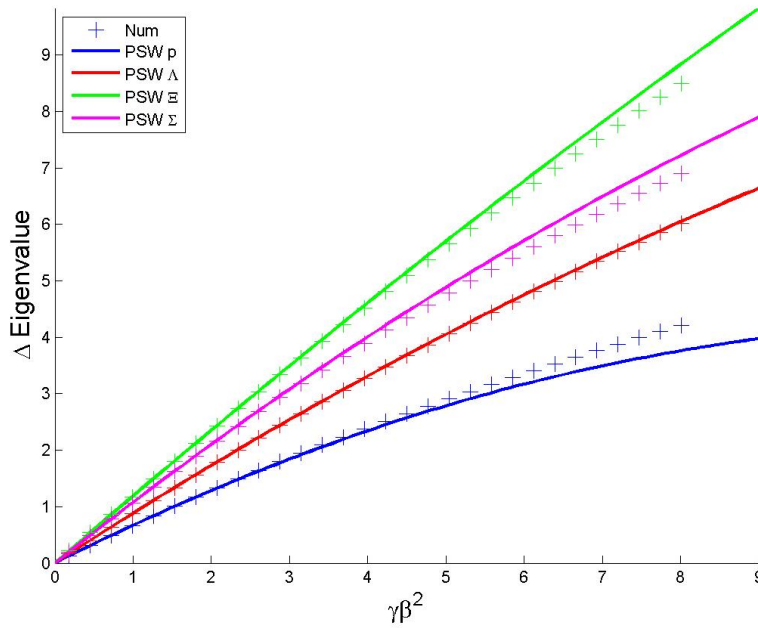


Figure 5.3: Comparison between numerical and 2^{nd} order perturbation theory calculations (by Park *et al.* (1989)) of eigen-energies as a function of flavour symmetry breaking strength for light baryons.

Fig. 5.4 shows how the eigenvalue changes for different values of $\gamma\beta^2$ and it shows both numeric results and the third order perturbation theory of Park *et al.* (1989). We also show the same comparison in fig. 5.3 but only up to second order perturbation theory. Comparing the two figures we can see the improvement obtained by including the third order correction.

From figs. 5.2 and 5.4 we can see that when $\gamma\beta^2 = 0$, i.e. when there is no symmetry breaking, the eigenvalue is just the first eigenvalue of the relevant representation in $SU(3)$. As one turns on symmetry breaking though,

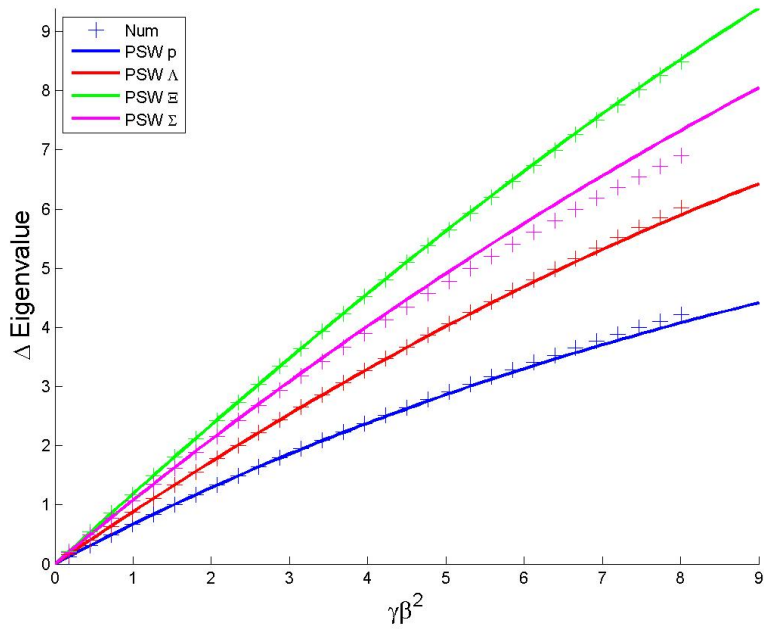


Figure 5.4: Comparison between numerical and 3rd order perturbation theory calculations (by Park *et al.* (1989)) of eigen-energies as a function of flavour symmetry breaking strength for light baryons.

the eigenvalues start changing. Though perturbation theory can give decent results for low values of $\gamma\beta^2$, as it increases one is forced to go to higher orders of perturbation theory. This complicates matters and requires the calculation of many Clebsch-Gordan coefficients. On the other hand, the numerical approach is simpler and the complexity does not grow for higher symmetry breaking strengths.

Chapter 6

Heavy Flavour Symmetry

Thus far we have only considered three flavours (up, down and strange), but eventually we want to be able to include the charm and bottom flavours as well. The solitons discussed in the previous chapters were all built up from an effective meson theory, where the current quark masses were assumed to be much lighter than typical interaction energies. This was a good approximation because the current quark masses are much smaller than the QCD scale¹, Λ_{QCD} . Flavour symmetry breaking for the effective theory (and thus for the soliton) are then brought about by looking at the pion and kaon. When considering quarks with masses much greater than Λ_{QCD} , i.e., charm or bottom quarks, the $m_Q \rightarrow \infty$ limit in QCD is a good approximation. In this limit, the dynamics are the same, regardless of which flavour of heavy quark is used, so this is called heavy flavour symmetry.

6.1 Parity Degeneracy

In order to look at the $m_Q \rightarrow \infty$ limit, it is convenient to use an effective field theory, called heavy quark effective theory (HQET). This description of hadrons, containing a single heavy quark, is valid as long as the momenta are much smaller than the mass of the heavy quark. After transforming to the heavy quark rest frame, the effective Lagrangian only contains terms with non-positive powers of m_Q . Moreover, the contribution of zeroth power in m_Q does not have spin operators. Hence the spin-dependent interactions are suppressed. Therefore, the dynamics are not affected by a change in the heavy quark spin. This is called heavy quark spin symmetry, and leads to a degeneracy between pseudoscalar and vector mesons, consisting of the same quarks. This symmetry is very well reflected in the data.

Table 6.1 shows the masses of pseudoscalar (0^-) and vector (1^-) components of some mesons. For light mesons, the respective mass differences are

¹For the energy scale of the mass of the Z-boson, $\Lambda_{\text{QCD}} \approx 250\text{MeV}$

quite large compared to the actual masses. It is therefore sufficient to have independent models for the pseudoscalar and vector components. As the mass increases though, the difference becomes much smaller to the point where the difference is less than 1% for mesons containing the bottom quark. Therefore it is clear that any model of heavy meson masses must take into account both the pseudoscalar and vector components.

Mesons	0^- mass(MeV)	1^- mass(MeV)	ΔM (MeV)	quark content
(π, ρ)	138	770	632	(q,q)
(K, K^*)	494	892	398	(q,s)
(D, D^*)	1870	2010	140	(q,c)
(B, B^*)	5279	5325	46	(q,b)

Table 6.1: Masses of pseudoscalar and vector mesons where ‘q’ indicates an up or down quark and 0^- and 1^- represent the pseudoscalar and vector components respectively. All masses were taken from Olive *et al.* (2014)

6.2 Heavy Meson Lagrangian

In order to take into account the near degeneracy in the masses of the pseudoscalar and vector mesons, we first reparametrise them so that the large masses are accounted for by the frequency of fluctuating modes (see Manohar and Wise (2000)),

$$\begin{aligned}\tilde{P} &= e^{iM V \cdot x} P \\ \tilde{Q}_\mu &= e^{iM^* V \cdot x} Q_\mu,\end{aligned}\tag{6.2.1}$$

where M and M^* are the pseudoscalar and vector masses respectively. We have factorised the mass dependence of all the fields in an exponential to set the stage for a large mass expansion. Then the leading order terms will cancel in the respective effective meson Lagrangian. The reference frame of the heavy quark is characterised by the four-velocity, V^μ . In order to account for the (near) degeneracy discussed above, we combine these fields into a single heavy meson multiplet,

$$\mathcal{H} = \frac{1}{2}(1 + \gamma_\mu V^\mu)(i\gamma_5 \tilde{P} + \gamma^\nu \tilde{Q}_\nu),\tag{6.2.2}$$

which refers to the heavy quark component of the heavy meson while,

$$\bar{\mathcal{H}} = \gamma_0 \mathcal{H}^\dagger \gamma_0\tag{6.2.3}$$

refers to the light (up or down) anti-quark component. The interaction between light and heavy mesons should be governed by chiral symmetry for the light degrees of freedom of \mathcal{H} . We want the smallest possible number of derivatives acting on the light pseudoscalar field in our model Lagrangian, so it must be of the form,

$$\frac{1}{M}\mathcal{L}_H \approx iV^\mu \text{tr}\{\mathcal{H}(\partial_\mu - iv_\mu)\bar{\mathcal{H}}\} - d \text{tr}\{\mathcal{H}\gamma_\mu\gamma_5 p^\mu\bar{\mathcal{H}}\} + \dots \quad (6.2.4)$$

The elipsis indicates terms that are subleading in $\frac{1}{M}$. The pseudovector (p_μ) and vector (v_μ) currents of the light mesons are defined as

$$p_\mu = \frac{i}{2}(\xi\partial_\mu\xi^\dagger - \xi^\dagger\partial_\mu\xi) \quad (6.2.5)$$

$$v_\mu = \frac{i}{2}(\xi\partial_\mu\xi^\dagger + \xi^\dagger\partial_\mu\xi), \quad (6.2.6)$$

where ξ is a square root of the chiral field,

$$U = \xi^2. \quad (6.2.7)$$

The parameter, d , can be determined from the semi-leptonic $D \rightarrow K$ transition and is found to be $d \approx 0.53$ (see Gupta *et al.* (1993)).

6.3 Covariant Heavy Meson Lagrangian

In our model we will consider the heavy baryon as consisting of a heavy meson bound in the background field of a Skyrmion. We have already discussed the Lagrangian of the Skyrmion, so now we need the parts of the action corresponding to the pseudoscalar mesons in the Skyrme model coupling to their counterparts in the heavy meson. We will follow the same approach as Schechter *et al.* (1995), except that we ignore the effect of the vector mesons (ω_0 and $\rho_{i,a}$). The Lagrange density of the heavy meson coupling to the background of the Skyrmion, is then given by

$$\begin{aligned} \mathcal{L}_H = & D_\mu P(D^\mu P)^\dagger - \frac{1}{2}Q_{\mu\nu}(Q^{\mu\nu})^\dagger - M^2 P P^\dagger + M^{*2} Q_\mu Q^{\mu\dagger} \\ & + 2iMd(Pp_\mu Q^{\mu\dagger} - Q_\mu p^\mu P^\dagger) \\ & - \frac{d}{2}\epsilon^{\alpha\beta\mu\nu}[Q_{\nu\alpha}p_\mu Q_\beta^\dagger + Q_\beta p_\mu(Q_{\nu\alpha})^\dagger]. \end{aligned} \quad (6.3.1)$$

Performing the transition in eq.(6.2.1) on eq.(6.3.1) confirms that this Lagrange density is of the correct form (the same form as eq.(6.2.4)) in the limit where $M \rightarrow \infty$. The masses M and M^* are listed in table 6.1 under 0^- and 1^- respectively. The definition of Q_μ is as a row vector in light flavour space. We define the covariant derivative similar to Schechter *et al.* (1995),

$$D_\mu P^\dagger = (\partial_\mu - iv_\mu)P^\dagger, \quad (6.3.2)$$

and the covariant field strength tensor exactly like Schechter *et al.* (1995),

$$(Q_{\mu\nu})^\dagger = D_\mu Q_\nu^\dagger - D_\nu Q_\mu^\dagger. \quad (6.3.3)$$

Usually one would expect a term such as $[Q_\mu, Q_\nu]$ to appear in the field strength tensor, but in our case this would lead to terms in the Lagrangian that are higher than second order, and we do not need such terms to explore heavy meson fluctuations in the Skyrmion background.

In eq.(6.2.4) we see the coupling constant, d , affecting the heavy meson multiplet. In the Lagrangian this leads to the same coupling constant, d , for terms involving the coupling of the heavy pseudoscalar field, as well as the heavy vector fields to the light pseudoscalar fields, as shown in the fifth and sixth terms in eq.(6.3.1). The equality of the coupling constant reflects the heavy flavour symmetry. Without that, independent coupling constants would have been permitted.

Chapter 7

Heavy Meson Solitons

In this chapter we will discuss the calculation of the bound states of a heavy meson in the background of a Skyrmion. Before looking at the heavy meson, however, we will take a brief look at the initial use of the bound state approach.

7.1 The Bound State Approach

In sections 5.3 and 5.4 we treated the three flavour soliton in $SU(3)$. This was possible by considering the strangeness symmetry breaking as a large amplitude fluctuation in the direction of strangeness. The collective coordinate Hamiltonian could then be exactly diagonalized according to the Yabu-Ando approach (see Yabu and Ando (1988)). If we approximate the flavour rotations by their small amplitude content, we need to treat the symmetry breaking in the bound state approach (BSA), initiated by Callan and Klebanov (1985). These two approaches are indeed identical in the large N_c limit (see Walliser and Weigel (2005)). In the BSA, baryons with heavy flavour are described as a heavy meson in the background field of a Skyrmion.

Since strangeness is considered a heavy flavour in the BSA, strangeness degrees of freedom are introduced via small fluctuations in the kaonic directions around the pionic Skyrmion, parameterised as,

$$U_K(\vec{x}, t) = \xi e^{iZ} \xi, \quad (7.1.1)$$

where

$$Z = \frac{2}{f_K} \left(\begin{array}{c|c} 0 & K(\vec{x}, t) \\ \hline K^\dagger(\vec{x}, t) & 0 \end{array} \right). \quad (7.1.2)$$

Here $K(\vec{x}, t)$ is the isospinor used to parameterise the kaon field and ξ is defined in eq.(6.2.7). Expanding up to second order in K results in the following

Lagrange density (see Schat *et al.* (1995) and Oh *et al.* (1991)):

$$\begin{aligned}
 \mathcal{L}_K &= (D_\mu)^\dagger D^\mu K - m_K^2 K^\dagger K - \frac{f_\pi^2 m_\pi^2}{4f_K^2} (\xi + \xi^\dagger - 2)K \\
 &\quad - \frac{1}{2} K^\dagger K \text{tr} \left(p_\mu p^\mu + \frac{1}{16e_{\text{sk}}^2 f_K^2} [\xi^\dagger \partial_\mu \xi, \xi^\dagger \partial_\nu \xi]^2 \right) \\
 &\quad + \frac{1}{2e_{\text{sk}} f_K^2} \left\{ (D_\mu K)^\dagger D_\nu K \text{tr}(p^\mu p^\nu) - (D_\mu K)^\dagger D^\mu K (p_\nu p^\nu) \right. \\
 &\quad \left. - 3(D_\mu K)^\dagger [p^\mu, p^\nu] D_\nu K \right\} \\
 &\quad - \frac{iN_c}{4f_K^2} B_\mu [K^\dagger D^\mu K - (D_\mu K)^\dagger K].
 \end{aligned} \tag{7.1.3}$$

Here, the covariant derivative is the same as is defined in eq.(6.3.2), and p_μ is defined in eq.(6.2.5). The term containing B_μ , the baryon number current, arises from the Wess-Zumino term. Due to the factor $\frac{1}{f_K}$ in eq.(7.1.2), the $K(\vec{x}, t)$ has a smooth limit as $N_c \rightarrow \infty$. Terms of higher order in K (or K^\dagger) contain additional factors of $\frac{1}{f_K}$, and therefore disappear in the large N_c limit. Hence, the bound state approach is exact in large N_c .

In order to investigate the static properties, and spectrum, of low lying baryons, with strangeness (in the bound state approach), we must look at the P-wave channel. The *ansatz* for the P-wave is given by,

$$K^{(P)}(\vec{x}, t) = \int \frac{d\omega}{2\pi} e^{i\omega t} k^{(P)}(r, \omega) \hat{x} \cdot \vec{\tau} \begin{pmatrix} a_1(\omega) \\ a_2(\omega) \end{pmatrix}. \tag{7.1.4}$$

Canonical quantization will lead to the spectral functions, $a_1(\omega)$ and $a_2(\omega)$ becoming creation and annihilation operators. The term containing these operators is, importantly, an (iso)spinor. Therefore, $K(\vec{x}, t)$ is built up from an (iso)spinor and some radial function, $k^{(P)}(r, \omega)$. From the Lagrange density in eq.(7.1.3) we can get the modified Klein-Gordon equation,

$$\begin{aligned}
 0 &= k^{(P)}(r, \omega) \left\{ -\frac{1}{r^2} \frac{d}{dr} \left(r^2 h(r) \frac{d}{dr} \right) + m_K^2 \right. \\
 &\quad \left. + V^{(P)}(r) - f(r)\omega^2 + 2\lambda(r)\omega \right\}.
 \end{aligned} \tag{7.1.5}$$

Here, the potential, $V^{(P)}(r)$, is generated by the Skyrmion. The radial functions h , $V^{(P)}$, f and λ can be found in Callan and Klebanov (1985). The radial function, $k^{(P)}(r, \omega)$, can be found by solving this second order DEQ. Normalizable (i.e. bound state) solutions can only be found for certain frequencies, ω . These frequencies ultimately determine the mass of the strange baryons like the Λ or Σ .

The last term in eq.(7.1.5) arises from the Wess Zumino action. Because of this term, a solution with $\omega > 0$ cannot also be satisfied for $\omega < 0$. This means that, in the bound state approach, pentaquark states are presumably heavier than ordinary baryons, and only emerge for strong enough coupling via the Wess-Zumino term. For physically motivated parameters, then do not emerge.

This concludes our look at how the bound state approach was first used to describe strange baryons as a strange meson bound to the Skyrmion.

7.2 S & P wave bound states

For heavy baryons there are two major differences compared to the just discussed BSA: (i) the small amplitude Lagrangian is not a chiral theory, but a HQET, (ii) we cannot reduce the fluctuation to the pseudoscalar channel. We will first address the second difference and look at the *ansätze* for the heavy meson fields. Similarly to eq.(7.1.4), they are built up from a spinor and one or more radial functions. We will make the same *ansätze* for the heavy meson fields as Schechter *et al.* (1995). For the P-wave (1^-):

$$\begin{aligned} P^\dagger &= \frac{1}{\sqrt{4\pi}} \Phi(r) \hat{r} \cdot \vec{\tau} \chi e^{i\epsilon t} \\ Q_0^\dagger &= \frac{1}{\sqrt{4\pi}} \Psi_0(r) \chi e^{i\epsilon t} \\ Q_i^\dagger &= \frac{1}{\sqrt{4\pi}} \left[i\Psi_1(r) \hat{r}_i + \frac{1}{2} \Psi_2(r) (\hat{r} \times \vec{\tau})_i \right] \chi e^{i\epsilon t}, \end{aligned} \quad (7.2.1)$$

and the S-wave (0^-):

$$\begin{aligned} P^\dagger &= \frac{1}{\sqrt{4\pi}} \Phi(r) \chi e^{i\epsilon t} \\ Q_0^\dagger &= \frac{1}{\sqrt{4\pi}} \Psi_0(r) \hat{r} \cdot \vec{\tau} \chi e^{i\epsilon t} \\ Q_i^\dagger &= \frac{i}{\sqrt{4\pi}} [\Psi_1(r) \hat{r} \cdot \vec{\tau} \hat{r}_i + \Psi_2(r) r (\vec{\tau} \cdot \partial_i \hat{r})] \chi e^{i\epsilon t}, \end{aligned} \quad (7.2.2)$$

where Φ and Ψ_i are our four radial functions (one for the pseudoscalar and three for the vector fields). Since we seek solutions to different frequencies, ϵ , the radial functions depend on ϵ , but it is not necessary to make that dependence explicit. In eqs.(7.2.1) and (7.2.2) χ is the Fourier amplitude, defined as a column spinor,

$$\chi = \begin{pmatrix} u \\ d \\ s \end{pmatrix}, \quad (7.2.3)$$

relating to the light flavour content of the heavy meson. Notice that we are multiplying 2×2 τ matrices by the three component spinor. The τ matrices are really embedded in the top left corner of a 3×3 matrix or, to put it differently, τ_i are really the first three Gell-Mann matrices, λ_i (see Appendix B.1.1). Therefore the third entry in χ is not really important here, but it will be later on.

Substituting everything back into 6.3.1 we get the following results for \mathcal{L}_H^1 .
P-Wave:

$$\begin{aligned}
\mathcal{L}_H^{(P)} &= \Phi'^2 + \left[M^2 - \epsilon^2 + \frac{2}{r^2} \left(1 + \frac{R_\alpha}{2} \right) \right] \Phi^2 \\
&+ M^{*2} \left(\Psi_1^2 + \frac{1}{2} \Psi_2^2 - \Psi_0^2 \right) + \frac{1}{2} \left(\Psi_2' - \frac{1}{r} \Psi_2 \right)^2 + \frac{R_\alpha}{r} \Psi_1 \Psi_2' \\
&\frac{R_\alpha}{r^2} (\Psi_1 + \Psi_2) \Psi_2 + \frac{R_\alpha^2}{2r^2} \left(\Psi_1^2 + \frac{1}{2} \Psi_2^2 \right) \\
&- (\Psi_0' - \epsilon \Psi_1)^2 - \frac{1}{2} \left(\frac{R_\alpha}{r} \Psi_0 + \epsilon \Psi_2 \right)^2 \\
&- d \left[\frac{2 \sin F}{r} \left(\Psi_2 \Psi_0' - \frac{R_\alpha}{r} \Psi_0 \Psi_1 - \epsilon \Psi_1 \Psi_2 \right) \right. \\
&\left. + F' \left(\frac{\epsilon}{2} \Psi_2^2 + \frac{R_\alpha}{r} \Psi_0 \Psi_2 \right) \right] \\
&+ 2Md \left(F' \Psi_1 - \frac{\sin F}{r} \Psi_2 \right) \Phi. \tag{7.2.4}
\end{aligned}$$

S-wave:

$$\begin{aligned}
\mathcal{L}_H^{(S)} &= \Phi'^2 + \left[M^2 - \epsilon^2 + \frac{R_\alpha^2}{2r^2} \right] \Phi^2 + M^{*2} (\Psi_1^2 + 2\Psi_2^2 - \Psi_0^2) \\
&+ \frac{2}{r^2} \left(r\Psi_2' + \Psi_2 - \frac{R_\alpha + 2}{2} \Psi_1 \right)^2 + \frac{R_\alpha^2}{r^2} \Psi_2^2 \\
&- (\Psi_0' - \epsilon \Psi_1)^2 - 2 \left(\epsilon \Psi_2 - \frac{R_\alpha + 2}{2r} \Psi_0 \right)^2 \\
&+ 2d \left[F' \left(\frac{1}{r} (1 + \cos F) \Psi_0 \Psi_2 - \epsilon \Psi_2^2 \right) \right. \\
&\left. + \frac{2 \sin F}{r} \left(\Psi_2 \Psi_0' - \epsilon \Psi_1 \Psi_2 + \frac{R_\alpha + 2}{2r} \Psi_0 \Psi_1 \right) \right] \\
&+ 2Md \left(F' \Psi_1 + \frac{2 \sin F}{r} \Psi_2 \right) \Phi, \tag{7.2.5}
\end{aligned}$$

¹Some total derivative terms are discarded, since they result in zeros when integrating the Lagrange density to obtain the Lagrange function.

where $R_\alpha = \cos F - 1$. We have left out a global factor of $\chi^\dagger \chi$ in the Lagrange densities.

A quick glance at eqs.(7.2.4) and (7.2.5) will show that we are dealing with four radial functions and their derivatives, but a closer look will reveal that there is no $(\Psi'_1)^2$ component, so we must eliminate Ψ_1 when setting up the differential equations. Terms with a single derivative Ψ'_1 have been transformed to Ψ_1 via integration by parts. First we will write the Lagrange density in a more general form, containing all the combinations of the radial functions,

$$\mathcal{L}_H = \frac{a_i}{2} \zeta_i'^2 + b_{ij} \zeta_i \zeta_j' + \frac{c_{ij}}{2} \zeta_i \zeta_j + \frac{f_1}{2} \Psi_1^2 + (g_i \zeta_i + h_i \zeta_i') \Psi_1, \quad (7.2.6)$$

where $\zeta = (\Phi, \Psi_0, \Psi_2)$ represents the three radial functions that we have derivatives of. Now the two different waves can be done in the same way, but with slightly different matrices a, b, c, f and g . These are read off straight from eqs.(7.2.4) and (7.2.5) and shown explicitly in Appendix C. We do need to be careful when reading off the entries for c_{ij} since there is the possibility for double counting on the off-diagonal terms. This can be avoided, by either dividing the problematic terms by two, as we have done, and keeping the matrix symmetric, or by making the upper or lower triangle all zeros.

In order to eliminate Ψ_1 from eq.(7.2.6), we apply the Euler-Lagrange equation to get an equation of motion for Ψ_1 ,

$$\Psi_1 = -\frac{1}{f_1} (g_i \zeta_i + h_i \zeta_i'). \quad (7.2.7)$$

Because Ψ_1 acts as a constraint on the other radial functions rather than having an independent equation of motion, we can rewrite \mathcal{L}_H in terms of ζ_i only by defining new coefficient matrices as follows:

$$A_{ij} = a_i \delta_{ij} - \frac{h_i h_j}{f_1} \quad (7.2.8)$$

$$B_{ij} = b_{ij} - \frac{h_i g_j}{f_1} \quad (7.2.9)$$

$$C_{ij} = c_{ij} - \frac{g_i g_j}{f_1} \quad (7.2.10)$$

$$\mathcal{L}_H = \frac{1}{2} A_{ij} \zeta_i' \zeta_j' + B_{ij} \zeta_i \zeta_j' + \frac{1}{2} C_{ij} \zeta_i \zeta_j. \quad (7.2.11)$$

Now we apply the Euler-Lagrange equation on ζ_i to get our differential equations,

$$0 = \frac{\partial(r^2\mathcal{L}_H)}{\partial\zeta} - \frac{\partial}{\partial r} \left(\frac{\partial(r^2\mathcal{L}_H)}{\partial\zeta'} \right) \quad (7.2.12)$$

$$\begin{aligned} \Rightarrow A\zeta'' &= \left(-\frac{\partial A}{\partial r} - \frac{2A}{r} + B^T - B \right) \zeta' \\ &+ \left(\frac{1}{2}C + \frac{1}{2}C^T - \frac{\partial B}{\partial r} - \frac{2B}{r} \right) \zeta. \end{aligned} \quad (7.2.13)$$

The identical result arises, of course, when first deriving the equations of motion from eq.(7.2.6) for all four fields and subsequently eliminating Ψ_1 via the construction (7.2.7). Eq.(7.2.13) gives three coupled second order linear differential equations for the three fields (Φ, Ψ_0, Ψ_2) . The background potentials in A , B and C are generated by the chiral angle, $F(r)$. The energy (ϵ) acts as a parameter in these differential equations. In solving these differential equations, it is worth mentioning that calculating analytic expressions for A_{ij} , B_{ij} and C_{ij} is not advisable, since they do become extremely large, which gives a lot of room for problems when programming. It is more practical to program the coefficients matrices in eq.(7.2.6) and the calculations according to eq.(7.2.8) through eq.(7.2.10). Even though these calculations will be repeated for every iteration of the program, it is not that costly in terms of calculation time.

In order to solve these DEQs, we employ the same numerical method used to solve the DEQs in eq.(5.4.19). Good solutions (eg. asymptotically decaying profile functions) to these differential equations occur only for bound state energies. The bound state energy of the heavy meson in the presence of a soliton (the soliton contribution comes via. the chiral angle, F), is then given by²,

$$\epsilon_H = M - |\epsilon|. \quad (7.2.14)$$

Figs. 7.1 and 7.2 show the wave functions for the first bound state in the P and S wave of a meson containing a bottom quark. In these plots, $e_{sk} = 6.62$, in order to match the results and the wave functions in Fig. 5.4 of Schechter *et al.* (1995). Higher energy states will contain more oscillations of the wave functions, but for now we are mainly interested in the ground states.

²Notice that it is the absolute value of ϵ that enters the expression for the bound state energy. Baryons will have $\epsilon > 0$, but pentaquarks will have $\epsilon < 0$.

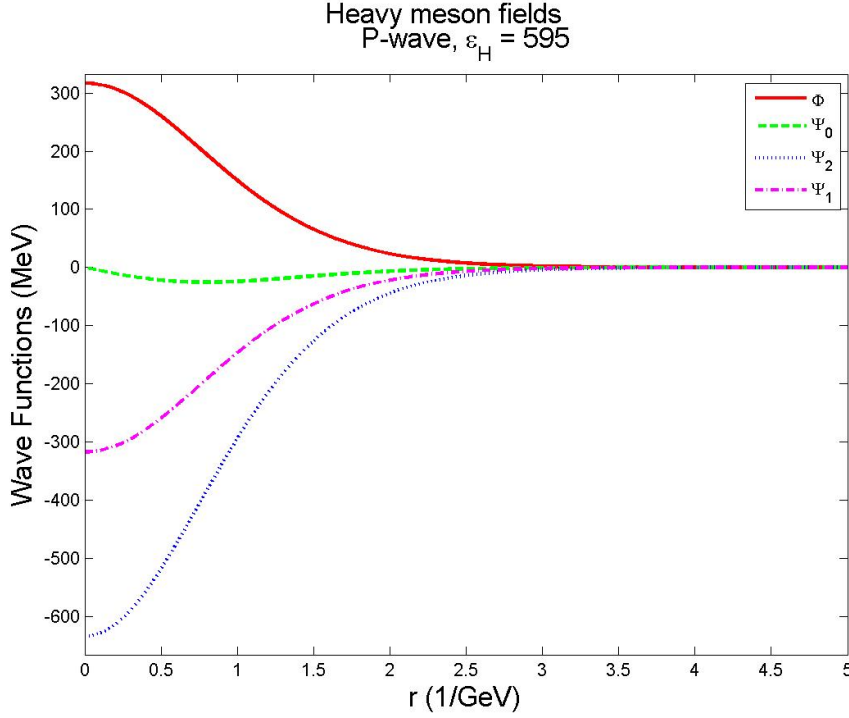


Figure 7.1: Wave functions of the pseudoscalar and vector fields for the P-wave of the heavy meson containing a bottom quark with $\epsilon_H = 595$ MeV and $e_{sk} = 6.62$.

7.3 Normalisation of bound state wave functions

The wave functions ($\Phi, \Psi_0, \Psi_1, \Psi_2$) in figs. 7.1 and 7.2 are displayed with arbitrary normalisation, so we still need to apply a physically sensible normalisation, which goes beyond solving a linear system of differential equations. In eqs.(7.2.1) and (7.2.2) we can see that all the fields contain a factor e^{ict} which is exactly the phase of the heavy meson field. The invariance under changing this phase, generates the Noether current for the heavy flavour under consideration. The corresponding charge (ie. the spatial integral of the time component) must be an integer. Applying, for example, the Gell-Mann-Lévy method to construct the Noether current, reveals that the charge is identical to the derivative, $\frac{\partial L_H}{\partial \epsilon}$. Hence the appropriate normalisation condition for the bound state wave function is

$$\left| \frac{\partial L_H}{\partial \epsilon} \right| = 1. \quad (7.3.1)$$

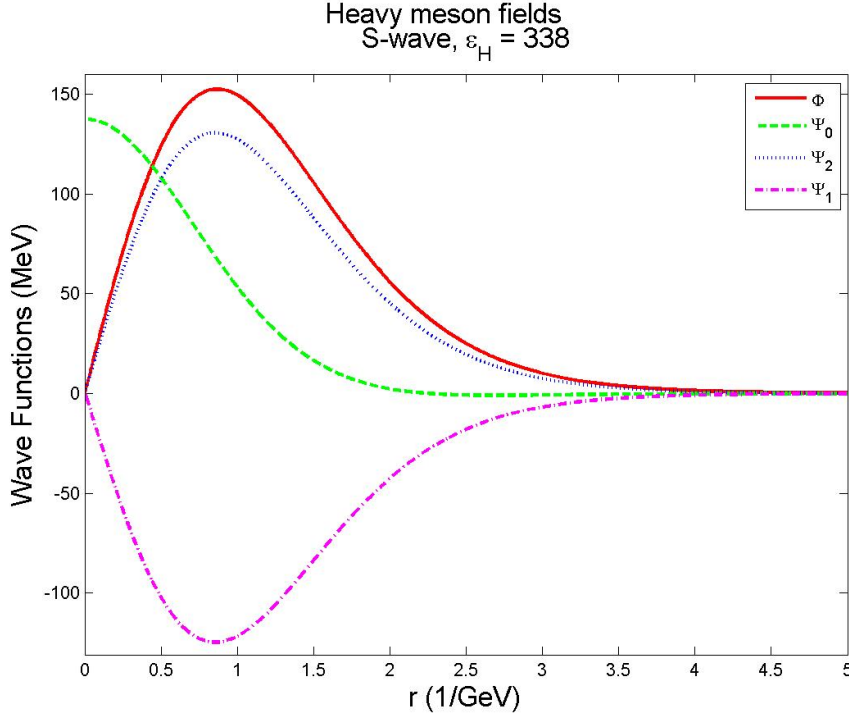


Figure 7.2: Wave functions of the pseudoscalar and vector fields for the S-wave of the heavy meson containing a bottom quark with $\epsilon_H = 338$ MeV and $e_{sk} = 6.62$.

For the P-wave this translates to

$$1 = \left| \int dr r^2 \left[2\epsilon\Phi^2 - 2(\Psi'_0 - \epsilon\Psi_1)\Psi_1 + \left(\frac{R_\alpha}{r}\Psi_0 + \epsilon\Psi_2 \right) \Psi_2 - d \left(\frac{2\sin F}{r}\Psi_1 - \frac{F'}{2}\Psi_2 \right) \Psi_2 \right] \right| \quad (7.3.2)$$

and for the S-wave

$$1 = \left| \int dr r^2 \left[2\epsilon\Phi^2 - 2(\Psi'_0 - \epsilon\Psi_1)\Psi_1 + 4 \left(\epsilon\Psi_2 - \frac{R_\alpha + 2}{2r}\Psi_0 \right) \Psi_2 - 2d \left(\frac{2\sin F}{r}\Psi_1 + F'\Psi_2 \right) \Psi_2 \right] \right|. \quad (7.3.3)$$

These normalised wave functions will be important to us when we deal with hyperfine splitting in chapter 9 and they are, of course, crucial for any calculation that involves the bound state wave functions.

Chapter 8

Heavy Solitons in Flavour $SU(3)$

In section 5.3 we discussed the quantisation of the soliton in flavour $SU(3)$. That discussion contained the light flavours (up, down and strange). In this chapter we want to build on that, to encompass the case where heavy flavours (charm and bottom) are involved.

8.1 Modified constraint on R_8

We have already shown the collective coordinate lagrangian for a light soliton in eq.(5.3.10). In order to take into account the heavy meson, we need to apply the same collective coordinate quantisation as in section 5.3 to the Lagrange density in eq.(6.3.1). The time dependent collective coordinates $A(t) \in SU(3)$ are introduced as a generalisation of eq.(5.3.9),

$$\tilde{\xi}(t, \vec{r}) = A(t)\xi(\vec{r})A(t)^\dagger \quad (8.1.1)$$

$$\tilde{P}^\dagger(t, \vec{r}) = A(t)P^\dagger(t, \vec{r}) \quad (8.1.2)$$

$$\tilde{Q}_\mu^\dagger(t, \vec{r}) = A(t)Q_\mu^\dagger(t, \vec{r}). \quad (8.1.3)$$

As an example of the effect this has, we will look at the first term in eq.(6.3.1),

$$D_\mu P(D^\mu P)^\dagger \rightarrow D_\mu \tilde{P}(D^\mu \tilde{P})^\dagger. \quad (8.1.4)$$

Since $A(t)$ is only dependent on time, only the $\mu = 0$ case will be affected by the inclusion of the collective coordinates. For clarity of the description, we will ignore the v_0 component and look only at the $\partial_0 \tilde{P}$ components.

$$\partial_0 \tilde{P} \partial_0 \tilde{P}^\dagger = \partial_0(PA^\dagger) \partial_0(AP^\dagger) \quad (8.1.5)$$

$$\begin{aligned} &= \dot{P}A^\dagger A\dot{P}^\dagger + \dot{P}A^\dagger \dot{A}P^\dagger \\ &\quad + P\dot{A}^\dagger A\dot{P}^\dagger + P\dot{A}^\dagger \dot{A}P^\dagger. \end{aligned} \quad (8.1.6)$$

The first term in eq.(8.1.6) is just $\dot{P}\dot{P}^\dagger$ and already forms part (the ϵ^2 term) of the results in eqs.(7.2.4) and (7.2.5). The final term in eq.(8.1.6) is quadratic

in \dot{A} , and therefore of no interest to us, since it would give us a subdominant contribution to the moments of inertia, α^2 and β^2 . The second and third terms are the ones we are really interested in now, since they are linear in the angular velocity,

$$A^\dagger \dot{A} = \frac{i}{2} \Omega \cdot \lambda. \quad (8.1.7)$$

If we look at this term in the P-wave, the terms linear in the angular velocity in eq.(8.1.6) have the form

$$\dot{P} A^\dagger \dot{A} P^\dagger = \frac{1}{4\pi} \frac{\epsilon}{2} \Phi(r)^2 \chi^\dagger (\hat{r} \cdot \vec{\tau}) (\Omega \cdot \lambda) (\hat{r} \cdot \vec{\tau}) \chi. \quad (8.1.8)$$

Since the bound state wave functions do not carry strangeness, only those λ_a which conserve strangeness will contribute to the sum

$$\Omega \cdot \lambda = \sum_{a=1}^8 \Omega_a \lambda_a. \quad (8.1.9)$$

Therefore eq.(8.1.8) can be rewritten as

$$\dot{P} A^\dagger \dot{A} P^\dagger = \frac{1}{4\pi} \frac{\epsilon}{2} \Phi(r)^2 \chi^\dagger (\hat{r} \cdot \vec{\tau}) (\vec{\Omega} \cdot \vec{\tau} + \frac{1}{\sqrt{3}} \Omega_8) (\hat{r} \cdot \vec{\tau}) \chi. \quad (8.1.10)$$

The term containing $\vec{\Omega} \cdot \vec{\tau}$ relates to the hyperfine splitting in chapter 9, but for now we are more interested in the Ω_8 term. When we first quantised the soliton in SU(3) in section 5.3, we found that the Ω_8 term in eq.(5.3.10) results in a constraint on the right generator, R_8 , which forces the soliton to have half-integer spin, and therefore be quantised as a baryon. We have just seen however, that the heavy meson will also contribute a term, proportional to Ω_8 , to the Lagrangian. The new form of the Lagrangian is (see Momen *et al.* (1994)),

$$\begin{aligned} L(A, \Omega_\alpha) = & -E_{\text{cl}} + \frac{1}{2} \alpha^2 \sum_{i=1}^3 \Omega_i^2 + \frac{1}{2} \beta^2 \sum_{\alpha=4}^7 \Omega_\alpha^2 \\ & - \frac{\sqrt{3}}{2} \Omega_8 + \frac{\sqrt{3}}{6} \Omega_8 \chi^\dagger \chi \hat{P}. \end{aligned} \quad (8.1.11)$$

The coefficient of the last term is, in principle, an integral over the heavy meson radial functions. However, this integral is equal to the normalisation conditions in eqs.(7.3.2) and (7.3.3). The reason for this identity is that $\Omega_8 \lambda_8$ essentially acts like a phase transformation on the heavy meson bound states that have zero strangeness. In eq.(8.1.11), \hat{P} is the projection onto the heavy flavour subspace. Therefore, in the absence of heavy flavours (no charm or bottom flavour), $\hat{P} = 0$ so that the Lagrangian returns to the form of eq.(5.3.10). If a

heavy flavour is present though, $\hat{P} = 1$ and summing over the $\chi^\dagger \chi$ also yields one, which leads to a change in the overall coefficient of Ω_8 . This changes the constraint on R_8 in eq.(5.3.15) so we have (see Momen *et al.* (1994)),

$$R_8 = \begin{cases} \frac{\sqrt{3}}{2} & \text{light baryons} \\ \frac{1}{\sqrt{3}} & \text{heavy baryons} \end{cases} \quad (8.1.12)$$

This new constraint on R_8 constrains Y_R to $\frac{2}{3}$ according to eq.(3.4.1). Therefore we must quantise the soliton (or more precisely, the collective coordinates) as a diquark rather than a baryon¹. This very important factor has been mentioned repeatedly in earlier chapters.

8.2 Heavy symmetry breaking

We have already discussed light flavour symmetry breaking in section 5.4. Since we were interested in the difference between up, down and strange flavours there, the theory required input from mesons which showed these differences, which is why we included the differences between the masses and decay constants of the π and K . Now we are interested in the effect of a heavy flavour, such as bottom or charm, so we need input from the mesons containing these flavours. In order to do this, we will add a term to the Lagrangian proportional to the masses squared of heavy mesons,

$$\mathcal{L}_{\text{Hm}} = -\frac{1}{2} P M_H P^\dagger - \frac{1}{2} Q_\mu M_H^* Q^{\mu\dagger}, \quad (8.2.1)$$

where M_H and M_H^* contain the masses of the heavy pseudoscalar and vector mesons respectively. The subscript H denotes the heavy flavour we are interested in, and can be either charm or bottom. These matrices are of the form,

$$M_H = \begin{bmatrix} m_H^2 & 0 & 0 \\ 0 & m_H^2 & 0 \\ 0 & 0 & m_{H_s}^2 \end{bmatrix}, \quad (8.2.2)$$

where the subscript s indicates the meson containing strangeness. The masses that enter the matrices, M_H and M_H^* are shown in table 8.1.

Eq.(8.2.2) can be rewritten as

$$M_H = \frac{1}{3} m_H^2 (2I + \sqrt{3} \lambda_8) + \frac{1}{3} m_{H_s}^2 (I - \sqrt{3} \lambda_8) \quad (8.2.3)$$

$$= \frac{1}{3} (2m_H^2 + m_{H_s}^2) I + \frac{1}{3} (m_H^2 - m_{H_s}^2) \sqrt{3} \lambda_8, \quad (8.2.4)$$

¹This arises from considerations of the SU(3) irreps and is explained in section 3.3

Flavour	$m_H(\text{MeV})$	$m_{H_s}(\text{MeV})$	$m_H^*(\text{MeV})$	$m_{H_s}^*(\text{MeV})$
C	1864.86	1968.49	2006.98	2112.3
B	5279.58	5366.77	5325.2	5415.4

Table 8.1: Heavy pseudoscalar and vector meson masses according to Olive *et al.* (2014).

where I is the 3×3 identity matrix. Using definitions (7.2.1) and (7.2.2) we get the change of the Lagrangian due to SU(3) symmetry breaking in the heavy sector

$$\Delta L_{\text{Hm}} = -\frac{1}{2}\gamma_{\text{H}}(1 - D_{88}) \quad (8.2.5)$$

with

$$\begin{aligned} \gamma_{\text{H}}^{(P)} = \int dr r^2 & \left[(m_{\text{H}}^2 - m_{\text{H}_s}^2)\Phi^2 \right. \\ & \left. + (m_{\text{H}}^{*2} - m_{\text{H}_s}^{*2}) \left(-\Psi_0^2 + \Psi_1^2 + \frac{1}{2}\Psi_2^2 \right) \right], \end{aligned} \quad (8.2.6)$$

$$\begin{aligned} \gamma_{\text{H}}^{(S)} = \int dr r^2 & \left[(m_{\text{H}}^2 - m_{\text{H}_s}^2)\Phi^2 \right. \\ & \left. + (m_{\text{H}}^{*2} - m_{\text{H}_s}^{*2}) \left(-\Psi_0^2 + \Psi_1^2 + 2\Psi_2^2 \right) \right], \end{aligned} \quad (8.2.7)$$

for the P and S waves respectively. In order to simplify matters we redefine L_{sb} from definition (5.4.14) to include this heavy flavour symmetry breaking,

$$L_{\text{sb}} = -\frac{1}{2}(\gamma + \gamma_{\text{H}})(1 - D_{88}). \quad (8.2.8)$$

This obviously alters the eigenvalue equation (5.4.17),

$$[C_2 + (\gamma + \gamma_{\text{H}})\beta^2(1 - D_{88})]\Psi = \epsilon_{\text{sb}}\Psi. \quad (8.2.9)$$

Of course this means that the bound state energy of the soliton will change, and since γ_{H} differs for the S and P waves, this will lead to additional mass differences between states of different parity.

Chapter 9

Hyperfine Splitting

Differences in the masses for baryons with different spatial isospin, already emerge in the eigenvalue equation (8.2.9) as the quantum numbers are contained in C_2 in eq.(5.4.18). Additional differences arise from the $\vec{\Omega} \cdot \vec{\tau}$ term in eq.(8.1.10). We will discuss that addition in this chapter.

9.1 Flavour Rotations and Spin

The differences in mass between heavy meson states of different spin, is called hyperfine splitting. In order to incorporate this into our model, we will first look at a time dependent coordinate rotation of our radial vector,

$$\hat{r}_i \rightarrow D_{ij}\hat{r}_j, \quad (9.1.1)$$

where D has the same type of definition as in eq.(5.3.6), but here we will redefine it in terms of a new time dependent rotation matrix, R_0 ,

$$D_{ij}(R_0) \equiv \frac{1}{2}\text{tr} [\lambda_i R_0 \lambda_j R_0^\dagger], \quad (9.1.2)$$

where

$$R_0 = 1 + \frac{1}{2}\vec{\delta}(t) \cdot \vec{\tau}, \quad (9.1.3)$$

is an infinitesimal rotation in coordinate space and the spin (of the baryon), \vec{J} , is the Noether current associated with this rotation. By construction, this is the total spin (The corresponding transformation must be applied to Q_μ , the vector component of the heavy meson field.). Let us now consider the effect of this rotation on the pseudoscalar field, P , in the P-wave.

$$\tilde{P}^\dagger = \frac{1}{4\pi}\Phi A(t)(\hat{r} \cdot \vec{\tau})\chi e^{i\epsilon t} \quad (9.1.4)$$

$$\rightarrow \frac{1}{4\pi}\Phi A(t)D_{ij}\hat{r}_i\tau_j\chi e^{i\epsilon t} \quad (9.1.5)$$

$$= \frac{1}{4\pi}\Phi A(t)R_0(t)(\vec{r} \cdot \vec{\tau})R_0(t)^\dagger\chi e^{i\epsilon t}. \quad (9.1.6)$$

Now we can see that the coordinate rotation in eq.(9.1.1) is equivalent to the simultaneous rotation in flavour space and a rotation among the different Fourier amplitudes of the bound states,

$$A(t) \rightarrow A(t)R_0(t) \quad (9.1.7)$$

$$\chi \rightarrow R_0(t)^\dagger \chi. \quad (9.1.8)$$

It is important to note that neither of these two rotations correspond to a conserved quantity on their own, but together they do correspond to a conserved quantity, the total spin,

$$\vec{J} = \left. \frac{\partial L}{\partial \dot{\vec{\delta}}(t)} \right|_{\delta=0}. \quad (9.1.9)$$

Notice that we are taking the derivative of the Lagrange function, and not the Lagrange density. This is possible because R_0 is no longer considered to be a coordinate rotation. The rotation in eq.(9.1.7) relates to the spin of the soliton,

$$\begin{aligned} \vec{J}^{\text{sol}} &= -\frac{\partial L}{\partial \vec{\Omega}} \\ &= -\vec{R}. \end{aligned} \quad (9.1.10)$$

The total spin, \vec{J} , is given by,

$$\vec{J} = \vec{J}^{\text{sol}} + \vec{G}, \quad (9.1.11)$$

where \vec{G} is the grand spin or spin of the heavy meson, which must then be

$$\vec{G} = -\frac{1}{2}\chi^\dagger \vec{\tau} \chi. \quad (9.1.12)$$

It arises from the transformation in eq.(9.1.8) together with the normalisation conditions in eqs.(7.3.2) and (7.3.3). Again, neither the soliton spin or the grand spin is conserved on their own, but their sum is conserved.

We finally have all the tools we need to set up the Lagrangian for our heavy baryon,

$$\begin{aligned} L &= -E_{\text{cl}} + \frac{1}{2}\alpha^2 \vec{\Omega}^2 + \frac{1}{2}\beta^2 \sum_{a=4}^7 \Omega_a^2 \\ &\quad - \frac{\sqrt{3}}{2}\Omega_8 + \frac{\sqrt{3}}{6}\Omega_8 \chi^\dagger \chi P - \rho \vec{\Omega} \cdot \vec{G}, \end{aligned} \quad (9.1.13)$$

where $\vec{\Omega}$ represents the first three components of Ω . Here ρ is given by

$$\begin{aligned} \rho^{(P)} = & \frac{2}{3} \int_0^\infty dr r^2 \left\{ \epsilon \Phi^2 (1 - 2 \cos F) \right. \\ & + (\epsilon \Psi_1^2 - \Psi_0' \Psi_1) (1 + 2 \cos F) - \frac{1}{2} \Psi_2 \left(\frac{R_\alpha}{r} \Psi_0 + \epsilon \Psi_2 \right) \\ & + 4M d\Phi \Psi_0 \sin F \\ & \left. - \frac{d}{r} \Psi_2 \left(\frac{r}{4} \Psi_2 F' + \Psi_1 \sin F (2 + \cos F + R_\alpha) \right) \right\} \end{aligned} \quad (9.1.14)$$

and

$$\begin{aligned} \rho^{(S)} = & \frac{2}{3} \int_0^\infty dr r^2 \left\{ \epsilon \Phi^2 (1 + 2 \cos F) \right. \\ & + (\epsilon \Psi_1^2 - \Psi_0' \Psi_1) (1 - 2 \cos F) + \Psi_2 \left(\frac{2 + R_\alpha}{r} \Psi_0 - 2\epsilon \Psi_2 \right) \\ & - 4M d\Phi \Psi_0 \sin F \\ & \left. - \frac{d}{r} \Psi_2 \left(r \Psi_2 F' + 2\Psi_1 \sin F (\cos F + R_\alpha) \right) \right\}, \end{aligned} \quad (9.1.15)$$

for the P and S waves respectively. We find the relevant Hamiltonian from the Legendre transformation,

$$H = \sum_{i=1}^3 \Omega_i \frac{\partial L}{\partial \Omega_i} - L. \quad (9.1.16)$$

Now we use the definition (9.1.10) and solve for

$$\vec{\Omega} = \frac{1}{\alpha^2} (\rho \vec{G} - \vec{R}). \quad (9.1.17)$$

We also know that

$$R_a = \frac{\partial L}{\partial \Omega_a} = J_a^{\text{sol}} \quad (9.1.18)$$

$$= -\beta^2 \Omega_a \quad a = 4, 5, 6, 7. \quad (9.1.19)$$

Of course the 3 component right generator \vec{R} is just the negative of the soliton spin \vec{J}^{sol} so the total spin of the baryon is given by

$$\vec{J} = -\vec{R} + \vec{G} \quad (9.1.20)$$

$$\Rightarrow \vec{J}^2 = \vec{R}^2 - 2\vec{R} \cdot \vec{G} \quad (9.1.21)$$

$$\Rightarrow \vec{R} \cdot \vec{G} = \frac{1}{2} (\vec{R}^2 - \vec{J}^2), \quad (9.1.22)$$

where we have neglected the term quadratic in \vec{G} because such terms would be quartic in the Fourier amplitude, χ . Using all of these, we can simplify the expression for the Hamiltonian to

$$H = \left(\frac{1}{2\alpha^2} - \frac{1}{2\beta^2} \right) \vec{R}^2 - \frac{1}{2\alpha^2} \rho(\vec{R}^2 - \vec{J}^2) + \frac{1}{2\beta^2} \sum_{a=1}^8 R_a^2 - \frac{1}{2\beta^2} R_8^2 + E_{\text{cl}} + \epsilon_H, \quad (9.1.23)$$

where R_a is just the Casimir operator. Of course \vec{R} and \vec{J} both represent spin quantum numbers, so they are squared according to,

$$\vec{J}^2 = \vec{J}(\vec{J} + 1). \quad (9.1.24)$$

The expressions for α^2 and β^2 can be found in eqs.(5.3.12) and (5.3.13) respectively. We saw in section 8.1 that the soliton must be quantised as a diquark, and therefore the soliton spin must be integer valued. Hence \vec{R}^2 is also integer valued, whereas \vec{J} is the baryon spin and therefore must be half-integer valued¹. Incorporating light and heavy flavour symmetry breaking, we replace the Casimir operator in eq.(9.1.23) by $\vec{\epsilon}_{\text{sb}}$, the symmetry breaking eigenvalue in eq.(8.2.9). The quantum number \vec{R} must be identified with the isospin of the $Y = Y_R$ member in the corresponding SU(3) irrep. The possible values of R_8 are given in eq.(8.1.12). The expression for the classical energy functional, E_{cl} , is given in eq.(4.3.24). The heavy meson energy eigenvalue, ϵ_H , is given in eq.(7.2.14).

We would like to stress that the inclusion of hyperfine splitting with strangeness to the Yabu-Ando approach is a really novel work in this study.

¹For good static baryons, $\vec{J} = \frac{1}{2}$, and for rotational excitations, $\vec{J} = \frac{3}{2}$

Chapter 10

Numerical Results

In section 5.4.1 we have already discussed our numerical results for the quantisation of the soliton, and we have compared these results to those found by Momen *et al.* (1994) and Park *et al.* (1989) using perturbation theory.

In section 7.2 we discussed the calculation of the bound states of a heavy meson in the background of a Skyrmion, including the differences between the S and P wave bound states. Table 10.1 shows the bound state energies of heavy mesons for the Skyrme parameter, $e_{\text{sk}} = 6.62$. These results show good comparison with the results in table 5.1 of Schechter *et al.* (1995). We have already shown the wave functions for the bottom mesons in figs. 7.1 and 7.2. The corresponding wave functions for the charm mesons are shown in figs. 10.1 and 10.2.

Flavour	$\epsilon_{\text{H}}^{(P)}$ (MeV)	$\epsilon_{\text{H}}^{(S)}$ (MeV)	$\epsilon_{\text{H}}^{(P)} - \epsilon_{\text{H}}^{(S)}$ (MeV)
Charm	314	28	286
Bottom	595	338	257

Table 10.1: Bound state energies of bottom and charm mesons where ϵ_H is defined in eq.(7.2.14).

The S and P waves refer to the 0^- and 1^- parity states respectively. Therefore the difference between $\epsilon_{\text{H}}^{(S)}$ and $\epsilon_{\text{H}}^{(P)}$ give us the difference between the masses of the 0^- and 1^- parity states of the same heavy meson. Table 10.2 shows the numerical and experimental results for these mass differences for bound state mesons, containing either a charm or a bottom quark. These results are satisfactory, and so can be applied to the model for heavy baryons.

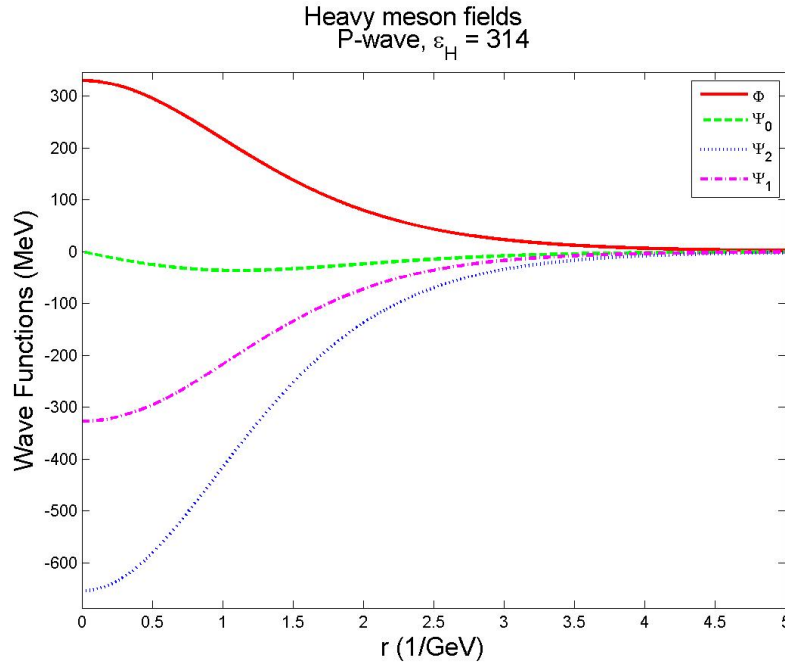


Figure 10.1: Wave functions of the pseudoscalar and vector fields for the P-wave of the heavy meson containing a charm quark with $\epsilon_B = 314$ MeV. Here the vertical axis is in arbitrary units.

Flavour	$\Delta\epsilon_B$ (MeV)	Baryon	Δm (MeV)(exp)
B	257	Λ_b	293
C	286	Λ_c	306

Table 10.2: Comparison of mass differences between S and P-wave to experimentally observed mass differences between heavy mesons of opposite parity. Here $e_{sk} = 6.62$. The experimentally determined masses were taken from Olive *et al.* (2014).

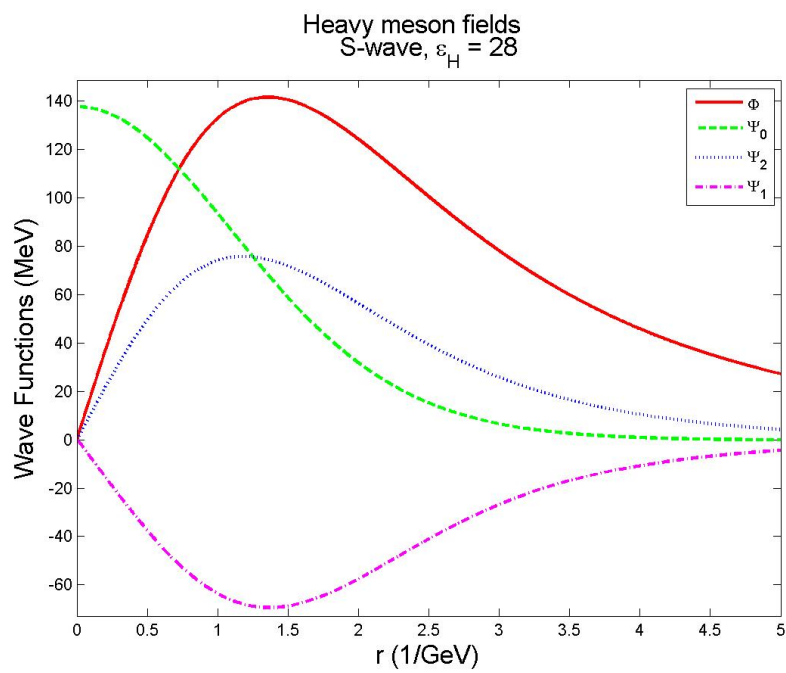


Figure 10.2: Wave functions of the pseudoscalar and vector fields for the S-wave of the heavy meson containing a charm quark with $\epsilon_B = 28$ MeV. Here the vertical axis is in arbitrary units.

We can now compute the relative masses of heavy baryons. The relevant quantum numbers that go into the calculations are shown in table 10.3. We show all masses relative to the Λ_c mass for our numerical results, in comparison to experimental results obtained from Olive *et al.* (2014). Tables 10.4 and 10.5 show the relative masses for the $J = 1/2$ and $J = 3/2$ baryons respectively with $e_{\text{sk}} = 6.62$, as used in Schechter *et al.* (1995). Adjusting e_{sk} to reproduce the mass difference between the N and the Δ though, we get $e_{\text{sk}} = 4.25$, just like Harada *et al.* (1997). The corresponding mass differences are shown in tables 10.6 and 10.7.

Baryon	Lowest SU(3) irrep	J	Y	I	R	Wave
Λ_c	$\bar{\mathbf{3}}$	$\frac{1}{2}$	$\frac{2}{3}$	0	0	P
$\Lambda_c(2595)$	$\bar{\mathbf{3}}$	$\frac{1}{2}$	$\frac{2}{3}$	0	0	S
Ξ_c	$\bar{\mathbf{3}}$	$\frac{1}{2}$	$-\frac{1}{3}$	$\frac{1}{2}$	0	P
$\Xi_c(2645)^*$	$\mathbf{6}$	$\frac{3}{2}$	$-\frac{1}{3}$	$\frac{1}{2}$	1	P
$\Xi_c(2790)$	$\bar{\mathbf{3}}$	$\frac{1}{2}$	$-\frac{1}{3}$	$\frac{1}{2}$	0	S
$\Xi_c(2815)^*$	$\mathbf{6}$	$\frac{3}{2}$	$-\frac{1}{3}$	$\frac{1}{2}$	1	S
Ω_c	$\mathbf{6}$	$\frac{1}{2}$	$-\frac{4}{3}$	0	1	P
Ω_c^*	$\mathbf{6}$	$\frac{3}{2}$	$-\frac{4}{3}$	0	1	P
Ξ_c'	$\mathbf{6}$	$\frac{1}{2}$	$-\frac{1}{3}$	$\frac{1}{2}$	1	P
$\Sigma_c(2455)$	$\mathbf{6}$	$\frac{1}{2}$	$\frac{2}{3}$	1	1	P
$\Sigma_c(2520)^*$	$\mathbf{6}$	$\frac{3}{2}$	$\frac{2}{3}$	1	1	P
Λ_b	$\bar{\mathbf{3}}$	$\frac{1}{2}$	$\frac{2}{3}$	0	0	P
$\Lambda_b(5912)$	$\bar{\mathbf{3}}$	$\frac{1}{2}$	$\frac{2}{3}$	0	0	S
Ξ_b	$\bar{\mathbf{3}}$	$\frac{1}{2}$	$-\frac{1}{3}$	$\frac{1}{2}$	0	P
$\Xi_b(5945)^*$	$\mathbf{6}$	$\frac{3}{2}$	$-\frac{1}{3}$	$\frac{1}{2}$	1	P
Ω_b	$\mathbf{6}$	$\frac{1}{2}$	$-\frac{4}{3}$	0	1	P
Σ_b	$\mathbf{6}$	$\frac{1}{2}$	$\frac{2}{3}$	1	1	P
Σ_b^*	$\mathbf{6}$	$\frac{3}{2}$	$\frac{2}{3}$	1	1	P

Table 10.3: Relevant quantum numbers for the baryons under investigation.

The lower value of e_{sk} does show much better agreement with experimental data than the higher value. Of course Harada *et al.* (1997) included the effects of the light vector mesons, which is expected to greatly improve the results.

Baryon	$M_{\text{Num}}(\text{MeV})$	$M_{\text{Exp}}(\text{MeV})$
Λ_c	0	0
Ξ_c	103	181
Ω_c	735	409
Ξ'_c	692	289
$\Sigma_c(2455)$	649	167
Λ_b	3116	3333
Ξ_b	3215	3505
Ω_b	3871	3762
Ξ'_b	3830	
Σ_b	3788	3524

Table 10.4: Numerical and experimental results for masses of $J = 1/2$ heavy baryons relative to the mass of the Λ_c with $e_{\text{sk}} = 6.62$.

Baryon	$M_{\text{Num}}(\text{MeV})$	$M_{\text{Exp}}(\text{MeV})$
Ξ_c^*	701	
Ω_c^*	976	480
$\Xi_c(2645)^{*'}$	933	360
$\Sigma_c(2520)^*$	890	232
Ξ_b^*	3149	
Ω_b^*	3769	
$\Xi_b(5945)^{*'}$	3728	
Σ_b^*	3686	3546

Table 10.5: Numerical and experimental results for masses of $J = 3/2$ heavy baryons relative to the mass of the Λ_c with $e_{\text{sk}} = 6.62$.

Adkins and Nappi (1984) adjusted the parameters of the skyrme model in order to fit the N , Δ and π masses. They used $e_{\text{sk}} = 4.84$ and $f_\pi = 54$ MeV¹. Throughout this study we have considered f_π to have its experimentally verified value, rather than a free parameter, but it is still interesting to see the results obtained from setting it to the value used by Adkins and Nappi (1984). Of course they did not consider strangeness, and so there is no f_K in their publication, but we will keep a constant ratio of $f_K = 1.21f_\pi$. Tables 10.8 and

¹In the actual publication they report $F_\pi = 108$ MeV, but they are using a different convention that is related to our convention by a factor 2.

Baryon	$M_{\text{Num}}(\text{MeV})$	$M_{\text{Exp}}(\text{MeV})$
Λ_c	0	0
Ξ_c	244	181
Ω_c	490	409
Ξ'_c	366	289
$\Sigma_c(2455)$	235	167
Λ_b	3214	3333
Ξ_b	3454	3505
Ω_b	3706	3762
Ξ'_b	3585	
Σ_b	3456	3524

Table 10.6: Numerical and experimental results for masses of $J = 1/2$ heavy baryons relative to the mass of the Λ_c with $e_{\text{sk}} = 4.25$.

Baryon	$M_{\text{Num}}(\text{MeV})$	$M_{\text{Exp}}(\text{MeV})$
Ξ_c^*	357	
Ω_c^*	541	480
$\Xi_c(2645)^{*'}$	417	360
$\Sigma_c(2520)^*$	286	232
Ξ_b^*	3417	
Ω_b^*	3665	
$\Xi_b(5945)^{*'}$	3543	
Σ_b^*	3415	3546

Table 10.7: Numerical and experimental results for masses of $J = 3/2$ heavy baryons relative to the mass of the Λ_c with $e_{\text{sk}} = 4.25$.

10.9 show our results for these parameters. The agreement with the experiment is surprisingly good, in light of the fact that the parameters were chosen to fit light baryons without strangeness. This gives us great confidence in the model.

Thus far we have only looked at the masses of the P-wave states because there is very little data available for comparison of S-wave states. Tables 10.10 and 10.11 show the comparison of the three different sets of parameters we have discussed, as well as the available experimental data.

Baryon	$M_{\text{Num}}(\text{MeV})$	$M_{\text{Exp}}(\text{MeV})$
Λ_c	0	0
Ξ_c	208	181
Ω_c	435	409
Ξ'_c	333	289
$\Sigma_c(2455)$	225	167
Λ_b	3262	3333
Ξ_b	3465	3505
Ω_b	3703	3762
Ξ'_b	3604	
Σ_b	3499	3524

Table 10.8: Numerical and experimental results for masses of $J = 1/2$ heavy baryons relative to the mass of the Λ_c with $e_{\text{sk}} = 4.84$ and $f_\pi = 54$ as used by Adkins and Nappi (1984).

Baryon	$M_{\text{Num}}(\text{MeV})$	$M_{\text{Exp}}(\text{MeV})$
Ξ_c^*	294	
Ω_c^*	483	480
$\Xi_c(2645)^{*'}$	381	360
$\Sigma_c(2520)^*$	274	232
Ξ_b^*	3441	
Ω_b^*	3680	
$\Xi_b(5945)^{*'}$	3581	
Σ_b^*	3476	3546

Table 10.9: Numerical and experimental results for masses of $J = 3/2$ heavy baryons relative to the mass of the Λ_c with $e_{\text{sk}} = 4.84$ and $f_\pi = 54$ as used by Adkins and Nappi (1984).

Baryon	$M_{\text{Num}}(\text{MeV})$	$M_{\text{Num}}(\text{MeV})$	$M_{\text{Num}}(\text{MeV})$	$M_{\text{Exp}}(\text{MeV})$
	$e_{\text{sk}} = 6.62$	$e_{\text{sk}} = 4.25$	$e_{\text{sk}} = 4.84, f_{\pi} = 54 \text{ MeV}$	
$\Lambda_c(2595)$	417	199	121	306
$\Xi_c(2790)$	519	442	328	505
Ω_c	793	626	517	
Ξ'_c	751	502	415	
Σ_c	708	371	308	
$\Lambda_b(5912)$	3387	3360	3348	3626
Ξ_b	3486	3600	3551	
Ω_b	4105	3849	3790	
Ξ'_b	4064	3727	3691	
Σ_b	4023	3599	3586	

Table 10.10: Numerical and experimental results for S-wave masses of $J = 1/2$ heavy baryons relative to the ground state mass of the Λ_c with different values of e_{sk} and f_{π} .

Baryon	$M_{\text{Num}}(\text{MeV})$	$M_{\text{Num}}(\text{MeV})$	$M_{\text{Num}}(\text{MeV})$	$M_{\text{Exp}}(\text{MeV})$
	$e_{\text{sk}} = 6.62$	$e_{\text{sk}} = 4.25$	$e_{\text{sk}} = 4.84, f_{\pi} = 54 \text{ MeV}$	
Ξ_c^*	-251	66	116	
Ω_c^*	381	312	344	
$\Xi_c(2815)^{*}$	338	188	242	531
Σ_c^*	295	57	134	
Ξ_b^*	2824	3264	3356	
Ω_b^*	3480	3516	3594	
Ξ_b^{*}	3439	3395	3495	3663
Σ_b^*	3397	3266	3390	

Table 10.11: Numerical and experimental results for S-wave masses of $J = 3/2$ heavy baryons relative to the ground state mass of the Λ_c with different values of e_{sk} and f_{π} .

Chapter 11

Conclusion

In this study we have found that one can build a comprehensive picture of heavy baryons in an effective meson theory by considering the baryon as consisting of a heavy meson bound in the background of a light soliton. In such a picture the Wess-Zumino term needs to be included in order for the meson action to display the correct parity transformations. This Wess-Zumino term is then directly responsible, via the right generator, R_8 , for enforcing the correct spin on the baryon. In the case of heavy baryons this, forces the soliton to be quantised as a diquark.

We also found that in order to incorporate strangeness into the model, one needs to break the $SU(3)$ symmetry in the collective coordinate quantisation of the soliton. This symmetry is then further broken by inclusion of the heavy meson bound in the background of the soliton.

When considering heavy mesons, one cannot consider the pseudoscalar and vector mesons separately, since there is some degeneracy between them. Therefore any model containing heavy mesons must contain both pseudoscalar and vector mesons and, in fact, their interactions are governed by the same coupling constant.

Finally we found that hyperfine splitting is crucial to building a model of heavy baryons with sensible spin quantum numbers.

In chapter 10 we found that we could calculate the ground state mass differences of heavy baryons to within around 10% of their experimentally determined values, depending on the set of parameters used. Further improvements should be obtained by including the effects of the light vector mesons as was done by Harada *et al.* (1997). Therefore the model presented in this study is a good first approach to a model describing baryons containing strangeness as well as a single heavy quark.

Appendices

Appendix A

Notation & Conventions

In this study, we use aspects of different fields of specialisation, each with their own conventional notations. This leads to potential overlap in the used notation. Rather than redefining the symbols used in well known formalisms, in order to prevent ambiguities, we have opted to use the popular symbols. This does lead to some duplication, but the meaning should be clear, from the context. For instance, in section 2.5, $\vec{\alpha}$ indicates Dirac matrices as used in Bhaduri (1988). In eq.(4.3.17), α_μ is defined as the derivative of the field, as part of the Skyrme term. In eq.(5.1.4), α^2 is introduced as a moment of inertia which is straightforwardly calculated from the chiral angle. Finally, in eq.(5.3.2), α and α' indicate two of the eight Euler angles. These different meanings of the same symbol are used in separate sections, and therefore confusion should be avoidable.

Unless otherwise indicated in the text, we use the following conventions. Three-component vectors or operators are indicated by an arrow as in \vec{p} or $\vec{\tau}$. Einstein summation is used wherever indices are repeated, and in such cases Latin indices indicate a sum from 1 to 3 and Greek indices indicate a sum from 0 to 3, except where it is explicit that there is a longer range such as in eq.(5.2.5). Four-component vectors are taken, according to particle physics conventions, to be,

$$\begin{aligned} x^\mu &= (t, -\vec{x}) \\ \partial_\mu &= (\partial_0, -\vec{\partial}). \end{aligned} \tag{A.1}$$

Therefore changing between covariant and contravariant derivatives have the following signs,

$$\begin{aligned} \partial_0 Q_0 &= \partial^0 Q^0 \\ \partial_i Q_j &= \partial^i Q^j \\ \partial_0 Q_i &= -\partial^0 Q^i \\ \partial_i Q_0 &= -\partial^i Q^0. \end{aligned} \tag{A.2}$$

Time derivatives are denoted with a dot as in \dot{A} . Spatial derivatives are denoted with a prime as in F' , but this should not be confused with the prime sometimes used to indicate small transformations. This distinction should be explicit from the context, though.

It is common practice in literature to make little distinction between the Lagrangian (Lagrange function) and the Lagrange density, since the Lagrangian is just the spatial integral of the Lagrange density. In this text we will make the distinction by indicating a Lagrangian by L , and a Lagrange density by \mathcal{L} . The Lagrangian should not be confused with the left generator, which is indicated with L_i , where the subscript will be some summation index. The distinction between a Lagrangian with a label as subscript, and the left generators should be clear from the context.

In order to relate our notation to that in Schechter *et al.* (1995), the following replacements must be made:

$$e_{sk} \rightarrow g.$$

In order to relate our notation to that in Harada *et al.* (1997), the following replacements must be made:

$$\chi \rightarrow \rho \tag{A.3}$$

$$L_H \rightarrow I_\epsilon \tag{A.4}$$

$$\rho \rightarrow \chi \tag{A.5}$$

Appendix B

Conventional Matrices

B.1 Gell-Mann Matrices

The flavour $SU(3)$ group is fundamental to our study and therefore its generators are very important. In chapter 3 we show how these generators are defined in terms of the eight Gell-Mann matrices. These matrices are traceless, hermitian and unitary. They appear again in section 5.3 when we define the eight Euler angles in order to quantise the collective coordinates of the soliton. We list these Gell-Mann matrices below:

$$\begin{aligned}
 \lambda_1 &= \begin{pmatrix} 0 & 1 & 0 \\ 1 & 0 & 0 \\ 0 & 0 & 0 \end{pmatrix} & \lambda_2 &= \begin{pmatrix} 0 & -i & 0 \\ i & 0 & 0 \\ 0 & 0 & 0 \end{pmatrix} & \lambda_3 &= \begin{pmatrix} 1 & 0 & 0 \\ 0 & -1 & 0 \\ 0 & 0 & 0 \end{pmatrix} \\
 \lambda_4 &= \begin{pmatrix} 0 & 0 & 1 \\ 0 & 0 & 0 \\ 1 & 0 & 0 \end{pmatrix} & \lambda_5 &= \begin{pmatrix} 0 & 0 & -i \\ 0 & 0 & 0 \\ i & 0 & 0 \end{pmatrix} & \lambda_6 &= \begin{pmatrix} 0 & 0 & 0 \\ 0 & 0 & 1 \\ 0 & 1 & 0 \end{pmatrix} \\
 \lambda_7 &= \begin{pmatrix} 0 & 0 & 0 \\ 0 & 0 & -i \\ 0 & i & 0 \end{pmatrix} & \lambda_8 &= \frac{1}{\sqrt{3}} \begin{pmatrix} 1 & 0 & 0 \\ 0 & 1 & 0 \\ 0 & 0 & -2 \end{pmatrix}
 \end{aligned} \tag{B.1.1}$$

B.2 Dirac Matrices

In section 2.5 we introduce the Dirac equation which requires the Dirac matrices listed below in the standard representation:

$$\begin{aligned} \gamma^0 &= \begin{pmatrix} 1 & 0 & 0 & 0 \\ 0 & 1 & 0 & 0 \\ 0 & 0 & -1 & 0 \\ 0 & 0 & 0 & -1 \end{pmatrix} & \gamma^1 &= \begin{pmatrix} 0 & 0 & 0 & 1 \\ 0 & 0 & 1 & 0 \\ 0 & -1 & 0 & 0 \\ -1 & 0 & 0 & 0 \end{pmatrix} \\ \gamma^2 &= \begin{pmatrix} 0 & 0 & 0 & -i \\ 0 & 0 & i & 0 \\ 0 & i & 0 & 0 \\ -i & 0 & 0 & 0 \end{pmatrix} & \gamma^3 &= \begin{pmatrix} 0 & 0 & 1 & 0 \\ 0 & 0 & 0 & -1 \\ -1 & 0 & 0 & 0 \\ 0 & 1 & 0 & 0 \end{pmatrix}. \end{aligned} \quad (\text{B.2.1})$$

We also introduce γ^5 which is not strictly one of the Dirac matrices, but is defined from their product,

$$\gamma^5 = i\gamma^0\gamma^1\gamma^2\gamma^3 \quad (\text{B.2.2})$$

$$= \begin{pmatrix} 0 & 0 & 1 & 0 \\ 0 & 0 & 0 & 1 \\ 1 & 0 & 0 & 0 \\ 0 & 1 & 0 & 0 \end{pmatrix}. \quad (\text{B.2.3})$$

This matrix plays a crucial role in the chiral symmetry of the massless Dirac equation and, by extension, QCD.

Appendix C

Radial Functions

In this appendix we will show the explicit forms of the matrices used in the generalisation of the the radial functions for section 7.2. For the sake of completeness we will reiterate 7.2.6 here.

$$\mathcal{L}_H = \frac{a_i}{2}\zeta_i'^2 + b_{ij}\zeta_i\zeta_j' + \frac{c_{ij}}{2}\zeta_i\zeta_j + \frac{f_1}{2}\Psi_1^2 + (g_i\zeta_i + h_i\zeta_i')\Psi_1 \quad (\text{C.1})$$

$$\zeta = (\Phi, \Psi_0, \Psi_2). \quad (\text{C.2})$$

Now the coefficient matrices are

$$\begin{aligned} a &= \begin{bmatrix} 2 & -2 & 1 \end{bmatrix} \\ b &= \begin{bmatrix} 0 & 0 & 0 \\ 0 & 0 & 0 \\ 0 & -\frac{2d\sin F}{r} & -\frac{1}{r} \end{bmatrix} \\ c &= \begin{bmatrix} 2M^2 + \frac{4(1+\frac{R_\alpha}{2})^2}{r^2} - 2\epsilon^2 & 0 & -4Md\frac{\sin F}{r} \\ 0 & -2M^{*2} - \left(\frac{R_\alpha}{r}\right)^2 & -2\frac{R_\alpha}{r}(\epsilon + dF') \\ -4Md\frac{\sin F}{r} & -2\frac{R_\alpha}{r}(\epsilon + dF') & M^{*2} + \frac{2+4R_\alpha+R_\alpha^2}{2r^2} \\ & & -\epsilon^2 + -dF'\epsilon \end{bmatrix} \\ f &= 2M^{*2} - 2\epsilon^2 + \left(\frac{R_\alpha}{r}\right)^2 \\ g &= 2d \begin{bmatrix} MF' & R_\alpha\frac{\sin F}{r^2} & \frac{R_\alpha}{r^2} + \epsilon\frac{\sin F}{r} \end{bmatrix} \\ h &= \begin{bmatrix} 0 & 2\epsilon & \frac{R_\alpha}{r} \end{bmatrix} \end{aligned} \quad (\text{C.3})$$

and

$$\begin{aligned}
a &= \begin{bmatrix} 2 & -2 & 4 \end{bmatrix} \\
b &= \frac{4}{r} \begin{bmatrix} 0 & 0 & 0 \\ 0 & 0 & 0 \\ 0 & d \sin F & 1 \end{bmatrix} \\
c &= \begin{bmatrix} 2M^2 + \left(\frac{R_\alpha}{r}\right)^2 - 2\epsilon^2 & 0 & 8dM\frac{\sin F}{r} \\ 0 & -2M^{*2} - \left(\frac{R_\alpha+2}{r}\right)^2 & \frac{4}{r}\{\epsilon(R_\alpha+2) + dF'(1+\cos F)\} \\ 8dM\frac{\sin F}{r} & \frac{4}{r}\{\epsilon(R_\alpha+2) + dF'(1+\cos F)\} & 4\left(M^{*2} + \frac{1}{r^2} + \frac{R_\alpha^2}{2r^2} - dF'\epsilon - \epsilon^2\right) \end{bmatrix} \\
f &= 2M^{*2} - 2\epsilon^2 + \left(\frac{R_\alpha+2}{r}\right)^2 \\
g &= 2 \left[dMF' \quad d(R_\alpha+2)\frac{\sin F}{r^2} \quad -\frac{R_\alpha+2}{r^2} - 2d\epsilon\frac{\sin F}{r} \right] \\
h &= \begin{bmatrix} 0 & 2\epsilon & -2\frac{R_\alpha+2}{r} \end{bmatrix}. \tag{C.4}
\end{aligned}$$

for the P and S-wave respectively.

List of References

- Adkins, G.S. and Nappi, C.R. (1984). The Skyrme model with pion masses. *Nuclear Physics B*, vol. 233, no. 1, pp. 109 – 115.
Available at: <http://www.sciencedirect.com/science/article/pii/055032138490172X>
- Adkins, G.S., Nappi, C.R. and Witten, E. (1983). Static properties of nucleons in the Skyrme model. *Nuclear Physics B*, vol. 228, no. 3, pp. 552 – 566.
Available at: <http://www.sciencedirect.com/science/article/pii/055032138390559X>
- Alkofer, R. and Reinhardt, H. (1995). *Chiral Quark Dynamics*. No. v. 33 in Chiral Quark Dynamics. Springer-Verlag. ISBN 9783540601371.
Available at: <http://books.google.co.za/books?id=fDENwIMAc50C>
- Bhaduri, R. (1988). *Models of the nucleon: from quarks to soliton*. Lecture notes and supplements in physics. Addison-Wesley, Advanced Book Program. ISBN 9780201156737.
Available at: <http://books.google.co.za/books?id=7smBAAAIAAJ>
- Blanckenberg, J. and Weigel, H. (2014). Heavy Baryons with Strangeness. In: Botha, R. and Jili, T. (eds.), *Proceedings of SAIP2013, the 58th Annual Conference of the South African Institute of Physics*, pp. 525 – 530. ISBN 978-0-620-62819-8.
Available at: <http://events.saip.org.za/internalPage.py?pageId=13&confId=32>
- Callan, C. and Klebanov, I. (1985). Bound-state approach to strangeness in the skyrme model. *Nuclear Physics B*, vol. 262, no. 2, pp. 365 – 382.
Available at: <http://www.sciencedirect.com/science/article/pii/0550321385902925>
- Cheng, T. and Li, L. (1984). *Gauge Theory of Elementary Particle Physics*. Oxford science publications. Clarendon Press. ISBN 9780198519614.
Available at: <http://books.google.co.za/books?id=lk8GEzVNB10C>
- Collaboration, L. (2014 Jun). Observation of the resonant character of the $Z(4430)^-$ state. *Phys. Rev. Lett.*, vol. 112, p. 222002.
Available at: <http://link.aps.org/doi/10.1103/PhysRevLett.112.222002>

- Gupta, K.S., Momen, M.A., Schechter, J. and Subbaraman, A. (1993 Jun). Heavy quark solitons. *Phys. Rev. D*, vol. 47, pp. R4835–R4839.
Available at: <http://link.aps.org/doi/10.1103/PhysRevD.47.R4835>
- Harada, M., Qamar, A., Sannino, F., Schechter, J. and Weigel, H. (1997). Hyperfine splitting of low-lying heavy baryons. *Nuclear Physics A*, vol. 625, no. 4, pp. 789 – 816.
Available at: <http://www.sciencedirect.com/science/article/pii/S0375947497004004>
- Hooft, G. (1974). A planar diagram theory for strong interactions. *Nuclear Physics B*, vol. 72, no. 3, pp. 461 – 473.
Available at: <http://www.sciencedirect.com/science/article/pii/0550321374901540>
- Ioffe, B. and Shifman, M. (1982). Baryons in multicolor chromodynamics. *Nuclear Physics B*, vol. 202, no. 2, pp. 221 – 237.
Available at: <http://www.sciencedirect.com/science/article/pii/0550321382900694>
- Lee, T. (1982). *Particle Physics and Introduction to Field Theory*. Harwood Academic Publishers.
- Manohar, A.V. and Wise, M.B. (2000). *Heavy Quark Physics*. Cambridge University Press. ISBN 9780511529351. Cambridge Books Online.
Available at: <http://dx.doi.org/10.1017/CB09780511529351>
- Meissner, U.-G. (1988). Low-energy hadron physics from effective chiral lagrangians with vector mesons. *Physics Reports*, vol. 161, no. 5-6, pp. 213 – 361.
Available at: <http://www.sciencedirect.com/science/article/pii/0370157388900907>
- Momen, A., Schechter, J. and Subbaraman, A. (1994). Heavy quark solitons: Strangeness and symmetry breaking. *Phys.Rev.*, vol. D49, pp. 5970–5978. hep-ph/9401209.
- Oh, Y., Min, D.-P., Rho, M. and Scoccola, N.N. (1991). Massive-quark baryons as skyrmions: Magnetic moments. *Nuclear Physics A*, vol. 534, no. 34, pp. 493 – 512.
Available at: <http://www.sciencedirect.com/science/article/pii/037594749190458I>
- Olive, K. *et al.* (2014). Particle data group. *Chin. Phys. C*38, 090001.
Available at: <http://pdg.lbl.gov/>
- Park, N., Schechter, J. and Weigel, H. (1989). Higher order perturbation theory for the SU(3) Skyrme model. *Physics Letters B*, vol. 224, no. 1-2, pp. 171 – 176.
Available at: <http://www.sciencedirect.com/science/article/pii/0370269389910691>

- Pauli, W. (1946). *Meson Theory of Nuclear Forces*. Interscience Publishers, Inc. New York.
- Schat, C.L., Scoccola, N.N. and Gobbi, C. (1995). $\Lambda(1405)$ in the bound-state soliton model. *Nuclear Physics A*, vol. 585, no. 4, pp. 627 – 640.
Available at: <http://www.sciencedirect.com/science/article/pii/037594749400798R>
- Schechter, J., Subbaraman, A., Vaidya, S. and Weigel, H. (1995). Heavy quark solitons: Towards realistic masses. *Nuclear Physics A*, vol. 590, pp. 655–679.
<http://www.sciencedirect.com/science/article/pii/037594749500182Z>.
- Schwesinger, B., Weigel, H., Holzwarth, G. and Hayashi, A. (1989). The Skyrme soliton in pion, vector- and scalar-meson fields: π N-scattering and photoproduction. *Physics Reports*, vol. 173, no. 4, pp. 173 – 255.
Available at: <http://www.sciencedirect.com/science/article/pii/0370157389900227>
- Skyrme, T.H.R. (1961). A non-linear field theory. *Proceedings of the Royal Society of London. Series A. Mathematical and Physical Sciences*, vol. 260, no. 1300, pp. 127–138. <http://rspa.royalsocietypublishing.org/content/260/1300/127.full.pdf+html>.
Available at: <http://rspa.royalsocietypublishing.org/content/260/1300/127.abstract>
- Walliser, H. and Weigel, H. (2005). Bound-state versus collective-coordinate approaches in chiral soliton models and the width of the Θ^+ pentaquark. *The European Physical Journal A - Hadrons and Nuclei*, vol. 26, no. 3, pp. 361–382.
Available at: <http://dx.doi.org/10.1140/epja/i2005-10180-5>
- Weigel, H. (2008). *Chiral Soliton Models for Baryons*. Lecture Notes in Physics. Springer. ISBN 9783540754350.
Available at: <http://link.springer.com/book/10.1007/978-3-540-75436-7>
- Witten, E. (1979). Baryons in the $1/N$ expansion. *Nuclear Physics B*, vol. 160, no. 1, pp. 57 – 115.
Available at: <http://www.sciencedirect.com/science/article/pii/0550321379902323>
- Witten, E. (1983). Global aspects of current algebra. *Nuclear Physics B*, vol. 223, no. 2, pp. 422 – 432.
Available at: <http://www.sciencedirect.com/science/article/pii/0550321383900639>
- Yabu, H. and Ando, K. (1988). A new approach to the SU(3) Skyrme model: Exact treatment of the SU(3) symmetry breaking. *Nuclear Physics B*, vol. 301, no. 4, pp. 601 – 626.
Available at: <http://www.sciencedirect.com/science/article/pii/0550321388902799>

- Zahed, I. and Brown, G. (1986). The Skyrme model. *Physics Reports*, vol. 142, no. 1-2, pp. 1 – 102.
Available at: <http://www.sciencedirect.com/science/article/pii/0370157386901420>